Sorting and membrane integration of mitochondrial outer membrane proteins

Dissertation

der Mathematisch-Naturwissenschaftlichen Fakultät
der Eberhard Karls Universität Tübingen
zur Erlangung des Grades eines
Doktors der Naturwissenschaften
(Dr. rer. nat.)

vorgelegt von
Daniela Giulia Vitali
aus Bergamo, Italy

Tübingen
2018

Gedruckt mit Genehmigung der Mathematisch-Naturwissenschaftlichen Fakultät der Eberhard Karls Universität Tübingen.

Tag der mündlichen Qualifikation:	24.07.2018
Dekan:	Prof. Dr. Wolfgang Rosenstiel
1. Berichterstatter:	Prof. Dr. Doron Rapaport
2. Berichterstatter:	Prof. Dr. Ana J. García Sáez

Table of Contents

1. Abbreviations

ATOM	archaic translocase of the outer membrane
BN-PAGE	blue native-polyacrylamide gel electrophoresis
CTE	C-terminal element
EMC	endoplasmic reticulum membrane protein complex
ER	endoplasmic reticulum
ERAD	endoplasmic reticulum-associated degradation
GET	guided entry of tail-anchored proteins
IMM	inner mitochondrial membrane
IMP	inner membrane peptidase
IMS	intermembrane space
kDNA	kinetoplast DNA
LECA	last eukaryotic common ancestor
MIA	mitochondrial import and assembly
MIM	mitochondria import
MPP	mitochondrial processing peptidase
MTS	mitochondria targeting signal
OMM	outer mitochondrial membrane
OXA	oxidase assembly
PAM	presequence translocase-associated motor
pATOM36	peripheral archaic translocase of the outer membrane 36
PK	proteinase K
PTP1B	protein tyrosine phosphatase 1B
RER	rough endoplasmic reticulum
SDS-PAGE	sodium dodecyl sulfate polyacrylamide gel electrophoresis
SER	smooth endoplasmic reticulum
SND	signal recognition particle-independent targeting
SR	signal recognition particle receptor
SRP	signal recognition particle
sTIMs	small TIM chaperones
TA	tail-anchored
TAC	tripartite attachment complex
TIM22/23	translocase of the inner mitochondrial membrane 22/23

TMS	transmembrane segment
TOB	topogenesis of the outer membrane β-barrel protein
TOM	translocase of the outer mitochondrial membrane
UBL	ubiquitin-like
WT	wild type

2. Summary

The various cellular activities of eukaryotic cells are confined in different organelles. The compartmentalization of the cytosol requires a fine regulation of the distribution of newly synthesized proteins to the destined organelle. Targeting pathways ensure the accurate sorting of protein and help to avoid mislocalization. They are organelle-specific and discriminate among the substrate proteins according to their topology and targeting signals.

Tail-anchored (TA) proteins are inserted into the lipid bilayer via a single C-terminal transmembrane segment that constitutes also the targeting signal. These proteins are mainly imported into the endoplasmic reticulum (ER) and the outer mitochondrial membrane (OMM). TA proteins are targeted to the ER by the guided entry of TA proteins (GET) pathway, while it is unclear how they are directed and inserted into the OMM. Interestingly, when the mitochondrial targeting is inefficient, OMM TA proteins are mislocalized to the ER. In this study, I analysed the role of the GET pathway in the missorting of TA proteins and I proved that this machinery could recognize mitochondrial proteins and direct them to the ER. These findings suggest the existence of a, yet unknown, mitochondrial targeting pathway that under physiological conditions is more efficient and wins the kinetic competition against other pathways.

One important factor that mediates the membrane insertion of several OMM α-helical proteins is the MIM complex. It is composed by the proteins Mim1 and Mim2, which have been identified only in fungi, while no homologues could be found in other eukaryotes. The MIM complex is important for mitochondrial functionality and its loss causes impaired mitochondria biogenesis, alteration of mitochondrial morphology and severe growth defects. It is still unclear how the crucial functions of this complex are mediated in other eukaryotes. In this work, I analysed the capacity of the trypanosomal OMM protein pATOM36 to rescue the phenotypes caused by the absence of the MIM complex. Reciprocal complementation studies demonstrated that this protein is a functional analogue of the MIM complex. This discovery suggests that pATOM36 and the Mim1/Mim2 complex are the result of a convergent evolution that happened after fungi and trypanosomatids diverged.

3. List of publications contained in this thesis

1. Vitali, D.G., M. Sinzel, E.P. Bulthuis, A. Kolb, S. Zabel, D.G. Mehlhorn, B. Figueiredo Costa, A. Farkas, A. Clancy, M. Schuldiner, C. Grefen, B. Schwappach, N. Borgese, and D. Rapaport. 2018. The GET pathway can increase the risk of mitochondrial outer membrane proteins to be mistargeted to the ER. *Journal of Cell Science*. 131.

2. Vitali, D.G.*, S. Käser*, A. Kolb*, K.S. Dimmer, A. Schneider, D. Rapaport. 2018. Independent evolution of functionally exchangeable mitochondrial outer membrane import complexes. *eLIFE*. 7.
   * equal contribution.

4. Personal contribution

1. Vitali, D.G., M. Sinzel, E.P. Bulthuis, A. Kolb, S. Zabel, D.G. Mehlhorn, B. Figueiredo Costa, A. Farkas, A. Clancy, M. Schuldiner, C. Grefen, B. Schwappach, N. Borgese, and D. Rapaport. 2018. The GET pathway can increase the risk of mitochondrial outer membrane proteins to be mistargeted to the ER. *Journal of Cell Science*. 131.

I analysed the membrane topology and the glycosylation state of HA-cytochrome b5 RR in the ER by PK treatment, carbonate extraction and glycosylation assays (Fig. 1D-F). To understand the effect of the deletion of GET component on the localization of GFP-Mcp3, I performed subcellular fractionation (Fig. 2B and 2F-H) and statistical analysis of the fluorescence microscopy localization (Fig. 2E). I also analysed the subcellular localization of GFP-Mim1 in WT, *get3Δ* and *get1Δ* cells (Fig. 3B, 3G-I) and of Mim1-GFP and Mim1 in WT and *get3Δ* strains (Fig. S2A-B). Moreover, I investigated whether Mim1 is glycosylated in the ER (Fig. S2C). I also analysed by fluorescence microscopy the localization of GFP-Mim1 (Fig. 3F). Furthermore, I assessed the physical interaction of Get3 with Mcp3 and Mim1 (Fig. 4A-B). I participated in writing the manuscript and prepared all the figures.

2. Vitali, D.G.*, S. Käser*, A. Kolb*, K.S. Dimmer, A. Schneider, D. Rapaport. 2018. Independent evolution of functionally exchangeable mitochondrial outer membrane import complexes. *eLIFE.* 7.
   * equal contribution.

I analysed the steady states levels of proteins in mitochondria isolated from WT and *mim1Δ mim2Δ* cells expressing pATOM36-HA (Fig. 3A-B). Moreover, I analysed the *in vitro* interaction of Tom70 with Mim1 or pATOM36 (Fig. 3E). Furthermore, I performed some of the *in vitro* import assay of radiolabelled Tom20 and Ugo1 into mitochondria from various strains (Fig. 4B-C). I participated in writing the manuscript and prepared part of the figures.

5. Introduction

5.1 Intracellular membrane protein sorting

One of the main characteristics of eukaryotic cells is the compartmentalization of the cytosol, which leads to the isolation of different cellular activities in specialized organelles. This division allows more efficient, rapid and controlled reactions. Along with this progress, it became crucial to sort the proteins, which are synthetized in the cytosol, precisely to the right compartment (Schlacht et al., 2014). This fine-tuning is achieved by an orchestral symphony of several cytosolic factors, chaperones, membrane receptors and translocases working in coordinated fashion not only to localize the required protein in a specific organelle, but also to avoid its erroneous targeting to another compartment (Sommer et al., 2014). The regulation of this sorting is extremely important for integral membrane proteins, which constitute 20-30% of the cellular proteome, due to the presence of hydrophobic transmembrane segments (TMSs) that are prone to aggregate in an aqueous environment (Guna et al., 2018a). Therefore, during the sorting of these proteins it is essential that the TMS is shielded as soon as it emerges from the ribosome until it reaches the target membrane. There, the cell faces another challenge in inserting the protein into the lipid bilayer with the correct orientation and conformation (Shao et al., 2011). The aforementioned processes lead to the import of membrane proteins into three organelles: peroxisomes, mitochondria and endoplasmic reticulum (ER), from where membrane proteins are distributed to their final destination along the secretory pathway.

5.2 Structure and function of the ER

The ER is a multifunctional organelle distributed through the entire cell, formed by a continuous membrane bilayer that defines a connected lumen and organized in functional and morphological different subdomains. It is arranged in a nuclear and a peripheral ER, which is constituted of large convoluted cisternae and an interconnected tubular network (Voeltz et al., 2002). The nuclear envelop surrounds the nucleus as a flat cisterna, which is composed of a double membrane bilayer separated by the nuclear membrane space and interconnected with nuclear

pores. The peripheral tubular ER is considered ribosome-free and is also defined as smooth ER (SER), while the cisternae are also called rough ER (RER) because of the high concentration of membrane-associated ribosomes on them (English et al., 2013). The ER plays a crucial role in protein folding and quality control of the secretory pathway and the translation of new protein on its surface can improve the control of their maturation. Indeed, around 30% of human proteins are targeted to the ER, where they can be retained or further distributed to their final location through vesicles that travels until the Golgi apparatus and can reach the plasma membrane, via the so-called secretory pathway (Bellucci et al., 2017; Benham, 2012; Glick et al., 2011). Before the distribution to their ultimate target, these proteins undergo several maturation steps comprising the addition of covalent N-linked glycans, the formation of disulphide bonds, the addition of co-factors, and the folding into their functional conformation or eventually the assembly into complexes (Araki et al., 2011; Braakman et al., 2011; Ellgaard et al., 2003). Additionally to its role in protein quality control and homeostasis, the ER also controls the degradation of unfolded proteins via the ER-associated degradation (ERAD) pathway (Olzmann et al., 2013; Thibault et al., 2012). Furthermore, it is also required for lipid biosynthesis and ions homeostasis (mainly calcium) (Breslow et al., 2010; Fagone et al., 2009; Gault et al., 2010; Jakobsson et al., 2006; Sammels et al., 2010; Sorger et al., 2003). Given all the aforementioned activities performed by the ER, the efficient regulation of its functions is essential for cell survival.

5.3 Co-translational protein import into the ER

Most of the proteins targeted to ER, both membrane and soluble, are co-translationally inserted via the conserved signal recognition particle (SRP) pathway (Nyathi et al., 2013) (Fig. 1, pathway 1). The ribonucleoprotein complex SRP associates with the nascent chain at the ribosome exit tunnel and recognizes an N-terminal hydrophobic segment, which can be either a cleavable signal sequence in soluble proteins, or an α-helical TMS in membrane proteins (Zhang et al., 2014). This interaction stalls the translation until the SRP binds the SRP receptor (SR) on the ER surfaces, allowing the recruitment of the protein synthesis machinery in close proximity to the organelle (Halic et al., 2004). Afterwards, a GTPase-dependent mechanism induces the release of the nascent chain from the SRP and its transfer

to the Sec61 translocon, which mediates the translocation of the protein through the membrane. Ultimately, the translation resumes and the protein is released into the lumen or inserted in the ER membrane (Osborne et al., 2005; Shao et al., 2011).

5.4 Post-translational protein import into the ER

5.4.1 Tail-anchored proteins

Tail-anchored (TA) proteins are a class of proteins representing 3-5% of eukaryotic membrane proteins (Kalbfleisch et al., 2007). They are characterized by a large N-terminal domain facing the cytosol and a single α-helical TMS, which is located less than 30 residues from the C-terminus. TA proteins can be imported only in a post-translational manner, because the TMS, representing the targeting signal, cannot interact with SRP since it is still inside the ribosome exit tunnel when the translation terminates (Hegde et al., 2011). These proteins are found in all cellular compartments and are involved in various cellular activities such as protein import, quality control, vesicular transport, apoptosis, organelles dynamics, and contact sites formation (Borgese et al., 2011; Chio et al., 2017a; Krumpe et al., 2012).

The target organelle for TA proteins is mainly dictated by the physicochemical properties of the targeting signal. Mitochondrial TA proteins have generally a short and less hydrophobic TMS, which is flanked by positive charges and has low helical content. Similarly, low hydrophobicity and helical content of the TMS with a basic C-terminal element (CTE) lead TA proteins to peroxisomes. Conversely, ER TA proteins have the longest and more hydrophobic TMS with a higher helical content. Moreover, those that are retained in the ER have on average a shorter and less hydrophobic TMS compared to those that are distributed along the secretory pathway (Beilharz et al., 2003; Chio et al., 2017a; Costello et al., 2017; Rao et al., 2016).

These different signals are recognized by organelle-specific import machineries. The most characterized targeting pathway is the guided entry of TA proteins (GET), which directs these proteins to the ER (Fig. 1, pathway 2) (see section 6.4.2) (Chartron et al., 2012; Chio et al., 2017a; Denic et al., 2013; Hegde et al., 2011). The regulation of the insertion into peroxisomes membranes is more debated, since it is unclear whether TA proteins are directly inserted into these organelles or first targeted to the ER and then are carried to peroxisomes via

vesicles. Indeed, it is known that the cytosolic factor Pex19 can bind TA proteins and mediate their import into peroxisomes through its interaction with the membrane receptor Pex3. Moreover, it has been described that in yeast the GET machinery can target some peroxisomal proteins, such as Pex15, to the ER (Chio et al., 2017a; Mayerhofer, 2016). Mitochondrial TA proteins are localized only in the outer mitochondrial membrane (OMM) and it is still puzzling how they are directed to this location (see section 6.7.1). In fact, the insertion of these proteins is independent of the known components of the OMM translocases and do not require membrane potential (Kemper et al., 2008; Setoguchi et al., 2006). Instead, it has been shown that in yeast the unique lipid composition of the OMM has an important role in the targeting of mitochondria TA proteins. Furthermore, *in vitro* studies demonstrated that the yeast mitochondrial TA protein Fis1 could spontaneously insert into liposomes (Kemper et al., 2008). Interestingly, the unassisted insertion of TA proteins was also observed in the case of ER proteins with less hydrophobic TMS, such as the mammalian cytochrome b5 and the protein tyrosine phosphatase 1B (PTP1B) (Brambillasca et al., 2006; Colombo et al., 2009; Fueller et al., 2015).

5.4.2 The GET pathway

The import of TA proteins to the ER is mediated by the conserved GET machinery (Fig. 1, pathway 2) (Schuldiner et al., 2008). The substrate recognition is mediated by the pretargeting complex, comprising Sgt2, Get4, and Get5. Sgt2 is a multidomain protein that associates with the ribosome and interacts with the nascent TA protein after its release from the exit tunnel (Wang et al., 2010). Since it binds specifically the TMS of ER TA proteins, it acts as a first selection filter for the correct substrates (Rao et al., 2016). Once Sgt2 binds the nascent TA protein, it associates with the Get4/5 complex. Get5 is a homodimer scaffold protein that interacts with Sgt2 trough an ubiquitin-like (UBL) domain and with Get4 via the N-terminal domain (Chartron et al., 2010). Get4 is required for recruiting Get3, the second substrate selection filter, with higher affinity for ER TA proteins (Rao et al., 2016). It is a cytosolic chaperone organized as a homodimer and is coordinated by one Zn^{2+} ion. Get3 has an ATPase domain that, in combination with the interaction with Get4 or Get1, regulates its conformational state and substrate affinity (Bozkurt et al., 2009; Hu et al., 2009; Mateja et al., 2009; Suloway et al., 2009). Since Get4 interacts with

the ATP-bound Get3, it stabilizes the chaperone in its open state, ready for capturing the TA protein (Rome et al., 2013). The interaction of Get3 with the TA protein causes a conformational change of the former protein to a closed state that induces the hydrolysis of ATP and the release of Get3 from the Get4/5 complex (Rome et al., 2014). Subsequently, the Get3-TA protein complex interacts with the Get1/2 receptors, embedded in the ER membrane (Rome et al., 2013; Schuldiner et al., 2008; Stefer et al., 2011). Both Get1 and Get2 have three TMSs, required for their heterodimerization, and a cytosolic domain that interacts with Get3 (Wang et al., 2014). Structural studies suggested that the ADP-Get3-TA protein complex binds first the long and flexible cytosolic domain of Get2 (Mariappan et al., 2011). Afterwards, the interaction with the cytosolic domain of Get1 causes the release of ADP, inducing the opening of Get3, the release of the TA protein and its membrane insertion (Wang et al., 2011). It is still not clear whether the receptors also actively mediate the membrane insertion of TA protein or if this happens in an unassisted way (Mariappan et al., 2011; Wang et al., 2014). Finally, Get3 is released from the receptors; it binds a new ATP molecule and interacts with the Get4/5 complex, ready to mediate the targeting of another TA protein (Rome et al., 2014). Interestingly, under oxidative stress Get3 has an additional function as ATP-independent chaperone holdase protecting the cell from protein aggregation (Powis et al., 2013; Voth et al., 2014).

5.5 SRP-independent targeting to the ER

Recently, the SRP-independent targeting (SND) pathway has been identified as another protein import machinery of the ER membrane (Fig. 1, pathway 3) (Aviram et al., 2016). Although it favours substrate membrane proteins with a TMS in the central region, the SND pathway can compensate the absence of either the SRP or the GET machinery (Aviram et al., 2016; Haßdenteufel et al., 2017). It is comprised of the cytosolic protein Snd1 and the ER membrane proteins Snd2 and Snd3. The molecular mechanism of this pathway has still to be unravelled, however it has been hypothesized that Snd1, which was suggested to interact with the ribosome, could recognize and bind the substrates during translation, while Snd2 and Snd3 could be membrane receptors, which capture the substrate and transfer it to the Sec61 translocon (Aviram et al., 2016).

Moreover, very recently it has been proposed that the ER-membrane protein complex (EMC), a conserved complex constituted by eight subunits, acts as an additional ER insertase for moderately hydrophobic TA proteins (Guna et al., 2018b).

These new discoveries suggest that there are several overlapping and redundant ER targeting pathways, which can reciprocally compensate the loss of a single pathway (Casson et al., 2017). This is particularly crucial for TA proteins, which have targeting signals with a broad range of physicochemical properties, leading to a higher risk of mislocalization and aggregation (Rao et al., 2016).

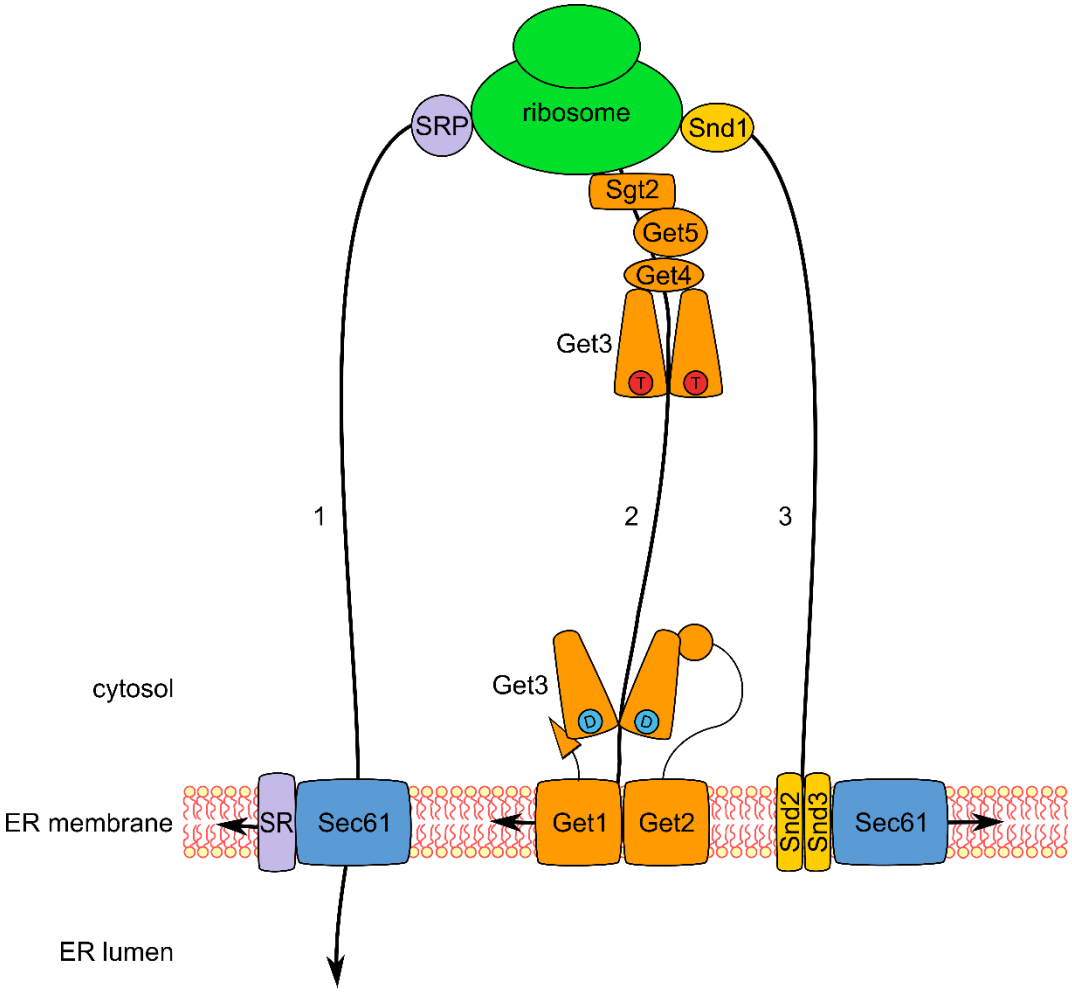

Figure 1. ER proteins import pathways. The SRP pathway mediates the co-translational import of soluble and membrane proteins with an N-terminal signal sequence **(1)**. The GET machinery mediates the insertion of TA proteins into the lipid bilayer. T, ATP; D, ADP. **(2)**. The SND pathway favours the insertion of membrane proteins with a TMS in the centre of the polypeptide **(3)**.

5.6 Mitochondria structure and function

Mitochondria are essential multifunctional organelles originated by endosymbiosis of an α-proteobacterium with an archaeal cell more than 1.5 billion years ago (Gray, 2012; Martin et al., 2015). After this event, the symbiont genomic material was transferred to the host nucleus, leaving only a small part of the original DNA in the resulting mitochondria (Dyall et al., 2004). Due to their origin, these organelles are constituted by two membranes (outer and inner mitochondrial membranes, OMM and IMM, respectively), delimiting a narrow intermembrane space (IMS) and an internal matrix. The IMM is arranged in cristae structures that harbour the respiratory chain complexes, required for the production of energy (Frey et al., 2000). Mitochondria are organized in the cell as interconnected tubules, which undergo continuous fusion and fission events in a very dynamic process (van der Bliek et al., 2013). In addition to the production of energy, mitochondria are involved in several metabolic pathways, like the tricarboxylic acid cycle, β-oxidation of fatty acids, amino acids biosynthesis, and heme and iron-sulphur clusters production (Lill, 2009; Osellame et al., 2012; Stehling et al., 2013). Moreover, they also participate in cell signalling, calcium storage and apoptosis (Nunnari et al., 2012).

5.7 Mitochondrial proteins import

Most of mitochondrial proteins are encoded in the nucleus and translated in the cytosol. Subsequently, they should be directed to the organelle and distributed to the correct intraorganelle compartment. The most known import pathways are acting in a post-translational manner, although recently the co-translational import of few proteins was described (Dukanovic et al., 2011; Wiedemann et al., 2017; Williams et al., 2014). Because of their post-translational import, many of the mitochondrial proteins are stabilized by cytosolic chaperones that subsequently carried them to their destination, where they interact with import receptors on the mitochondria surface (Chacinska et al., 2009; Dukanovic et al., 2011). The targeting signal of a large part of mitochondrial proteins is represented by an N-terminal cleavable presequence (mitochondrial targeting signal, MTS) of around 15-50 amino acids long, which forms an amphipathic α-helix with a positive charged side and a hydrophobic face (Vögtle et al., 2009; Wiedemann et al., 2017). However,

some proteins do not have an MTS and contain instead an internal targeting signal that is part of the mature protein.

The entry gate for most of mitochondrial proteins is the translocase of the OMM (TOM) complex, which is composed of the Tom40 channel, and the receptors Tom20, Tom22, and Tom70/71. The assembly and stability of this complex is regulated by the small subunits Tom5, Tom6, and Tom7. Tom20 and Tom22 recognize mainly proteins with an MTS (Moczko et al., 1993; Söllner et al., 1989; Vögtle et al., 2009), whereas Tom70/71 are required mostly for importing proteins with an internal targeting sequence (Hines et al., 1990). Moreover, recently it has been demonstrated that Tom20 can also recognize β-barrel precursor proteins (Jores et al., 2016). However, these receptors have also overlapping binding properties, allowing the reciprocal compensation of their loss (Yamano et al., 2008).

After the recognition of MTS-containing matrix proteins by the receptors Tom20 and Tom22, the precursor protein is translocated through the Tom40 pore and transferred to the translocase of the IMM (TIM) 23 complex (Chacinska et al., 2005). This complex mediates the transfer of the precursor to the matrix with the assistance of the presequence translocase-associated motor (PAM) in a membrane potential and ATP-dependent manner (Fig. 2, pathway 1a) (Mokranjac et al., 2010).

The targeting of precursor proteins to the IMM follows four different pathways according to the topology of the substrate. Nuclear-encoded membrane proteins containing an MTS follow a similar pathway to the matrix proteins. They are imported by the TOM and TIM23 complex and laterally released by the latter into the lipid bilayer (Fig. 2, pathway 1b) (Chacinska et al., 2005). In contrast to the matrix proteins, MTS-containing IMM proteins import requires membrane potential, but not ATP hydrolysis (van der Laan et al., 2007). Instead, multispan proteins containing an MTS are imported into the IMM via the so-called conservative sorting route. In this pathway the precursor protein is translocated via the TOM and TIM23 complexes into the matrix, from where the IMM oxidase assembly (OXA) translocase can insert it into the membrane (Fig. 2, pathway 1c) (Bohnert et al., 2010; Hell et al., 1998). Furthermore, multispan proteins of the carrier family do not contain an MTS and they are recognized by the Tom70 receptor. After their translocation through Tom40, they interact with the small TIM chaperones (sTIMs) in the IMS, which keep them in an unfolded state. This allows their transfer to the

TIM22 complex that inserts them into the IMM (Fig. 2, pathway 2a) (Ferramosca et al., 2013). In addition, around 1% of mitochondria proteins are encoded by the mitochondrial DNA and inserted co-translationally into the IMM by the OXA translocase (Fig. 2, pathway 3) (Hell et al., 2001).

IMS proteins generally contain cysteine rich motifs, which form disulphide bonds to keep them in the folded state and to retain them in mitochondria (Chacinska et al., 2004). These proteins are inserted into the organelle through the TOM complex. In the IMS, they are recognized by the mitochondrial import and assembly (MIA) machinery, constituted by Mia40 and Erv1 proteins, which catalyses the disulphide bonds formation for the maturation of the protein (Fig. 2, pathway 4) (Chacinska et al., 2004; Hell, 2008).

The import of OMM proteins is a heterogeneous combination of pathways dependent mostly on the final topology of the protein (Dukanovic et al., 2011; Wiedemann et al., 2017). OMM proteins can be embedded in the membrane as a β-barrel or via single or multiple α-helices (Ellenrieder et al., 2015). The targeting signal of β-barrel proteins consists of a hydrophobic β-hairpin, which is recognized by the Tom20 receptor allowing the translocation of the precursor through Tom40 (Jores et al., 2016). In the IMS, it interacts with the sTIMs chaperones, which guide it to the topogenesis of the OMM β-barrel proteins (TOB) complex. This complex is composed of the Tob55 central pore and two peripheral cytosolic proteins, Mas37 and Tob38, and it mediates the insertion of β-barrel proteins into the lipid bilayer (Fig. 2, pathway 2b) (Wiedemann et al., 2017).

5.7.1 Import of OMM α-helical proteins

Most OMM proteins are embedded in the membrane with α-helical TMSs, but they acquire various topologies. According to the number of TMSs, they can be defined as multispan or single-span proteins. The latter can be further divided in three groups: (i) signal-anchored proteins, which have the TMS at the N-terminus and a soluble domain facing the cytosol or the IMS, (ii) TA proteins, with the TMS at the C-terminus and an N-terminal cytosolic domain, and (iii) non-canonical TA proteins, which have an N-terminal cytosolic domain and an additional C-terminal soluble domain facing the IMS (Dukanovic et al., 2011; Ellenrieder et al., 2015). These diverse proteins follow a variety of import pathways.

To date, no import factor has been identified for the insertion of TA proteins into the OMM and none of the known import machineries is required for the biogenesis of TA proteins. In yeast cells, deletion of TOM or TOB subunits or the treatment of isolated organelles with external proteases did not affect the import of the TA protein Fis1 (Kemper et al., 2008). Similarly, in mammalian cells, the biogenesis of the TA proteins Bax, Bcl-XL and Omp25 was proposed to be independent of known import components (Horie et al., 2002; Setoguchi et al., 2006). Additionally, it has been shown that the membrane lipid composition affects the localization of Fis1 and Gem1; in particular these TA proteins insert preferentially in membranes with a low ergosterol content, like the OMM (Krumpe et al., 2012). Furthermore, it has been observed that Fis1 can spontaneously insert *in vitro* into liposomes, suggesting that TA proteins can insert in the OMM in an unassisted manner (Fig. 2, pathway 5) (Kemper et al., 2008). In contrast to this hypothesis, the small TOM subunits Tom5, Tom6 and Tom7 depend in yeast on the TOB and the mitochondria import (MIM) complexes. Moreover, in mammalian cells Tom5 import depends on Tom40 and VDAC2 affects the levels of Bak (Becker et al., 2008; Horie et al., 2002; Setoguchi et al., 2006; Stojanovski et al., 2007; Thornton et al., 2010).

The mechanism of import of non-canonical TA proteins is mainly unknown. It is clear that Tom22 and Mim1 follow unrelated import routes. Tom22 is imported via the TOM complex and subsequently inserted and assembled with the assistance of a sub-population of TOB complex, which is associated with the β-barrel protein Mdm10 (Dukanovic et al., 2009; Stojanovski et al., 2007; Thornton et al., 2010). In contrast, Mim1 interacts with the cytosolic Hsp40 co-chaperone Djp1 and probably with the Hsp70 chaperone. Subsequently, these cytosolic factors guide the precursor to the OMM where it is recognized by Tom70 and inserted into the membrane via a Tom40-independent mechanism, probably mediated by MIM complexes already present in the membrane (Papic et al., 2013).

Signal-anchored proteins are characterised by a short TMS with low hydrophobicity and positively charged residues at its extremities, which represents the targeting signal (Waizenegger et al., 2003). The import of Tom20 and Tom70 depends on the membrane embedded MIM complex for their integration into the OMM (Fig. 2, pathway 6) (Becker et al., 2008; Hulett et al., 2008; Popov-Celeketic et al., 2008). Interestingly, the signal-anchored protein Om45, which exposes the

soluble domain into the IMS, follows a unique import pathway. It first crosses the OMM through the TOM complex and then it is inserted into the membrane in a TIM23 and MIM-dependent manner (Song et al., 2014; Wenz et al., 2014).

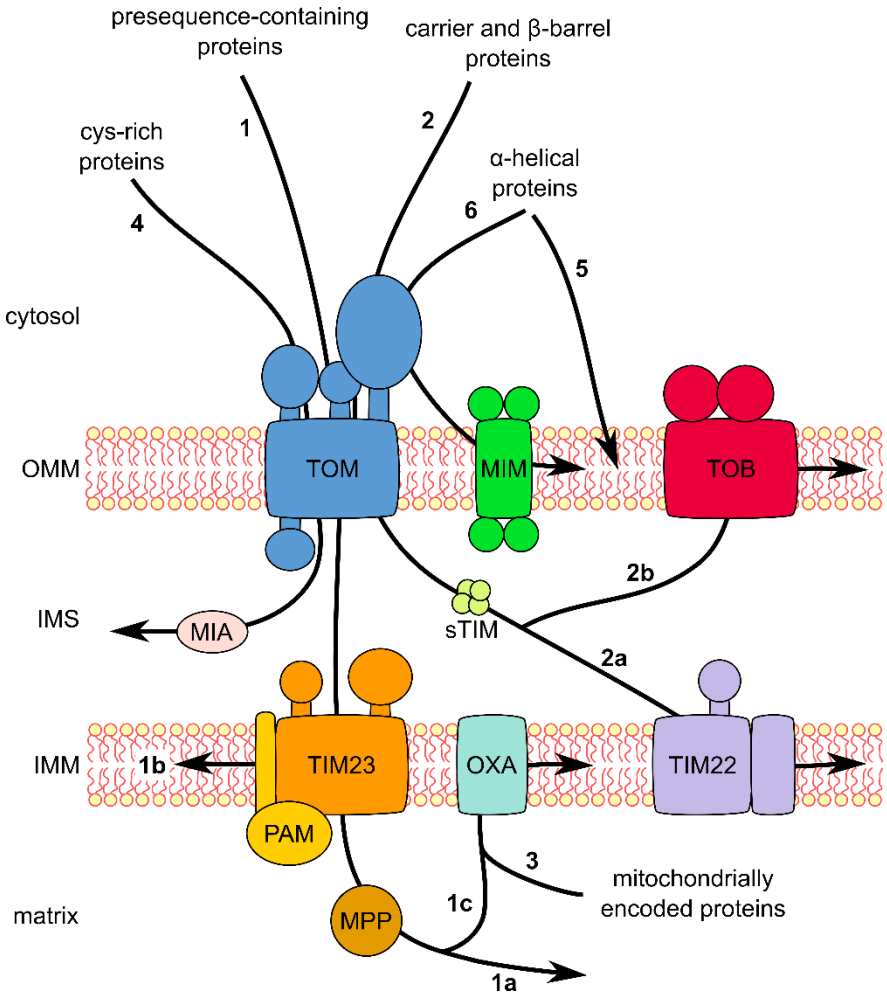

Figure 2. Mitochondrial protein import pathways. Proteins with a cleavable MTS are imported via the TOM and the TIM23 complexes and either released in the matrix **(1a)** or inserted into the IMM **(1b)**. Multispan proteins containing an MTS follow the same route but they are inserted into the IMM from the matrix side by OXA **(1c)**. Carrier proteins cross the OMM through the TOM pore, in the IMS they interact with the sTIM chaperones and then they are inserted into the IMM by the TIM22 complex **(2a)**. The import of β-barrel proteins requires also the TOM complex and the sTIM, but their insertion into the OMM is mediated by the TOB complex **(2b)**. Mitochondrially encoded proteins are inserted co-translationally into the IMM via OXA **(3)**. Cysteine-rich proteins reach the IMS via the TOM complex and their maturation via the formation of disulphide bonds is mediated by the MIA complex **(4)**. Some α-helical proteins (TA proteins) can insert spontaneously in the OMM **(5)**, while other (signal-anchored and multispan proteins) require the MIM complex **(6)**.

The import of multispan α-helical proteins into the OMM is also dependent on the MIM complex (Fig. 2, pathway 6). In particular, the precursor forms of Ugo1 and

Scm4 are recognized by Tom70 and subsequently transferred to the MIM complex for their insertion. Interestingly, the import of these proteins is independent of the TOM complex (Becker et al., 2011; Otera et al., 2007; Papic et al., 2011). An exception to this mechanism is the import of Mcp3, a protein with two predicted TMS and a cleavable presequence. This protein is recognized by Tom70 before it is translocated into the IMS through the Tom40 pore. Then, it interacts with the TIM23 complex and is processed by the inner membrane peptidase (IMP). At this point, the mature protein is inserted into the OMM, probably in a MIM-dependent manner (Sinzel et al., 2016).

5.7.2 The MIM complex

The MIM complex is an oligomeric complex of around 200 kDa with a crucial role in the biogenesis of α-helical OMM proteins. Although its stoichiometry is not defined yet, it has been suggested that it is composed of several molecules of Mim1 and one or two of Mim2 (Dimmer et al., 2012). Both proteins have a molecular weight of about 10-13 kDa, one putative TMS, and their N-terminus is facing the cytosol, while the C-terminus is in the IMS (Dimmer et al., 2012; Popov-Celeketic et al., 2008; Waizenegger et al., 2005). It has been recently reported that Mim1 alone or in combination with Mim2 can form a cation selective channel, suggesting that the TMSs of several copies of these proteins could organize in a pore-like structure (Krüger et al., 2017).

The MIM complex is required for the import of various α-helical OMM proteins, but the molecular mechanism of this process is not elucidated yet (Vögtle et al., 2015). Additionally, the MIM complex plays a crucial role in the assembly of the TOM complex (Becker et al., 2008; Dimmer et al., 2012; Hulett et al., 2008; Lueder et al., 2009). Given all the pivotal functions mediated by this complex, it is clear that the absence of one or both subunits of this complex leads to reduced substrates levels, hampered TOM complex assembly, and accumulation of mitochondrial precursor proteins in the cytosol. Subsequently, cells lacking this complex display a severe growth defect and altered mitochondria morphology (Dimmer et al., 2012; Ishikawa et al., 2004; Mnaimneh et al., 2004; Popov-Celeketic et al., 2008; Waizenegger et al., 2005).

Considering its relevant roles in mitochondrial protein biogenesis, it is surprising that Mim1 is conserved only in fungi, while no homologues were found in any other class, including higher eukaryotes (Waizenegger et al., 2005). Strikingly, sequence analysis revealed that the highest conservation among the fungal homologues is in the TMS, with two GXXXG(A) helix-dimerization motifs. In line with this observation, the functional part of Mim1 is the TMS, while the soluble domains are dispensable (Dimmer et al., 2012; Popov-Celeketic et al., 2008; Waizenegger et al., 2005). The lack of homologues in other eukaryotes raises the question how α-helical OMM proteins are imported in non-fungal organisms.

5.7.3 A putative functional orthologue of the MIM complex

The core components of the mitochondrial protein import machineries are conserved in all eukaryotes. In contrast, some additional subunits, which probably evolved later, are conserved only in some lineages (Dolezal et al., 2006). Even the parasitic protozoan *Trypanosoma brucei*, one of the earliest diverging eukaryotes with functional mitochondria, have a machinery similar to the yeast one. In this organism, the functional orthologue of the TOM complex is the archaic translocase of the outer membrane (ATOM) complex, which is constituted by the ATOM40 pore and the receptors ATOM14, ATOM11, ATOM12, ATOM46 and ATOM69. Of note, these proteins have no sequence similarities with yeast proteins, while ATOM40 and ATOM14 are only remote orthologues of the yeast Tom40 and Tom22, respectively. Despite the low similarity, ATOM mediates the import of a wide range of mitochondrial proteins suggesting a functional resemblance to the TOM complex in other eukaryotes (Pusnik et al., 2011).

Recently, the peripheral archaic translocase of the outer membrane 36 (pATOM36) protein of *T. brucei* was identified and characterized (Bruggisser et al., 2017; Harsman et al., 2017; Käser et al., 2016). This is a trypanosomatid specific integral OMM protein constituting a peripheral component of the ATOM complex. It has two predicted TMS, each containing a GXXXG(A) motif, and both the C- and the N-termini are proposed to face the cytosol. (Pusnik et al., 2012). Similar to the MIM complex, pATOM36 is required for the import of some OMM proteins and for the assembly of the ATOM components. Moreover, its depletion causes growth defect and alteration of mitochondrial morphology (Bruggisser et al., 2017; Pusnik

et al., 2012). Additionally, pATOM36 has a role in segregation of the mitochondrial genome, known as kinetoplast DNA (kDNA) in trypanosomes (Jensen et al., 2012). The kDNA is a single DNA unit connected to the cytosolic basal body via the tripartite attachment complex (TAC) and it has been shown that a part of pATOM36 molecules localizes with this complex (Käser et al., 2016). Given all the similarities with the yeast MIM proteins, it has been proposed that pATOM36 could be a functional orthologue of the MIM complex in Trypanosomatids (Bruggisser et al., 2017). However, this hypothesis was not tested experimentally.

6. Research objectives

The sort and assembly of membrane proteins in eukaryotic cells are crucial processes required to preserve many cellular functions. The specific targeting of such proteins to their correct compartments has to be finely regulated because in the crowded cytosolic environment the nascent proteins have to be examined by several factors and recognized by the ones that will lead them to their destined location. A multitude of targeting pathways has been characterized but many open questions remain. What is still not clear is how the different targeting machineries interplay in order to minimize protein mistargeting. Moreover, it is still unknown how TA proteins are targeted and inserted into the OMM. Additionally, the molecular mechanism by which the MIM complex mediates the insertion and assembly of various α-helical proteins is still unknown.

The main questions I addressed in this study are:

1. How is the targeting of TA proteins regulated between ER and mitochondria?

   In the article “The GET pathway can increase the risk of mitochondrial outer membrane proteins to be mistargeted to the ER” (Vitali et al., *J. Cell Science*, 2018) I investigated the effect of the GET machinery on the mistargeting of mitochondrial proteins to the ER.

2. How are the functions of the MIM complex fulfilled in non-fungi organisms?

   Reciprocal complementation experiments of Mim1/Mim2 and pATOM36 proteins in *S. cerevisiae* and *T. brucei* were performed in the article “Independent evolution of functionally exchangeable mitochondrial outer membrane import complexes” (Vitali et al., *eLife*, 2018).

7. Summary of the results

7.1 The GET pathway can increase the risk of mitochondrial outer membrane proteins to be mistargeted to the ER (Vitali et al., *Journal of Cell Science*, 2018)

The TA proteins targeting signal similarity between ER and mitochondria is one of the reasons for a high risk of protein mistargeting to the incorrect organelle. However, the mechanisms that dictate the accurate targeting of TA proteins towards ER or mitochondria are still unknown (Chio et al., 2017a; Costello et al., 2017; Rao et al., 2016).

In this study, we investigated the mislocalization of mitochondrial TA proteins to the ER due to inefficient or saturated mitochondrial targeting. To that aim, we examined three proteins that, according to their topology, could be potential substrates of the GET machinery.

The first protein we analysed was the mammalian TA protein cytochrome b5 (Fig. 1A). This protein has two isoforms with around 60% of sequence identity in the cytosolic domain that are localized in either the ER (b5-ER) or the OMM (b5-OM) (D'Arrigo et al., 1993). Their specific targeting is mediated by the C-terminal region, which is negatively charged in the ER isoform and mostly positively charged in the mitochondrial one (De Silvestris et al., 1995). In fact, the replacement of the C-terminal polar peptide of the ER protein (RLYMADD) with two arginine residues re-directs it to mitochondria (b5-RR) (Borgese et al., 2001) (Fig. 1A).

To gain insights into the mechanism that regulate the targeting of the two isoforms into their specific locations, we expressed the HA-tagged rabbit b5-ER and b5-RR proteins in yeast cells and analysed their localization by subcellular fractionation. We determined that, as expected, the b5-ER isoform is mainly localized in the ER (Fig. 1B). However, the b5-RR was surprisingly equally distributed between ER and mitochondria (Fig. 1C), suggesting that the targeting of mitochondrial TA proteins is not completely conserved between yeast and higher eukaryotes. Moreover, we observed that part of the b5-RR in the ER fraction migrated on SDS-PAGE slower than expected (Fig. 1C), indicating that it was subjected to post-translational modifications. To characterise the topology of the two

forms of b5-RR, we treated isolated microsomes with proteinase K (PK) and performed alkaline extraction (Fig. 1D-E). These experiments demonstrated that both the native and the modified b5-RR forms are membrane embedded, while only the native one has the typical TA orientation with the N-terminal domain exposed to the cytosol. In contrast, the modified protein was PK-protected, suggesting that the soluble domain was facing the ER lumen. This observation indicates that the N-terminal domain of the protein could be subjected to post-translational modification(s). Indeed, bioinformatics predictions allowed us to identify Asp21 as a potential glycosylation site (Fig. 1A). This prediction was confirmed by EndoH and PNGase treatment (Fig. 1F). In conclusion, the mitochondrial b5-RR version is partially mistargeted in yeast to the ER and is inserted either with the native topology or in an inverted orientation, which exposes a glycosylation site to the ER lumen.

Subsequently, we investigated whether the GET pathway mediates the targeting of the mislocalized b5-RR protein to the ER. Subcellular fractionation of cells lacking Get1 or Get3 showed a reduction of b5-RR levels in the microsomes fraction, indicating that the GET machinery is involved in the mistargeting (Fig. 1G-H). Nevertheless, around 40% of the protein was still in the ER implying that the GET system is not the only pathway involved in directing the cytochrome b5 to the ER.

The second protein we studied was Mcp3, an OMM protein with an MTS and two TMSs (Fig. 2A). The addition of an N-terminal GFP tag leads to a partial mislocalization of this protein to the ER probably because the presequence is masked by the tag (Fig. 2B). To obtain information about the membrane insertion of this protein, we performed alkaline extraction treatment, which demonstrated that GFP-Mcp3 is embedded in both the OMM and ER membrane (Fig. 2C). The presence of one TMS close to the C-terminus suggests a possible involvement of the GET pathway in directing GFP-Mcp3 to the ER. Indeed, fluorescence microscopy showed that this protein is mostly localized to the ER in WT cells, while the deletion of *GET3* alone, both *GET1* and *GET2*, or the triple deletion of *GET1/2/3*, drastically reduced the levels of GFP-Mcp3 in the ER and leaded to its correct targeting to mitochondria (Fig. 2D-E).

To confirm the effect of the GET machinery on the mistargeting of GFP-Mcp3 to the ER, we performed subcellular fractionation with the same strains employed in

the microscopy experiments and observed that upon deletion of the GET components, GFP-Mcp3 levels increased in the mitochondrial fraction (Fig. 2F-H). However, a fraction of the protein remained localized to the ER in the deleted strains suggesting the existence of some ER targeting pathways that are GET-independent. To confirm that the mistargeting of Mcp3 to the ER is due to the interference of the GFP-tag with the MTS, we analysed the localization of a construct lacking the presequence (GFP-Mcp3ΔN). Using fluorescence microscopy, we verified that this variant was also targeted to the ER in a GET-dependent manner. However, this truncated protein was not re-directed to mitochondria upon deletion of the GET components, but was evenly distributed in the cytosol or localized in puncta structures, which could represent aggregated particles (Fig. S1).

Finally, we examined Mim1, a mitochondrial non-canonical TA protein, with a single TMS in its centre (Fig. 3A). When an N-terminal GFP tagged version was overexpressed, this variant was partially mistargeted to the ER, as determined by subcellular fractionation (Fig. 3B). Furthermore, alkaline extraction assay demonstrated that this protein is membrane embedded both in the ER and in the mitochondrial fractions (Fig. 3C-D). Although Mim1 is not an optimal GET substrate, we investigated whether this machinery could lead to its mistargeting to the ER. First, we assessed by fluorescence microscopy the localization of GFP-Mim1 in WT cells or in cells lacking either Get1 or Get3. It was possible to observe a GFP signal in the ER of about 20% of WT cells, while this localization was significantly decreased in GET mutants (Fig. 3E-F).

Subcellular fractionation of these strains confirmed a reduction of the ER levels of GFP-Mim1 in the absence of the GET components (Fig. 3G-I). However, a portion of the protein was still present in the ER fraction of the mutant strains, suggesting the existence of GET-independent pathways. To exclude the possibility that the mistargeting of Mim1 depends on the GFP-tag, we tested a construct with the tag at the C-terminus and another one without any tag. Subcellular fractionation experiments showed that both constructs were mainly localized in mitochondria and only partially mislocalized in the ER (Fig. S2A-B). Moreover, the mistargeting was not affected by the deletion of *GET3*, confirming that Mim1 is not an ideal substrate for this machinery, especially in the constructs where the TMS is more towards the N-terminus of the protein. Interestingly, we observed that the non-tagged Mim1 was

modified in the ER of WT cells and not in *get3Δ* cells (Fig. S2B). This modification is not glycosylation, as indicated by PNGase treatment (Fig. S2C), and it is not clear why it is not observed in the *get3Δ* strain.

To further demonstrate that the GET machinery has a direct effect on mistargeting of the aforementioned mitochondrial proteins, we investigated the interaction of Get3 with these substrates. HA-Mim1, HA-Mcp3ΔN and the cytosolic protein DHFR-HA, serving as negative control, were translated *in vitro* in rabbit reticulocyte lysate. Next, the proteins were incubated with either the recombinant His-tagged Get3 or its ATP hydrolysis-defective mutant (D57N), which does not release the substrate (Chio et al., 2017b), followed by pulldown with anti-HA beads (Fig. 4A-B). This revealed a weak interaction of the native Get3 and a stronger association of the mutant protein with HA-Mim1 and HA-Mcp3ΔN, while no binding was observed with DHFR-HA. The interaction of Get3 and Mcp3 was confirmed *in vivo* by a cytosolic Split-Ubiquitin assay performed in collaboration with the Grefen's group (Fig. 4C).

In conclusion, these findings demonstrate that the GET machinery potentially could bind also mitochondrial proteins. This suggests that in normal condition the pathways leading to the two organelles are competing for the substrates and that the mitochondria targeting, although not identified yet, is faster and more efficient. Our data indicate additionally that the GET pathway is not the only route mediating mislocalization of mitochondrial proteins. Furthermore, we could demonstrate that this ER targeting machinery, commonly considered to direct only TA proteins, can recognize also proteins with a different topology.

7.2 Independent evolution of functionally exchangeable mitochondrial outer membrane import complexes (Vitali et al., *eLIFE*, 2018)

Our knowledge about the import of α-helical OMM proteins is still limited. To date, it has been reported that in *S. cerevisiae* both multispan and signal-anchored proteins requires the MIM complex (Becker et al., 2011; Papic et al., 2011; Waizenegger et al., 2005). The structure and the molecular mechanism of action of this complex are still unknown (Dimmer et al., 2012). Nevertheless, the MIM complex has been reported to affect mitochondrial proteins import, assembly of the

TOM complex, mitochondria morphology regulation, and cell viability. What is striking is the absence of a homologue in non-fungi organisms (Dimmer et al., 2012; Mnaimneh et al., 2004; Popov-Celeketic et al., 2008; Waizenegger et al., 2005).

Recently, it has been described that the *T. brucei* protein pATOM36 seems to be involved in similar functions. Hence, it has been proposed that this protein could be a functional analogue of the MIM complex, although no sequence or structural similarity could be identified (Bruggisser et al., 2017; Käser et al., 2016; Pusnik et al., 2012). In fact, the MIM subunits, Mim1 and Mim2, have a single TMS in the central region, with the C-terminal facing the IMS, while pATOM36 has two predicted TMS and the C-terminus is proposed to be in the cytosolic side. The only similarity between these proteins is the presence of GXXXG(A) motifs in their TMSs, although such a motif is frequently identified in TMSs (Teese et al., 2015) (Fig. 1 - Sup. 1).

To test whether pATOM36 and the MIM complex fulfil the same molecular functions, we analysed the ability of the trypanosomal protein to rescue the defects of yeast cells lacking Mim1, Mim2, or both. Therefore, we expressed pATOM36 with or without a C-terminal HA tag in WT cells or in cells lacking one or both the MIM subunits and verified its expression in all the strains (Fig. 1 - Sup. 2). Next, we confirmed, by PK treatment and carbonate extraction, that pATOM36-HA was embedded in the OMM with its C-terminus facing the cytosol (Fig. 1A). In trypanosoma, pATOM36 is organized in two types of high molecular weight complexes, one of approximately 140-250 kDa and another one that is larger than 480 kDa. The composition of the smaller structure is unknown, while the largest one corresponds to the population of pATOM36 associated with the TAC complex, required for maintaining the kDNA (Käser et al., 2016). To confirm whether pATOM36 could oligomerize into the same complexes also in yeast cells, we performed blue native (BN)-PAGE analysis. This analysis showed that in WT and *mim1Δmim2Δ* cells, pATOM36 formed complexes of 140-250 kDa, while the higher molecular weight structure is absent (Fig. 1B).

The confirmation that pATOM36 localization, topology and complex organization in yeast was the same as in *T. brucei* led us to investigate whether it could rescue the phenotypes resulting from the loss of the MIM complex. We analysed, by drop dilution assay, cells growth on respiratory carbon source, a

condition that is compromised in cells lacking a functional MIM complex (Dimmer et al., 2012; Mnaimneh et al., 2004). The outcome of this assay indicated that *mim1Δ* or *mim2Δ* cells expressing pATOM36 with or without HA-tag grow as good as cells complemented with the corresponding MIM protein (Fig. 2A). Moreover, we could show that the trypanosomal protein can rescue also the growth defect of cells lacking both MIM subunits (Fig. 2B and Fig. 2 - Sup. 1), demonstrating that it can complement the defects in a MIM-independent manner.

Due to its role in mitochondrial protein import, the absence of Mim1 and/or Mim2 leads to reduced steady-state levels of MIM substrates such as Tom20, Tom70, and Ugo1 (Dimmer et al., 2012; Popov-Celeketic et al., 2008; Waizenegger et al., 2005). Therefore, we investigated the effect of pATOM36 on the levels of such MIM substrates. Immunodecoration of isolated mitochondria demonstrated that the expression of pATOM36-HA could significantly restore the levels of Tom20 and Tom70 in *mim1Δmim2Δ* cells (Fig. 3A-B). Interestingly, pATOM36 did not affect the levels of the multispan protein Ugo1, indicating a preference towards some MIM substrates. As a control, we verified that the expression of the trypanosomal protein in WT cells influenced only marginally, if at all, the levels of the analysed proteins (Fig. 3A-B).

The loss of Mim1 and Mim2 impairs the TOM complex assembly consequently leading to the accumulation of mitochondrial precursor proteins, such as the mitochondrial Hsp60 (Ishikawa et al., 2004; Mnaimneh et al., 2004; Waizenegger et al., 2005). To investigate whether pATOM36 can rescue this phenotype, we analysed whole cell lysate of cells lacking one or both MIM subunits and expressing either pATOM36-HA or an empty plasmid as control (Fig. 3C). Our findings showed that the precursor of the mitochondrial Hsp60 completely disappeared upon expression of pATOM36-HA, suggesting the proper assembly of the TOM complex.

To confirm that pATOM36 can restore the TOM complex assembly in cells lacking the MIM complex, we analysed isolated mitochondria by BN-PAGE. Immunodecoration with antibodies against Tom40 and Tom22 revealed that the expression of pATOM36 restored the assembly of the TOM complex in *mim1Δmim2Δ* cells, while it did not affect it in WT cells (Fig. 3D). To ascertain that the complementation by pATOM36 is MIM-specific, we investigated its effects in

rescuing the loss of another OMM import factor. Therefore, we expressed pATOM36 in cells lacking Mas37, a subunit of the TOB complex, which is required for the biogenesis of β-barrel proteins and of Tom22 (Dukanovic et al., 2009; Stojanovski et al., 2007; Thornton et al., 2010). The deletion of *MAS37* causes an altered TOB complex assembly and reduced levels of its substrates. BN-PAGE and immunostaining with antibody against Tob55 showed that the expression of pATOM36 does not rescue the defect in the assembly of the TOB complex in *mas37Δ* cells (Fig. 3 - Sup. 1A). Moreover, the steady state levels of TOB substrates, such as Porin, Tom40, and Tom22, are not affected by the presence of the trypanosomal protein (Fig. 3 - Sup. 1B).

It has been suggested that the import of multispan OMM proteins requires the receptor Tom70, which cooperates with Mim1 (Becker et al., 2011; Papic et al., 2011). To investigate the relationship between pATOM36 and Tom70, we incubated *in vitro* synthesized radiolabelled pATOM36 or Mim1 with a recombinant fusion protein of the cytosolic domain of Tom70 with GST. The subsequent anti-GST pulldown revealed a specific binding of the radiolabelled proteins (Fig. 3E). This indicates that pATOM36 can cooperate with Tom70 during the import of α-helical OMM proteins. However, we cannot exclude the possibility that the Tom70 receptor can recognize Mim1 and pATOM36 as substrates rather that interaction partners.

Given that pATOM36 can compensate the loss of the MIM complex, we decided to investigate the direct role of pATOM36 in protein import. Hence, we performed *in vitro* import assay of the MIM substrates into isolated mitochondria. These experiments demonstrated that the presence of pATOM36 could improve the import and the assembly of Tom20 into mitochondria (Fig. 4A-B). In line with the steady state levels analysis, the import of Ugo1 was not rescued by the expression of pATOM36 (Fig. 4C). As controls, we performed *in vitro* import experiments of Fis1 and pSu9-DHFR, which are not impaired by the deletion of *MIM1* and *MIM2*. As expected the import of these proteins was not influenced by the presence of pATOM36 (Fig. 4D-E).

At last, we analysed the effect of the trypanosomal protein on the mitochondrial morphology alterations that are observed upon loss of Mim1 and Mim2. Fluorescence microscopy analysis revealed that pATOM36 could rescue the

mitochondrial fragmentation of cells lacking one or both MIM subunits, thus leading to tubular structures similar to WT cells (Fig. 5A-B).

In conclusion, our data indicated that pATOM36 could complement the defects in yeast cells resulted from the loss of the MIM complex.

To investigate the role of the yeast proteins in complementing the phenotypes derived from the lack of pATOM36, the Schneider's lab performed reciprocal experiments in *T. brucei* (Fig. 6-8).

8. Discussion

8.1 The GET pathway can increase the risk of mitochondrial outer membrane proteins to be mistargeted to the ER

The targeting of TA proteins to the destined organelle is one of the less characterized protein sorting mechanisms. While the pathway guiding these proteins to the ER via the GET machinery is well defined, the route directing these proteins to mitochondria is still unknown (Chio et al., 2017a). It is puzzling how the nascent protein is recognized by the correct pathway, leading it to the target organelle. In this study, we suggest that there is a kinetic competition between ER and mitochondrial targeting pathways. In normal conditions, the latter is more efficient, while when it is impaired the TA proteins have more chances to be recognized by the ER pathway (Fig. 3).

Often, the TA proteins targeting signal is not conserved between yeast and higher eukaryotes. For example, PTP1B and Bcl2, are localized in mammalian cells in ER and mitochondria, while they are exclusively localized in ER when expressed in yeast (Egan et al., 1999; Fueller et al., 2015). This is in line with our observation that expression of b5-RR in yeast leads to an even distribution of the protein between ER and mitochondria, while in mammalian cells, this isoform is exclusively localized in mitochondria (Figueiredo Costa et al., 2018). Therefore, either the b5-RR is not an optimal substrate for the yet unknown yeast mitochondrial targeting factors, or this protein, in contrast to the yeast mitochondrial TA proteins, does not have the ability to insert spontaneously into the OMM.

Our data show that the yeast GET machinery could partially direct b5-RR to the ER. This rather partial dependence on the GET components is consistent with a recent report that the GET machinery uses multiple selection filters to guarantee the correct targeting (Rao et al., 2016). Moreover, it suggests that ER alternative pathways, such as the SND and/or the SRP, exist and can compensate the absence of the GET machinery (Aviram et al., 2016; Casson et al., 2017). However, we cannot exclude the possibility that the b5-RR could insert into the membrane in an unassisted manner. In fact, it has been reported that the b5-ER isoform can insert in cholesterol-poor liposomes *in vitro* and that depletion of ER membrane translocation components does not interfere with its import (Brambillasca et al.,

2005). The presence of additional import machineries is also suggested by the observation that a portion of the b5-RR molecules that are mistargeted to the ER is inserted with the N-terminal domain in the lumen. In fact, it has been demonstrated that the SRP and the Sec61 translocon could mediate the targeting of b5 and other TA proteins to the ER (Casson et al., 2017; Haßdenteufel et al., 2017). These elements can insert, in principle, part of the b5-RR molecules with an inverted topology.

Our data regarding the cell sorting of Mcp3 and Mim1 also corroborated the hypothesis of a kinetic competition between ER and OMM targeting agents. In fact, the addition of a large tag as GFP at the N-terminus of Mcp3 probably masks its MTS resulting in a slower recognition by the mitochondrial import machinery. Hence, the GET machinery has a chance to bind the C-terminal TMS, which makes Mcp3 resemble a TA protein. Similarly, the overexpression of Mim1 could saturate the mitochondrial import pathway, allowing the GET components to redirect it to the ER. At a first glance, the dependence of Mim1 on the GET machinery could be surprising, since it is a non-canonical TA protein with the TMS in the central region. However, the insertion of a GFP-tag at the N-terminus of the protein moves the relative position of the TMS towards the C-terminal. Accordingly, when the tag was removed or placed at the C-terminus, the GET components did not have any effect on the protein localization. Moreover, the presence of residual proteins in the ER fraction confirmed the existence of alternative pathways directing such proteins to the ER.

In conclusion, we could demonstrate that the GET pathway does not recognize exclusively ER TA-proteins, but also binds mitochondrial ones. However, this interaction is probably slower and less efficient than the mitochondrial targeting pathway and it becomes significant only when the latter is impaired (Fig. 3). These observations shed light on the intracellular sorting of TA proteins, suggesting that a kinetic competition between the targeting pathways dictates the localization of these proteins. Moreover, these results corroborate the developing idea that the ER-delivery routes for TA proteins are partially overlapping and shading each other, and explain the broad range of physicochemical properties of the TMS with no distinct organelle-specific pattern.

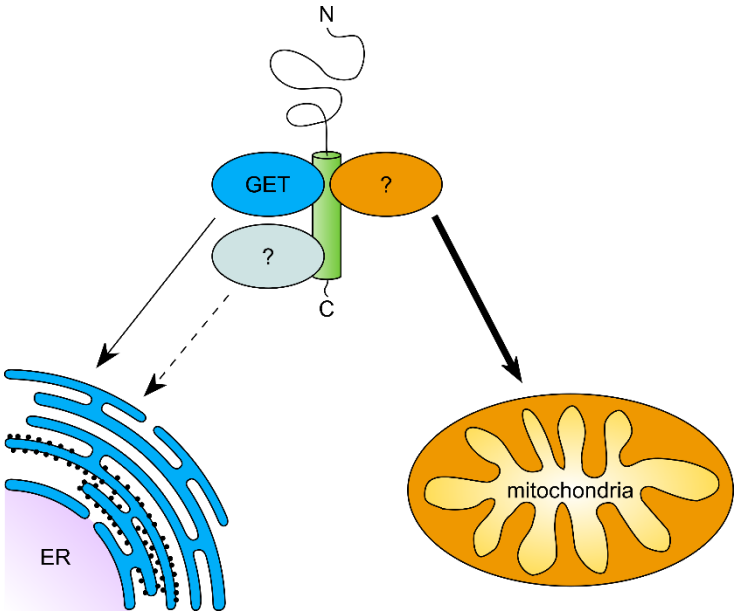

Figure 3. Working model for the kinetic competition between various targeting pathways. Newly synthesized mitochondrial TA proteins can interact in the cytosol with factors targeting to ER or to mitochondria. Under physiological conditions, the yet unknown mitochondrial pathway (orange) leads TA proteins to the OMM in a very efficient and fast way. However, when this route is impaired the GET machinery (dark blue) and/or an alternative pathway (light blue) can redirect mitochondrial TA proteins to the ER.

8.2 Independent evolution of functionally exchangeable mitochondrial outer membrane import complexes

The absence in non-fungi organisms of a homologue of such an important factor as the MIM complex has always been puzzling. Although α-helical proteins are localized in OMM of other eukaryotes, it is unknown which factors mediate their targeting and insertion. In our study, we demonstrated that the trypanosomal pATOM36 and the yeast MIM complex can reciprocally complement each other and thus have probably the same function. This is surprising, since these proteins do not share any sequence similarity, membrane topology or size. Furthermore, pATOM36 has the dual function to mediate protein import and assembly and to regulate mitochondrial DNA inheritance (Käser et al., 2016). As expected, the MIM complex could not rescue the latter role because it does not mediate this activity in yeast.

Since yeast and trypanosomes belongs to two unrelated supergroups, it is interesting that Mim1/2 and pATOM36 reciprocally complement each other. In fact,

yeast belongs to the eukaryotic super-group of Opisthokonts while trypanosomes to the Excavates, and both super-groups separated very early during eukaryotes evolution (Burki, 2014). This suggests that the two proteins evolved independently, after the two super-groups were established. Moreover, since the MIM complex is conserved only in fungi, we hypothesize that it evolved after fungi and metazoans diverged. The OMM protein import machineries of the last eukaryotic common ancestor (LECA) were simpler than the ones of the present organisms, presumably constituted only by their core components. In fact, the TOB complex pore, Tob55, is conserved in all eukaryotes and it could mediate the import of β-barrel proteins (Dolezal et al., 2006; Mani et al., 2016). Moreover, while Tom40 is conserved in all eukaryotes, the TOM receptors are unrelated in yeast, trypanosomes, and plants, organisms belonging to three distinct super-groups (Mani et al., 2015). This observation suggests that they evolved independently to increase specificity and efficiency of the import process (Mani et al., 2016). Hence, we can hypothesize that the appearance of α-helical membrane receptors required the evolution of import and assembly systems, such as the MIM complex and pATOM36.

Interestingly, pATOM36 expressed in yeast had a different rescue effect on different MIM substrates. In fact, the import of the mitochondrial fusion protein Ugo1 was not complemented. This can be explained by the fact that Ugo1 is a multispan carrier-like protein that has no clear homologues in higher eukaryotes (Coonrod et al., 2007; van der Bliek et al., 2013). Hence, we can speculate that pATOM36 has no similar substrates in the OMM of *T. brucei.*

The composition of the MIM complex and of the pATOM36-containing complex is still unknown (Dimmer et al., 2012; Pusnik et al., 2012). However, our observation that in the heterologous system these proteins can organize in complexes of similar size as in their respective organism, suggest that these structures do not contain any additional protein. Moreover, the reciprocal complementation experiments indicate that the MIM complex and pATOM36 do not need other factors for their activity.

The structure of these complexes is also poorly characterized. Mim1/2 and pATOM36 are dissimilar in their sequence or membrane topology. Mim1 and Mim2 have a single TMS with the C-terminus facing the IMS, whereas the topology of pATOM36 is not defined. It was reported that the C-terminus is in the cytosolic side,

while it has been predicted that the protein could have one, two or three TMSs (Pusnik et al., 2012). The only feature shared between the yeast and trypanosomal proteins is the presence of GXXXG(A) motifs in the putative TMSs (Käser et al., 2016). These motifs usually mediates the interaction between α-helices, reinforcing the idea that these proteins are organized in oligomeric structures (Teese et al., 2015). Moreover, it has been recently reported that Mim1 alone or in combination with Mim2 forms a cation-selective channel (Krüger et al., 2017). Therefore, it has been proposed that the α-helices form a pore-like structure in the MIM complex. It is tempting to speculate that pATOM36 organizes also in a similar structure, hence having the same molecular mechanism of function. However, we cannot exclude the possibility that the trypanosomal protein evolved with a different structure and mechanism of action for carrying the same functions.

Currently, it is widely accepted that both the MIM complex and pATOM36 are required for the assembly of the TOM/ATOM complex subunits and for the membrane insertion of some proteins (Becker et al., 2008; Becker et al., 2011; Dimmer et al., 2012; Hulett et al., 2008; Käser et al., 2016; Lueder et al., 2009; Papic et al., 2011; Thornton et al., 2010; Waizenegger et al., 2005). However, it has still to be elucidated whether these complexes mediates directly the import into the membrane or whether they form microdomains in the lipid bilayer that facilitates the integration of α-helical TMS. Nevertheless, we hypothesize that the two oligomers would act in the same manner.

In conclusion, our study revealed that the functions mediated by the MIM complex in yeast and by pATOM36 in trypanosoma evolved independently. This suggests that possible alternative factors could evolve in other eukaryotes, including metazoans. Comparative studies of the common fundamental features of the two complexes will shed light on their mechanism of action and on the evolution of the mitochondria import factors.

9. References

Araki, K., and K. Nagata. 2011. Protein folding and quality control in the ER. *Cold Spring Harb Perspect Biol*. 3:a007526.

Aviram, N., T. Ast, E.A. Costa, E.C. Arakel, S.G. Chuartzman, C.H. Jan, S. Haßdenteufel, J. Dudek, M. Jung, S. Schorr, R. Zimmermann, B. Schwappach, J.S. Weissman, and M. Schuldiner. 2016. The SND proteins constitute an alternative targeting route to the endoplasmic reticulum. *Nature*. 540:134-138.

Becker, T., S. Pfannschmidt, B. Guiard, D. Stojanovski, D. Milenkovic, S. Kutik, N. Pfanner, C. Meisinger, and N. Wiedemann. 2008. Biogenesis of the mitochondrial TOM complex: Mim1 promotes insertion and assembly of signal-anchored receptors. *J Biol Chem*. 283:120-127.

Becker, T., L.S. Wenz, V. Krüger, W. Lehmann, J.M. Müller, L. Goroncy, N. Zufall, T. Lithgow, B. Guiard, A. Chacinska, R. Wagner, C. Meisinger, and N. Pfanner. 2011. The mitochondrial import protein Mim1 promotes biogenesis of multispanning outer membrane proteins. *J Cell Biol*. 194:387-395.

Beilharz, T., B. Egan, P.A. Silver, K. Hofmann, and T. Lithgow. 2003. Bipartite signals mediate subcellular targeting of tail-anchored membrane proteins in Saccharomyces cerevisiae. *J Biol Chem*. 278:8219-8223.

Bellucci, M., F. De Marchis, and A. Pompa. 2017. The endoplasmic reticulum is a hub to sort proteins toward unconventional traffic pathways and endosymbiotic organelles. *J Exp Bot*. 69:7-20.

Benham, A.M. 2012. Protein secretion and the endoplasmic reticulum. *Cold Spring Harb Perspect Biol*. 4:a012872.

Bohnert, M., P. Rehling, B. Guiard, J.M. Herrmann, N. Pfanner, and M. van der Laan. 2010. Cooperation of Stop-Transfer and Conservative Sorting Mechanisms in Mitochondrial Protein Transport. *Current Biology*. 20:1227-1232.

Borgese, N., and E. Fasana. 2011. Targeting pathways of C-tail-anchored proteins. *Biochim Biophys Acta*. 1808:937-946.

Borgese, N., I. Gazzoni, M. Barberi, S. Colombo, and E. Pedrazzini. 2001. Targeting of a tail-anchored protein to endoplasmic reticulum and mitochondrial outer

membrane by independent but competing pathways. *Mol. Biol. Cell*. 12:2482-2496.

Bozkurt, G., G. Stjepanovic, F. Vilardi, S. Amlacher, K. Wild, G. Bange, V. Favaloro, K. Rippe, E. Hurt, B. Dobberstein, and I. Sinning. 2009. Structural insights into tail-anchored protein binding and membrane insertion by Get3. *Proc Natl Acad Sci U S A*. 106:21131-21136.

Braakman, I., and N.J. Bulleid. 2011. Protein folding and modification in the mammalian endoplasmic reticulum. *Annu Rev Biochem*. 80:71-99.

Brambillasca, S., M. Yabal, M. Makarow, and N. Borgese. 2006. Unassisted translocation of large polypeptide domains across phospholipid bilayers. *J Cell Biol*. 175:767-777.

Brambillasca, S., M. Yabal, P. Soffientini, S. Stefanovic, M. Makarow, R.S. Hegde, and N. Borgese. 2005. Transmembrane topogenesis of a tail-anchored protein is modulated by membrane lipid composition. *Embo j*. 24:2533-2542.

Breslow, D.K., and J.S. Weissman. 2010. Membranes in balance: mechanisms of sphingolipid homeostasis. *Mol Cell*. 40:267-279.

Bruggisser, J., S. Käser, J. Mani, and A. Schneider. 2017. Biogenesis of a Mitochondrial Outer Membrane Protein in Trypanosoma brucei: TARGETING SIGNAL AND DEPENDENCE ON A UNIQUE BIOGENESIS FACTOR. *J Biol Chem*. 292:3400-3410.

Burki, F. 2014. The eukaryotic tree of life from a global phylogenomic perspective. *Cold Spring Harb Perspect Biol*. 6:a016147.

Casson, J., M. McKenna, S. Haßdenteufel, N. Aviram, R. Zimmerman, and S. High. 2017. Multiple pathways facilitate the biogenesis of mammalian tail-anchored proteins. *J Cell Sci*. 130:3851-3861.

Chacinska, A., C.M. Koehler, D. Milenkovic, T. Lithgow, and N. Pfanner. 2009. Importing mitochondrial proteins: machineries and mechanisms. *Cell*. 138:628-644.

Chacinska, A., M. Lind, A.E. Frazier, J. Dudek, C. Meisinger, A. Geissler, A. Sickmann, H.E. Meyer, K.N. Truscott, B. Guiard, N. Pfanner, and P. Rehling. 2005. Mitochondrial presequence translocase: switching between TOM tethering and motor recruitment involves Tim21 and Tim17. *Cell*. 120:817-829.

Chacinska, A., S. Pfannschmidt, N. Wiedemann, V. Kozjak, L.K. Sanjuan Szklarz, A. Schulze-Specking, K.N. Truscott, B. Guiard, C. Meisinger, and N. Pfanner. 2004. Essential role of Mia40 in import and assembly of mitochondrial intermembrane space proteins. *Embo j*. 23:3735-3746.

Chartron, J.W., W.M. Clemons, Jr., and C.J. Suloway. 2012. The complex process of GETting tail-anchored membrane proteins to the ER. *Curr Opin Struct Biol*. 22:217-224.

Chartron, J.W., C.J. Suloway, M. Zaslaver, and W.M. Clemons, Jr. 2010. Structural characterization of the Get4/Get5 complex and its interaction with Get3. *Proc Natl Acad Sci U S A*. 107:12127-12132.

Chio, U.S., H. Cho, and S.O. Shan. 2017a. Mechanisms of Tail-Anchored Membrane Protein Targeting and Insertion. *Annu Rev Cell Dev Biol*. 33:417-438.

Chio, U.S., S. Chung, S. Weiss, and S.O. Shan. 2017b. A protean clamp guides membrane targeting of tail-anchored proteins. *Proc Natl Acad Sci U S A*. 114:E8585-E8594.

Colombo, S.F., R. Longhi, and N. Borgese. 2009. The role of cytosolic proteins in the insertion of tail-anchored proteins into phospholipid bilayers. *J Cell Sci*. 122:2383-2392.

Coonrod, E.M., M.A. Karren, and J.M. Shaw. 2007. Ugo1p is a multipass transmembrane protein with a single carrier domain required for mitochondrial fusion. *Traffic*. 8:500-511.

Costello, J.L., I.G. Castro, F. Camoes, T.A. Schrader, D. McNeall, J. Yang, E.A. Giannopoulou, S. Gomes, V. Pogenberg, N.A. Bonekamp, D. Ribeiro, M. Wilmanns, G. Jedd, M. Islinger, and M. Schrader. 2017. Predicting the targeting of tail-anchored proteins to subcellular compartments in mammalian cells. *J Cell Sci*. 130:1675-1687.

D'Arrigo, A., E. Manera, R. Longhi, and N. Borgese. 1993. The specific subcellular localization of two isoforms of cytochrome b5 suggests novel targeting pathways. *J Biol Chem*. 268:2802-2808.

De Silvestris, M., D.A. Antonello, and B. Nica. 1995. The targeting information of the mitochondrial outer membrane isoform of cytochrome b5 is contained within the carboxyl-terminal region. *FEBS Letters*. 370:69-74.

Denic, V., V. Dötsch, and I. Sinning. 2013. Endoplasmic reticulum targeting and insertion of tail-anchored membrane proteins by the GET pathway. *Cold Spring Harb Perspect Biol*. 5:a013334.

Dimmer, K.S., D. Papic, B. Schumann, D. Sperl, K. Krumpe, D.M. Walther, and D. Rapaport. 2012. A crucial role for Mim2 in the biogenesis of mitochondrial outer membrane proteins. *J Cell Sci*. 125:3464-3473.

Dolezal, P., V. Likic, J. Tachezy, and T. Lithgow. 2006. Evolution of the molecular machines for protein import into mitochondria. *Science*. 313:314-318.

Dukanovic, J., K.S. Dimmer, N. Bonnefoy, K. Krumpe, and D. Rapaport. 2009. Genetic and functional interactions between the mitochondrial outer membrane proteins Tom6 and Sam37. *Mol Cell Biol*. 29:5975-5988.

Dukanovic, J., and D. Rapaport. 2011. Multiple pathways in the integration of proteins into the mitochondrial outer membrane. *Biochim Biophys Acta*. 1808:971-980.

Dyall, S.D., M.T. Brown, and P.J. Johnson. 2004. Ancient invasions: from endosymbionts to organelles. *Science*. 304:253-257.

Egan, B., B. Traude, G. Rebecca, I. Sandra, G. Sabine, W. Binks, and L. Trevor. 1999. Targeting of tail-anchored proteins to yeast mitochondria in vivo. *FEBS Letters*. 451:243-248.

Ellenrieder, L., C.U. Martensson, and T. Becker. 2015. Biogenesis of mitochondrial outer membrane proteins, problems and diseases. *Biol Chem*. 396:1199-1213.

Ellgaard, L., and A. Helenius. 2003. Quality control in the endoplasmic reticulum. *Nat Rev Mol Cell Biol*. 4:181-191.

English, A.R., and G.K. Voeltz. 2013. Endoplasmic reticulum structure and interconnections with other organelles. *Cold Spring Harb Perspect Biol*. 5:a013227.

Fagone, P., and S. Jackowski. 2009. Membrane phospholipid synthesis and endoplasmic reticulum function. *J Lipid Res*. 50 Suppl:S311-316.

Ferramosca, A., and V. Zara. 2013. Biogenesis of mitochondrial carrier proteins: molecular mechanisms of import into mitochondria. *Biochim Biophys Acta*. 1833:494-502.

Figueiredo Costa, B., P. Cassella, S.F. Colombo, and N. Borgese. 2018. Discrimination between the endoplasmic reticulum and mitochondria by spontaneously inserting tail-anchored proteins. *Traffic*. 19:182-197.

Frey, T.G., and C.A. Mannella. 2000. The internal structure of mitochondria. *Trends Biochem Sci*. 25:319-324.

Fueller, J., M.V. Egorov, K.A. Walther, O. Sabet, J. Mallah, M. Grabenbauer, and A. Kinkhabwala. 2015. Subcellular Partitioning of Protein Tyrosine Phosphatase 1B to the Endoplasmic Reticulum and Mitochondria Depends Sensitively on the Composition of Its Tail Anchor. *PLoS One*. 10:e0139429.

Gault, C.R., L.M. Obeid, and Y.A. Hannun. 2010. An overview of sphingolipid metabolism: from synthesis to breakdown. *Adv Exp Med Biol*. 688:1-23.

Glick, B.S., and A. Luini. 2011. Models for Golgi traffic: a critical assessment. *Cold Spring Harb Perspect Biol*. 3:a005215.

Gray, M.W. 2012. Mitochondrial evolution. *Cold Spring Harb Perspect Biol*. 4:a011403.

Guna, A., and R.S. Hegde. 2018a. Transmembrane Domain Recognition during Membrane Protein Biogenesis and Quality Control. *Curr Biol*. 28:R498-r511.

Guna, A., N. Volkmar, J.C. Christianson, and R.S. Hegde. 2018b. The ER membrane protein complex is a transmembrane domain insertase. *Science*. 359:470-473.

Halic, M., T. Becker, M.R. Pool, C.M. Spahn, R.A. Grassucci, J. Frank, and R. Beckmann. 2004. Structure of the signal recognition particle interacting with the elongation-arrested ribosome. *Nature*. 427:808-814.

Harsman, A., and A. Schneider. 2017. Mitochondrial protein import in trypanosomes: Expect the unexpected. *Traffic*. 18:96-109.

Haßdenteufel, S., M. Sicking, S. Schorr, N. Aviram, C. Fecher-Trost, M. Schuldiner, M. Jung, R. Zimmermann, and S. Lang. 2017. hSnd2 protein represents an alternative targeting factor to the endoplasmic reticulum in human cells. *FEBS Lett*. 591:3211-3224.

Hegde, R.S., and R.J. Keenan. 2011. Tail-anchored membrane protein insertion into the endoplasmic reticulum. *Nat Rev Mol Cell Biol*. 12:787-798.

Hell, K. 2008. The Erv1-Mia40 disulfide relay system in the intermembrane space of mitochondria. *Biochim Biophys Acta*. 1783:601-609.

Hell, K., J.M. Herrmann, E. Pratje, W. Neupert, and R.A. Stuart. 1998. Oxa1p, an essential component of the N-tail protein export machinery in mitochondria. *Proc Natl Acad Sci U S A*. 95:2250-2255.

Hell, K., W. Neupert, and R.A. Stuart. 2001. Oxa1p acts as a general membrane insertion machinery for proteins encoded by mitochondrial DNA. *Embo j*. 20:1281-1288.

Hines, V., A. Brandt, G. Griffiths, H. Horstmann, H. Brütsch, and G. Schatz. 1990. Protein import into yeast mitochondria is accelerated by the outer membrane protein MAS70. *Embo j*. 9:3191-3200.

Horie, C., H. Suzuki, M. Sakaguchi, and K. Mihara. 2002. Characterization of signal that directs C-tail-anchored proteins to mammalian mitochondrial outer membrane. *Mol Biol Cell*. 13:1615-1625.

Hu, J., J. Li, X. Qian, V. Denic, and B. Sha. 2009. The crystal structures of yeast Get3 suggest a mechanism for tail-anchored protein membrane insertion. *PLoS One*. 4:e8061.

Hulett, J.M., F. Lueder, N.C. Chan, A.J. Perry, P. Wolynec, V.A. Likic, P.R. Gooley, and T. Lithgow. 2008. The transmembrane segment of Tom20 is recognized by Mim1 for docking to the mitochondrial TOM complex. *J Mol Biol*. 376:694-704.

Ishikawa, D., H. Yamamoto, Y. Tamura, K. Moritoh, and T. Endo. 2004. Two novel proteins in the mitochondrial outer membrane mediate beta-barrel protein assembly. *J Cell Biol*. 166:621-627.

Jakobsson, A., R. Westerberg, and A. Jacobsson. 2006. Fatty acid elongases in mammals: their regulation and roles in metabolism. *Prog Lipid Res*. 45:237-249.

Jensen, R.E., and P.T. Englund. 2012. Network news: the replication of kinetoplast DNA. *Annu Rev Microbiol*. 66:473-491.

Jores, T., A. Klinger, L.E. Groß, S. Kawano, N. Flinner, E. Duchardt-Ferner, J. Wöhnert, H. Kalbacher, T. Endo, E. Schleiff, and D. Rapaport. 2016. Characterization of the targeting signal in mitochondrial beta-barrel proteins. *Nat Commun*. 7:12036.

Kalbfleisch, T., A. Cambon, and B.W. Wattenberg. 2007. A bioinformatics approach to identifying tail-anchored proteins in the human genome. *Traffic*. 8:1687-1694.

Käser, S., S. Oeljeklaus, J. Tyc, S. Vaughan, B. Warscheid, and A. Schneider. 2016. Outer membrane protein functions as integrator of protein import and DNA inheritance in mitochondria. *Proc Natl Acad Sci U S A*. 113:E4467-4475.

Kemper, C., S.J. Habib, G. Engl, P. Heckmeyer, K.S. Dimmer, and D. Rapaport. 2008. Integration of tail-anchored proteins into the mitochondrial outer membrane does not require any known import components. *J Cell Sci*. 121:1990-1998.

Krüger, V., T. Becker, L. Becker, M. Montilla-Martinez, L. Ellenrieder, F.N. Vögtle, H.E. Meyer, M.T. Ryan, N. Wiedemann, B. Warscheid, N. Pfanner, R. Wagner, and C. Meisinger. 2017. Identification of new channels by systematic analysis of the mitochondrial outer membrane. *J Cell Biol*. 216:3485-3495.

Krumpe, K., I. Frumkin, Y. Herzig, N. Rimon, C. Özbalci, B. Brügger, D. Rapaport, and M. Schuldiner. 2012. Ergosterol content specifies targeting of tail-anchored proteins to mitochondrial outer membranes. *Mol Biol Cell*. 23:3927-3935.

Lill, R. 2009. Function and biogenesis of iron-sulphur proteins. *Nature*. 460:831-838.

Lueder, F., and T. Lithgow. 2009. The three domains of the mitochondrial outer membrane protein Mim1 have discrete functions in assembly of the TOM complex. *FEBS Lett*. 583:1475-1480.

Mani, J., S. Desy, M. Niemann, A. Chanfon, S. Oeljeklaus, M. Pusnik, O. Schmidt, C. Gerbeth, C. Meisinger, B. Warscheid, and A. Schneider. 2015. Mitochondrial protein import receptors in Kinetoplastids reveal convergent evolution over large phylogenetic distances. *Nat Commun*. 6:6646.

Mani, J., C. Meisinger, and A. Schneider. 2016. Peeping at TOMs-Diverse Entry Gates to Mitochondria Provide Insights into the Evolution of Eukaryotes. *Mol Biol Evol*. 33:337-351.

Mariappan, M., A. Mateja, M. Dobosz, E. Bove, R.S. Hegde, and R.J. Keenan. 2011. The mechanism of membrane-associated steps in tail-anchored protein insertion. *Nature*. 477:61-66.

Martin, W.F., S. Garg, and V. Zimorski. 2015. Endosymbiotic theories for eukaryote origin. *Philosophical transactions of the Royal Society of London. Series B, Biological sciences*. 370:20140330.

Mateja, A., A. Szlachcic, M.E. Downing, M. Dobosz, M. Mariappan, R.S. Hegde, and R.J. Keenan. 2009. The structural basis of tail-anchored membrane protein recognition by Get3. *Nature*. 461:361-366.

Mayerhofer, P.U. 2016. Targeting and insertion of peroxisomal membrane proteins: ER trafficking versus direct delivery to peroxisomes. *Biochim Biophys Acta*. 1863:870-880.

Mnaimneh, S., A.P. Davierwala, J. Haynes, J. Moffat, W.T. Peng, W. Zhang, X. Yang, J. Pootoolal, G. Chua, A. Lopez, M. Trochesset, D. Morse, N.J. Krogan, S.L. Hiley, Z. Li, Q. Morris, J. Grigull, N. Mitsakakis, C.J. Roberts, J.F. Greenblatt, C. Boone, C.A. Kaiser, B.J. Andrews, and T.R. Hughes. 2004. Exploration of essential gene functions via titratable promoter alleles. *Cell*. 118:31-44.

Moczko, M., F. Gärtner, and N. Pfanner. 1993. The protein import receptor MOM19 of yeast mitochondria. *FEBS Lett*. 326:251-254.

Mokranjac, D., and W. Neupert. 2010. The many faces of the mitochondrial TIM23 complex. *Biochim Biophys Acta*. 1797:1045-1054.

Nunnari, J., and A. Suomalainen. 2012. Mitochondria: in sickness and in health. *Cell*. 148:1145-1159.

Nyathi, Y., B.M. Wilkinson, and M.R. Pool. 2013. Co-translational targeting and translocation of proteins to the endoplasmic reticulum. *Biochim Biophys Acta*. 1833:2392-2402.

Olzmann, J.A., R.R. Kopito, and J.C. Christianson. 2013. The mammalian endoplasmic reticulum-associated degradation system. *Cold Spring Harb Perspect Biol*. 5.

Osborne, A.R., T.A. Rapoport, and B. van den Berg. 2005. Protein translocation by the Sec61/SecY channel. *Annu Rev Cell Dev Biol*. 21:529-550.

Osellame, L.D., T.S. Blacker, and M.R. Duchen. 2012. Cellular and molecular mechanisms of mitochondrial function. *Best practice & research. Clinical endocrinology & metabolism*. 26:711-723.

Otera, H., Y. Taira, C. Horie, Y. Suzuki, H. Suzuki, K. Setoguchi, H. Kato, T. Oka, and K. Mihara. 2007. A novel insertion pathway of mitochondrial outer membrane proteins with multiple transmembrane segments. *J Cell Biol*. 179:1355-1363.

Papic, D., Y. Elbaz-Alon, S.N. Koerdt, K. Leopold, D. Worm, M. Jung, M. Schuldiner, and D. Rapaport. 2013. The role of Djp1 in import of the mitochondrial protein Mim1 demonstrates specificity between a cochaperone and its substrate protein. *Mol Cell Biol*. 33:4083-4094.

Papic, D., K. Krumpe, J. Dukanovic, K.S. Dimmer, and D. Rapaport. 2011. Multispan mitochondrial outer membrane protein Ugo1 follows a unique Mim1-dependent import pathway. *J Cell Biol*. 194:397-405.

Popov-Celeketic, J., T. Waizenegger, and D. Rapaport. 2008. Mim1 functions in an oligomeric form to facilitate the integration of Tom20 into the mitochondrial outer membrane. *J Mol Biol*. 376:671-680.

Powis, K., B. Schrul, H. Tienson, I. Gostimskaya, M. Breker, S. High, M. Schuldiner, U. Jakob, and B. Schwappach. 2013. Get3 is a holdase chaperone and moves to deposition sites for aggregated proteins when membrane targeting is blocked. *J Cell Sci*. 126:473-483.

Pusnik, M., J. Mani, O. Schmidt, M. Niemann, S. Oeljeklaus, F. Schnarwiler, B. Warscheid, T. Lithgow, C. Meisinger, and A. Schneider. 2012. An essential novel component of the noncanonical mitochondrial outer membrane protein import system of trypanosomatids. *Mol Biol Cell*. 23:3420-3428.

Pusnik, M., O. Schmidt, A.J. Perry, S. Oeljeklaus, M. Niemann, B. Warscheid, T. Lithgow, C. Meisinger, and A. Schneider. 2011. Mitochondrial preprotein translocase of trypanosomatids has a bacterial origin. *Curr Biol*. 21:1738-1743.

Rao, M., V. Okreglak, U.S. Chio, H. Cho, P. Walter, and S.O. Shan. 2016. Multiple selection filters ensure accurate tail-anchored membrane protein targeting. *Elife*. 5.

Rome, M.E., U.S. Chio, M. Rao, H. Gristick, and S.O. Shan. 2014. Differential gradients of interaction affinities drive efficient targeting and recycling in the GET pathway. *Proc Natl Acad Sci U S A*. 111:E4929-4935.

Rome, M.E., M. Rao, W.M. Clemons, and S.O. Shan. 2013. Precise timing of ATPase activation drives targeting of tail-anchored proteins. *Proc Natl Acad Sci U S A*. 110:7666-7671.

Sammels, E., J.B. Parys, L. Missiaen, H. De Smedt, and G. Bultynck. 2010. Intracellular Ca2+ storage in health and disease: a dynamic equilibrium. *Cell Calcium*. 47:297-314.

Schlacht, A., E.K. Herman, M.J. Klute, M.C. Field, and J.B. Dacks. 2014. Missing pieces of an ancient puzzle: evolution of the eukaryotic membrane-trafficking system. *Cold Spring Harb Perspect Biol*. 6:a016048.

Schuldiner, M., J. Metz, V. Schmid, V. Denic, M. Rakwalska, H.D. Schmitt, B. Schwappach, and J.S. Weissman. 2008. The GET complex mediates insertion of tail-anchored proteins into the ER membrane. *Cell*. 134:634-645.

Setoguchi, K., H. Otera, and K. Mihara. 2006. Cytosolic factor- and TOM-independent import of C-tail-anchored mitochondrial outer membrane proteins. *EMBO J*. 25:5635-5647.

Shao, S., and R.S. Hegde. 2011. Membrane protein insertion at the endoplasmic reticulum. *Annu Rev Cell Dev Biol*. 27:25-56.

Sinzel, M., T. Tan, P. Wendling, H. Kalbacher, C. Özbalci, X. Chelius, B. Westermann, B. Brügger, D. Rapaport, and K.S. Dimmer. 2016. Mcp3 is a novel mitochondrial outer membrane protein that follows a unique IMP-dependent biogenesis pathway. *EMBO Rep*. 17:965-981.

Söllner, T., G. Griffiths, R. Pfaller, N. Pfanner, and W. Neupert. 1989. MOM19, an import receptor for mitochondrial precursor proteins. *Cell*. 59:1061-1070.

Sommer, M.S., and E. Schleiff. 2014. Protein targeting and transport as a necessary consequence of increased cellular complexity. *Cold Spring Harb Perspect Biol*. 6.

Song, J., Y. Tamura, T. Yoshihisa, and T. Endo. 2014. A novel import route for an N-anchor mitochondrial outer membrane protein aided by the TIM23 complex. *EMBO Rep*. 15:670-677.

Sorger, D., and G. Daum. 2003. Triacylglycerol biosynthesis in yeast. *Appl Microbiol Biotechnol*. 61:289-299.

Stefer, S., S. Reitz, F. Wang, K. Wild, Y.Y. Pang, D. Schwarz, J. Bomke, C. Hein, F. Löhr, F. Bernhard, V. Denic, V. Dötsch, and I. Sinning. 2011. Structural

basis for tail-anchored membrane protein biogenesis by the Get3-receptor complex. *Science*. 333:758-762.

Stehling, O., and R. Lill. 2013. The role of mitochondria in cellular iron-sulfur protein biogenesis: mechanisms, connected processes, and diseases. *Cold Spring Harb Perspect Biol*. 5:a011312.

Stojanovski, D., B. Guiard, V. Kozjak-Pavlovic, N. Pfanner, and C. Meisinger. 2007. Alternative function for the mitochondrial SAM complex in biogenesis of alpha-helical TOM proteins. *J Cell Biol*. 179:881-893.

Suloway, C.J., J.W. Chartron, M. Zaslaver, and W.M. Clemons, Jr. 2009. Model for eukaryotic tail-anchored protein binding based on the structure of Get3. *Proc Natl Acad Sci U S A*. 106:14849-14854.

Teese, M.G., and D. Langosch. 2015. Role of GxxxG Motifs in Transmembrane Domain Interactions. *Biochemistry*. 54:5125-5135.

Thibault, G., and D.T. Ng. 2012. The endoplasmic reticulum-associated degradation pathways of budding yeast. *Cold Spring Harb Perspect Biol*. 4.

Thornton, N., D.A. Stroud, D. Milenkovic, B. Guiard, N. Pfanner, and T. Becker. 2010. Two modular forms of the mitochondrial sorting and assembly machinery are involved in biogenesis of alpha-helical outer membrane proteins. *J Mol Biol*. 396:540-549.

van der Bliek, A.M., Q. Shen, and S. Kawajiri. 2013. Mechanisms of mitochondrial fission and fusion. *Cold Spring Harb Perspect Biol*. 5.

van der Laan, M., M. Meinecke, J. Dudek, D.P. Hutu, M. Lind, I. Perschil, B. Guiard, R. Wagner, N. Pfanner, and P. Rehling. 2007. Motor-free mitochondrial presequence translocase drives membrane integration of preproteins. *Nat Cell Biol*. 9:1152-1159.

Vitali, D.G., S. Käser, A. Kolb, K.S. Dimmer, A. Schneider, and D. Rapaport. 2018a. Independent evolution of functionally exchangeable mitochondrial outer membrane import complexes. *Elife*. 7.

Vitali, D.G., M. Sinzel, E.P. Bulthuis, A. Kolb, S. Zabel, D.G. Mehlhorn, B. Figueiredo Costa, A. Farkas, A. Clancy, M. Schuldiner, C. Grefen, B. Schwappach, N. Borgese, and D. Rapaport. 2018b. The GET pathway can increase the risk of mitochondrial outer membrane proteins to be mistargeted to the ER. *J Cell Sci*. 131.

Voeltz, G.K., M.M. Rolls, and T.A. Rapoport. 2002. Structural organization of the endoplasmic reticulum. *EMBO Rep*. 3:944-950.

Vögtle, F.N., M. Keller, A.A. Taskin, S.E. Horvath, X.L. Guan, C. Prinz, M. Opalinska, C. Zorzin, M. van der Laan, M.R. Wenk, R. Schubert, N. Wiedemann, M. Holzer, and C. Meisinger. 2015. The fusogenic lipid phosphatidic acid promotes the biogenesis of mitochondrial outer membrane protein Ugo1. *J Cell Biol*. 210:951-960.

Vögtle, F.N., S. Wortelkamp, R.P. Zahedi, D. Becker, C. Leidhold, K. Gevaert, J. Kellermann, W. Voos, A. Sickmann, N. Pfanner, and C. Meisinger. 2009. Global analysis of the mitochondrial N-proteome identifies a processing peptidase critical for protein stability. *Cell*. 139:428-439.

Voth, W., M. Schick, S. Gates, S. Li, F. Vilardi, I. Gostimskaya, D.R. Southworth, B. Schwappach, and U. Jakob. 2014. The protein targeting factor Get3 functions as ATP-independent chaperone under oxidative stress conditions. *Mol Cell*. 56:116-127.

Waizenegger, T., S. Schmitt, J. Zivkovic, W. Neupert, and D. Rapaport. 2005. Mim1, a protein required for the assembly of the TOM complex of mitochondria. *EMBO Rep*. 6:57-62.

Waizenegger, T., T. Stan, W. Neupert, and D. Rapaport. 2003. Signal-anchor domains of proteins of the outer membrane of mitochondria: structural and functional characteristics. *J Biol Chem*. 278:42064-42071.

Wang, F., E.C. Brown, G. Mak, J. Zhuang, and V. Denic. 2010. A chaperone cascade sorts proteins for posttranslational membrane insertion into the endoplasmic reticulum. *Mol Cell*. 40:159-171.

Wang, F., C. Chan, N.R. Weir, and V. Denic. 2014. The Get1/2 transmembrane complex is an endoplasmic-reticulum membrane protein insertase. *Nature*. 512:441-444.

Wang, F., A. Whynot, M. Tung, and V. Denic. 2011. The mechanism of tail-anchored protein insertion into the ER membrane. *Mol Cell*. 43:738-750.

Wenz, L.S., L. Opalinski, M.H. Schuler, L. Ellenrieder, R. Ieva, L. Böttinger, J. Qiu, M. van der Laan, N. Wiedemann, B. Guiard, N. Pfanner, and T. Becker. 2014. The presequence pathway is involved in protein sorting to the mitochondrial outer membrane. *EMBO Rep*. 15:678-685.

Wiedemann, N., and N. Pfanner. 2017. Mitochondrial Machineries for Protein Import and Assembly. *Annu Rev Biochem*. 86:685-714.

Williams, C.C., C.H. Jan, and J.S. Weissman. 2014. Targeting and plasticity of mitochondrial proteins revealed by proximity-specific ribosome profiling. *Science*. 346:748-751.

Yamano, K., Y. Yatsukawa, M. Esaki, A.E. Hobbs, R.E. Jensen, and T. Endo. 2008. Tom20 and Tom22 share the common signal recognition pathway in mitochondrial protein import. *J Biol Chem*. 283:3799-3807.

Zhang, X., and S.O. Shan. 2014. Fidelity of cotranslational protein targeting by the signal recognition particle. *Annual review of biophysics*. 43:381-408.

10. Acknowledgments

My sincere gratitude goes to Prof. Dr. Doron Rapaport for supervising my PhD work. He guided me through this tough but rewarding path and I learned a lot from him.

I want to thank Prof. Dr. Ana J. García Sáez, Prof. Dr. Rapf-Peter Jansen and Dr. Christopher Grefen for their valuable time dedicated in being part of my doctoral examination committee.

My thank goes to such good colleagues that create a nice working environment. To Elena for the professional help in the lab, avoiding it to collapse. To Diana, who shared this experience with me from day one and for often being me. To Janani, for bringing the drama in my life. To Bogdan for his constant optimism and for being at my side in the TAMPting experience. To Tobias, for being always there when I made a mistake, for his constant help and for keeping my glucose level always high. To Ravi for introducing me to the lab, for all the fun and for the good playlist and, together with Lena, for the tasty food and beers we shared. I want to thank all the present and past lab member for all the fun moments, science related and not: Kai, Moni, Layla, Jialin, Fenja, Thomas, and Hoda. A great thank goes to the student assistant, bachelor and master students for the precious contribution to my work: Susi, Elianne and Antonia. Especially to Antonia for the good work done in the last year and for adding some pink in my life. Moreover, I want to thank the collaborators in Tübingen and in Bern for the successful work, and all the TAMPting fellows and PIs for the nice time spent together, the helpful discussions and exchange of information.

A special thank goes to Enzo, who was always on my side, encouraging me and could always stand my craziness.

I also want to thank all my friends in Germany and in Italy for sharing with me many fun moments and for always making my life easier.

My gratitude goes also to my family. To my father, who always pushed me to give the maximum. To my sister Manuela for always believing in me and was always there when I needed. To Alessandro who is always able to put a smile on my face. To Sergio who was so patient with the Vitali sister for so many years. To uncle Bono and aunt Teresa for always taking care of me. To Nino and Anna for all the love.

11. Appendix

Accepted papers

1. Vitali, D.G., M. Sinzel, E.P. Bulthuis, A. Kolb, S. Zabel, D.G. Mehlhorn, B. Figueiredo Costa, A. Farkas, A. Clancy, M. Schuldiner, C. Grefen, B. Schwappach, N. Borgese, and D. Rapaport. 2018. The GET pathway can increase the risk of mitochondrial outer membrane proteins to be mistargeted to the ER. *Journal of Cell Science*. 131.

   doi:10.1242/jcs.211110.

2. Vitali, D.G.*, S. Käser*, A. Kolb*, K.S. Dimmer, A. Schneider, D. Rapaport. 2018. Independent evolution of functionally exchangeable mitochondrial outer membrane import complexes. *eLIFE*. 7.
   * equal contribution.

   doi: 10.7554/eLife.34488.

© 2018. Published by The Company of Biologists Ltd | Journal of Cell Science (2018) 131, jcs211110. doi:10.1242/jcs.211110

SHORT REPORT

The GET pathway can increase the risk of mitochondrial outer membrane proteins to be mistargeted to the ER

Daniela G. Vitali[1], Monika Sinzel[1], Elianne P. Bulthuis[1,*], Antonia Kolb[1], Susanne Zabel[1], Dietmar G. Mehlhorn[2], Bruna Figueiredo Costa[3,‡], Ákos Farkas[4], Anne Clancy[4], Maya Schuldiner[5], Christopher Grefen[2], Blanche Schwappach[4], Nica Borgese[3] and Doron Rapaport[1,§]

ABSTRACT

Tail-anchored (TA) proteins are anchored to their corresponding membrane via a single transmembrane segment (TMS) at their C-terminus. In yeast, the targeting of TA proteins to the endoplasmic reticulum (ER) can be mediated by the guided entry of TA proteins (GET) pathway, whereas it is not yet clear how mitochondrial TA proteins are targeted to their destination. It has been widely observed that some mitochondrial outer membrane (MOM) proteins are mistargeted to the ER when overexpressed or when their targeting signal is masked. However, the mechanism of this erroneous sorting is currently unknown. In this study, we demonstrate the involvement of the GET machinery in the mistargeting of suboptimal MOM proteins to the ER. These findings suggest that the GET machinery can, in principle, recognize and guide mitochondrial and non-canonical TA proteins. Hence, under normal conditions, an active mitochondrial targeting pathway must exist that dominates the kinetic competition against other pathways.

KEY WORDS: ER, GET, Mitochondria, Outer membrane, Protein sorting, Tail-anchor

INTRODUCTION

Eukaryotic cells face the challenge of directing newly synthesized membrane proteins to the right compartment because their mistargeting not only leads to their absence in the target organelle but also burdens the cytosol with aggregates of such proteins. Two main destinations for such proteins are mitochondria and the endoplasmic reticulum (ER). The mechanisms for targeting each membrane protein to its correct membrane depend on the protein topology and the targeting signals it contains.

Hundreds of eukaryotic membrane proteins have a single α-helical transmembrane segment (TMS) at their C-terminus (Kalbfleisch et al., 2007). The import of these proteins to the ER can be mediated by the guided entry of tail-anchored (TA) proteins (GET) pathway (Schuldiner et al., 2008). The recognition happens immediately after the release of the protein from the ribosome by the pre-targeting complex, which comprises Sgt2, Get4 and Get5. Sgt2 binds the TMS and discriminates between mitochondrial and ER TA proteins (Wang et al., 2010). Sgt2 then hands over the substrate to the Get4–Get5 complex that, in turn, recruits Get3, a cytosolic chaperone. Get3 shuttles TA proteins to the ER membrane, where Get1 and Get2 form a receptor complex that recognizes the Get3-TA protein complex and facilitates the release of the TA proteins (Schuldiner et al., 2008). It appears that the Get1-Get2 receptor can mediate the membrane insertion of some TA proteins (Wang et al., 2011), however, other TA proteins with a moderately hydrophobic TMS, as e.g. cytochrome b5 and the protein tyrosine phosphatase PTP1B, can spontaneously insert into the lipid bilayer (Brambillasca et al., 2005; Colombo et al., 2009). Recently, an additional ER membrane protein targeting pathway was identified, which can compensate the absence of either the signal recognition particle (SRP) or of the GET machinery and was named SRP-independent targeting (SND) pathway (Aviram et al., 2016; Hassdenteufel et al., 2017).

TA proteins are also targeted to the mitochondrial outer membrane (MOM), but none of the known mitochondrial import machineries are required for their insertion (Kemper et al., 2008; Dukanovic and Rapaport, 2011). It has been proposed that the difference in the lipid distribution (mainly of ergosterol) between ER and mitochondria plays a role in assuring specificity in targeting to mitochondria (Krumpe et al., 2012). Compared to ER-localized TA proteins, mitochondrial TA proteins generally have a moderately hydrophobic TMS flanked by positively charged residues. Despite these differences, the overall similarity of targeting signals between ER and mitochondrial destined TA proteins causes their mistargeting to the wrong organelles on different occasions. However, the mechanism by which mistargeting occurs is, so far, unresolved.

In this work, we used *Saccharomyces cerevisiae* to identify MOM proteins that are mislocalized to the ER because either their targeting sequence is masked or the membrane import machinery is saturated. We further demonstrate that their mistargeting to the ER membrane depends on the GET machinery, suggesting that under normal circumstances a mitochondrial targeting pathway counterbalances GET substrate capture.

RESULTS AND DISCUSSION

GET-dependent mislocalization of cytochrome b5-RR

The mammalian TA protein cytochrome b5 has two isoforms; one (b5-ER) is located in the ER and the other (b5-OM) in the MOM (D'Arrigo et al., 1993). The ER isoform has a predominantly negatively charged C-terminus while the mitochondrial isoform is mostly positively charged. Replacement of the C-terminal segment of b5-ER with two arginine residues – yielding substitution mutant

[1]Interfaculty Institute of Biochemistry, University of Tübingen, 72076 Tübingen, Germany. [2]Centre for Plant Molecular Biology, Developmental Genetics, University of Tübingen, Tübingen 72076, Germany. [3]Consiglio Nazionale delle Ricerche Institute of Neuroscience, Milan 20100, Italy. [4]Department of Molecular Biology, Universitätsmedizin Göttingen, Göttingen 37073, Germany. [5]Department of Molecular Genetics, Weizmann Institute of Science, Rehovot 7610001, Israel. *Present address: Department of Biochemistry, Radboud University Medical Centre, 6500HB Nijmegen, The Netherlands. ‡Present address: Telomeres and Cancer Laboratory, Champalimaud Centre for the Unknown, 1400-038 Lisbon, Portugal.

§Author for correspondence (doron.rapaport@uni-tuebingen.de)

D.R., 0000-0003-3136-1207

Received 4 October 2017; Accepted 10 April 2018

Journal of Cell Science (2018) 131, jcs211110. doi:10.1242/jcs.211110

b5-RR – leads to re-direction of the protein to mitochondria (Borgese et al., 2001) (Fig. 1A).

To understand better the distribution of the two isoforms between both organelles, we expressed rabbit b5-ER and its b5-RR variant in yeast cells, and analysed their localization by subcellular fractionation. As expected, we found the vast majority of the ER form in the ER (microsomal) fraction of yeast cells and only marginal amounts in their mitochondria (Fig. 1B). Surprisingly, ∼50% of the mitochondrial isoform was found in the ER fraction of yeast cells (Fig. 1C). This is in sharp contrast to the situation in mammalian cells where the vast majority of b5-RR is found in mitochondria (Borgese et al., 2001). Thus, it seems that those features that assure correct targeting in mammalian cells do not function properly in yeast cells. Similar differences between targeting in mammalian cells compared with that in yeast were observed for PTP1B and Bcl2. In mammalian cells, both proteins localize to the ER and mitochondria but are found, once expressed in yeast cells, solely in the ER (Egan et al., 1999; Fueller et al., 2015).

Furthermore, a substantial proportion of these b5-RR mistargeted molecules migrated at a higher than expected molecular mass, suggesting that they had been modified (Fig. 1C). To characterize the topology of the native and modified forms, we treated isolated microsomes with proteinase K. This treatment resulted in disappearance of the native protein signal suggesting that it adopted a classical TA topology. In contrast, the modified form was protease resistant, unless the membrane was solubilized with detergent (Fig. 1D). This outcome raised the possibility that the modified form flipped its topology such that the N-terminus faces the microsome lumen. Moreover, by using alkaline extraction both native and modified microsomal forms of b5-RR, as well as b5-RR localized in mitochondria, were found to be integrated into membranes (Fig. 1E).

The inside-out topology of the modified b5-RR suggests that its modification might be glycosylation. Hence, we treated b5-RR-containing microsomes with either endoglycosidase H (EndoH) or peptide:N-glycosidase (PNGase). Both enzymes caused the disappearance of the modified form of b5-RR and of protein disulfide-isomerase (Pdi1), which served as a control. Of note, the NetNGlyc 1.0 Server (http://www.cbs.dtu.dk/services/NetNGlyc/), which predicts N-glycosylation sites, suggested Asp residue 21 of cytochrome b5 as a potential glycosylation site (Fig. 1A). We concluded that a considerable portion of b5-RR molecules was mistargeted to the ER and some of those molecules had been inserted in the opposite orientation, i.e. with the N-terminus in the lumen. These findings can be explained by recent reports suggesting that the SRP and the Sec translocon are involved in the targeting of some TA proteins, including cytochrome b5, to the ER (Casson et al., 2017; Hassdenteufel et al., 2017). Thus, it might be that the Sec translocon mediates an integration of a sub-population of b5-RR into the ER membrane in the wrong topology.

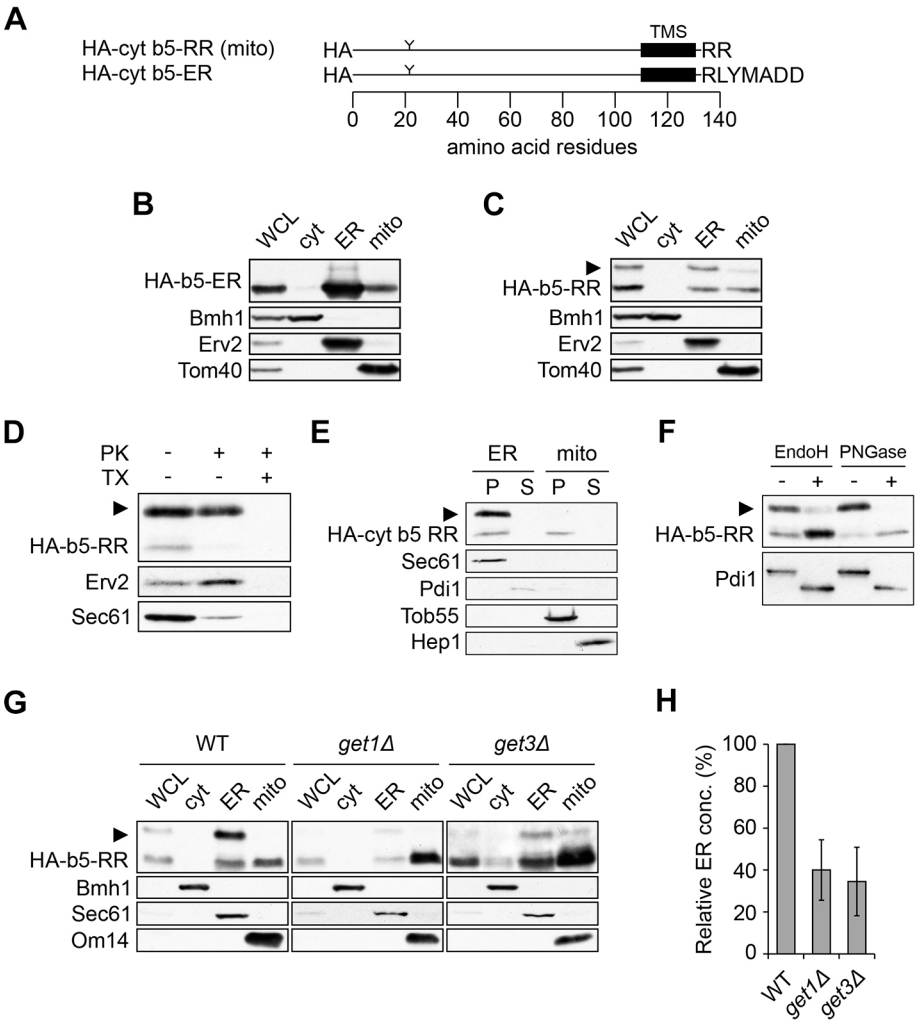

Fig. 1. Cytochrome b5-RR is partially mistargeted to ER in a GET-dependent manner. (A) Schematic representation of cytochrome b5 isoforms. Y represents a potential glycosylation site. (B,C) Whole-cell lysate (WCL) and fractions corresponding to cytosol (cyt), microsomes (ER) and mitochondria (mito) from cells expressing either b5-ER (B) or b5-RR (C) were analysed by SDS-PAGE and immunoblotting. (D) Western blot showing ER fractions treated with proteinase K (PK) in the absence or presence of Triton X-100 (TX). (E) Western blot showing ER and mitochondria fractions subjected to alkaline extraction. Pellet (P) and supernatant (S) fractions were analysed by SDS-PAGE and immunoblotting. (F) Western blot showing the ER fraction incubated in the presence (+) or absence (–) of either EndoH or PNGase. (G) Western blot showing WT, *get1Δ* and *get3Δ* cells expressing b5-RR subjected to subcellular fractionation and analysis as in (C). (H) Quantification of three independent experiments as in G; enrichment of the lower form of b5-RR in ER fractions is depicted. Arrowheads in C-G indicate the modified form of HA-b5-RR.

Journal of Cell Science (2018) 131, jcs211110. doi:10.1242/jcs.211110

Since ER TA proteins can be targeted to their destination by the GET machinery (Borgese and Fasana, 2011; Schuldiner et al., 2008), we wondered whether this system can participate in the missorting of b5-RR. To test this, we expressed b5-RR in cells that lack the ER receptor Get1 or the cytosolic chaperone Get3. We observed that, in both deletion strains, a smaller proportion of b5-RR molecules localized to the ER, whereas higher amounts were found in mitochondria (Fig. 1G,H). These findings suggest that the GET machinery deviates this substrate from its natural target membrane. Of note, we observed that ∼30-40% of b5-RR molecules are localized to ER, even in the absence of functional GET system. This partial dependence on the GET components is in line with the idea that multiple selection filters are used by the GET machinery to assure correct targeting (Rao et al., 2016), and that alternative pathways, involving SRP, hSnd2 and/or unassisted membrane integration, exist for ER TA protein targeting in the absence of GET (Casson et al., 2017; Hassdenteufel et al., 2017).

The GET machinery mediates mistargeting of Mcp3

In *S. cerevisiae* the MOM protein Mcp3 follows a unique import pathway that involves the TOM and TIM23 complexes, as well as processing by the inner membrane peptidases 1 and 2 (Imp1/2) (Sinzel et al., 2016). Mcp3 contains a presequence-like segment in its N-terminal region, whereas the C-terminal half contains two putative TMSs, one of them very close to the C-terminus (Fig. 2A). When Mcp3 was N-terminally labelled with GFP, we observed considerable mislocalization to the ER (Fig. 2B), potentially due to masking of the presequence by the GFP moiety.

Of note, alkaline extraction confirmed that the GFP-tagged version was integrated into the membranes of either mitochondria or

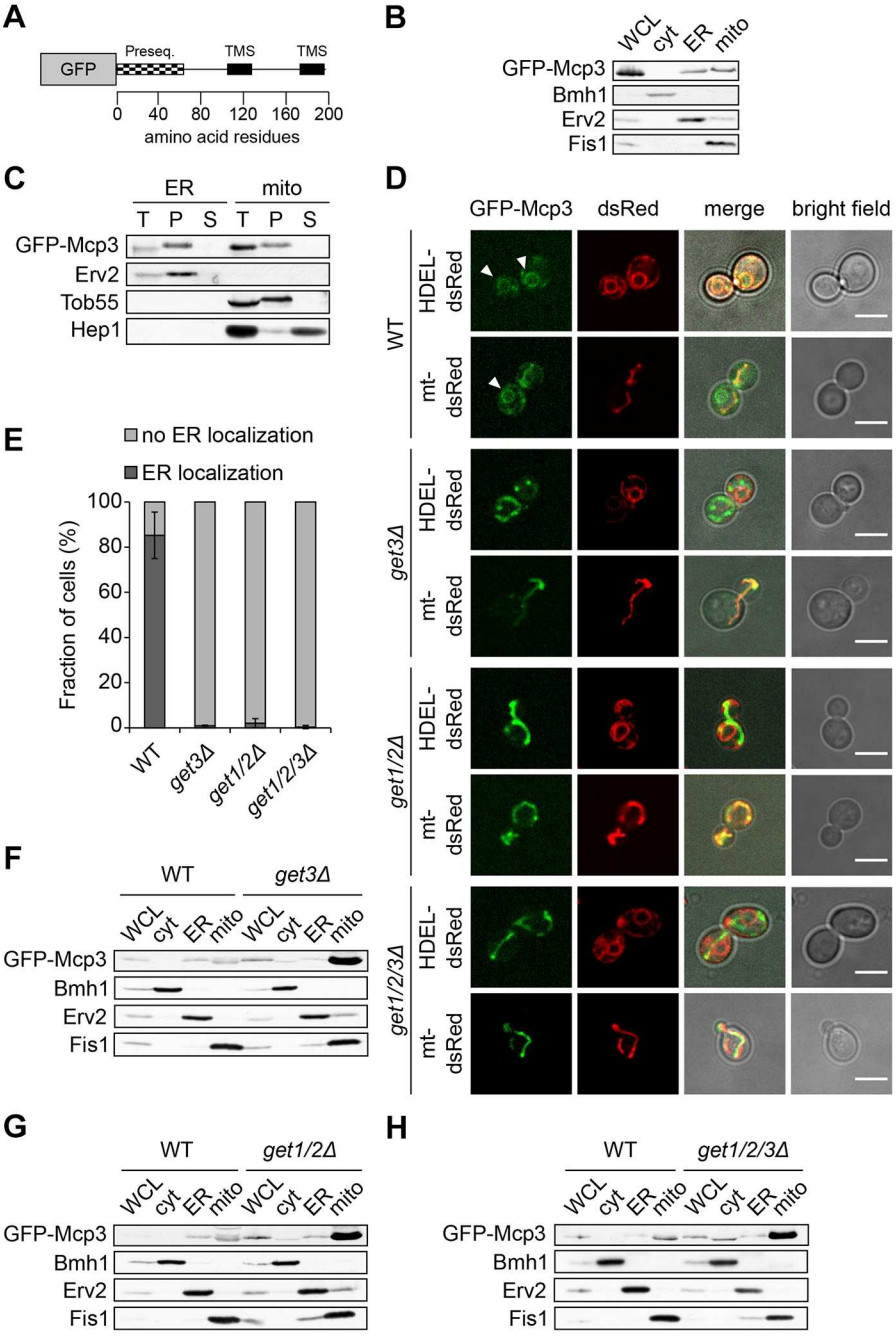

Fig. 2. The mistargeting of GFP-Mcp3 to ER requires the GET machinery. (A) Schematic representation of GFP-Mcp3. (B) Western blot showing cells expressing GFP-Mcp3 subjected to subcellular fractionation and analysis as described for Fig. 1B. (C) Western blot showing ER and mitochondrial fractions subjected to alkaline extraction as described for Fig. 1E. T, total; P, pellet; S, supernatant. (D) WT, *get3Δ*, *get1Δget2Δ*, and *get1Δget2Δget3Δ* cells expressing GFP-Mcp3 and either the ER marker HDEL-dsRed or the mitochondrial marker mt-dsRed were analysed by fluorescence microscopy and representative images are shown. Arrowheads indicate perinuclear ER localization. Scale bars: 5 µm. (E) Quantification of the intracellular localization of GFP-Mcp3 monitored as in D. The figure shows the average±s.d. of three independent experiments with at least 100 cells each. (F-H) Western blots showing WT, *get3Δ* (F), *get1/2Δ* (G), and *get1/2/3Δ* (H) cells expressing GFP-Mcp3 subjected to subcellular fractionation as described for Fig. 1B. WCL, whole-cell lysate; cyt, cytosol fraction; ER, microsome fraction; mito, mitochondria fraction; WT, wild type.

Journal of Cell Science (2018) 131, jcs211110. doi:10.1242/jcs.211110

the ER (Fig. 2C). Since Mcp3 has a TMS at its C-terminal region, we wondered whether GET components are required for its missorting. To address this point, we introduced GFP-Mcp3 into strains deleted for *GET3* alone (*get3Δ*), double-deleted for *GET1* and *GET2* (*get1/2Δ*), or triple deleted for *GET1*, *GET2* and *GET3* (*get1/2/3Δ*). Fluorescence microscopy verified the predominant ER localization of GFP-Mcp3 in WT cells. In sharp contrast, only negligible staining of the ER and a typical tubular pattern of mitochondria was observed in cells lacking one, two or all of the GET components (Fig. 2D,E).

To test our assumption that the N-terminal GFP interferes with the function of the presequence of Mcp3, we constructed a Mcp3 variant lacking its N-terminally presequence (Mcp3ΔN). Indeed, this construct behaved similarly to the GFP full-length Mcp3 and was localized to ER structures. This location disappeared upon deletion of either *GET1* or *GET3* (Fig. S1). However, in contrast to the full-length protein, the truncated variant, which lacks the mitochondrial targeting signal, was spread in the absence of the GET machinery in the cytosol or appeared in punctate structures, representing probably aggregated molecules (Fig. S1).

To support the fluorescence microscopy data, we performed subcellular fractionation of WT cells and *get* mutant cells expressing GFP-Mcp3. In all *get* mutant strains, we observed much higher amounts of GFP-Mcp3 in the mitochondrial fraction as compared to WT cells (Fig. 2F-H). Notably, the *get* mutant strains appear to contain a minor population of GFP-Mcp3 in their ER fraction. This, again, might be due to alternative targeting pathways supporting this rerouting but could also be due to cross-contamination between the ER and mitochondrial fractions. Markedly, the overall higher amounts of GFP-Mcp3 in the *get* mutants raise the possibility that GFP-Mcp3 is unstable in WT cells and undergoes degradation.

In summary, masking the mitochondrial targeting information in the N-terminal region with a GFP moiety probably slowed the association with mitochondria, thus providing the GET machinery a chance to recognize the C-terminal TMS of Mcp3 as a potential substrate. In the case of native Mcp3, the mitochondrial import is most likely so fast that it does not provide the GET machinery a time window to interfere with this process.

Overexpressed GFP-tagged Mim1 is partially targeted to the ER

The yeast mitochondrial import protein 1 (Mim1) is a MOM protein that harbours a central membrane-spanning hydrophobic stretch (Ishikawa et al., 2004; Waizenegger et al., 2005) (Fig. 3A). Subcellular fractionation indicated that, upon overexpression, GFP-Mim1 is mistargeted to the ER (Fig. 3B). It has been suggested that the GET pathway can also recognize TMSs that are not strictly at the C-terminus (Aviram et al., 2016), so it remained possible that it can even recognize proteins with a central TMS, like Mim1.

To understand better the mechanism of mistargeting, we first assayed whether the missorted overexpressed GFP-Mim1 is membrane-embedded, and observed that GFP-Mim1 behaved as a membrane protein in both ER and mitochondria fractions (Fig. 3C,D). We next investigated whether the ER localization is dependent on GET proteins. Hence, we expressed GFP-Mim1 in *get1Δ* or *get3Δ* cells and analysed the protein localization by fluorescence microscopy. Whereas in WT cells ∼20% of the cells had ER staining, only a negligible proportion of the *get* mutant cells displayed the GFP signal in the ER (Fig. 3E,F). We further checked the distribution of GFP-Mim1 in WT and *get* mutants by subcellular fractionation. Importantly, the amount of GFP-Mim1 in the ER was significantly reduced in the *get* deletion strains (Fig. 3G-I). The presence of a residual ER population of the protein, despite deletion of GET components, suggests that the GET pathway is not the only route for GFP-Mim1 targeting to the ER.

Next, we wondered if the mislocalization depends on the presence of the GFP moiety and on its location. To test this, we fused GFP to the C-terminus of Mim1 and analysed the subcellular distribution of the fusion protein. We observed the vast majority of the protein in the mitochondrial fraction, whereas only a minority was mistargeted to the ER (Fig. S2A). Similarly, overexpressed untagged Mim1 was very partially mislocalized to the ER where it was modified in WT, but not in *get3Δ* cells (Fig. S2B). This modification does not appear to be glycosylation (Fig. S2C), and it is not clear to us why we did not observe it in *get3Δ* cells. Of note, the GET machinery does not seem to contribute to the mistargeting of both Mim1 and Mim1-GFP (Fig. S2A,B). This finding is in agreement with the location of the TMS being positioned in the middle of the protein (as in Mim1) or in its N-terminal region (as in Mim1-GFP), rather than in the C-terminal region (as in GFP-Mim1).

Get3 interacts directly with Mcp3 and Mim1

The results described above, suggest that the GET machinery is involved in mistargeting of mitochondrial proteins. To test whether this effect is a direct one, we expressed a His-tagged version of the soluble component Get3 or of its ATP hydrolysis-deficient mutant (D57N) (Stefer et al., 2011), which fails to release substrate proteins, in *E. coli* cells. The purified proteins were incubated with rabbit reticulocyte lysate expressing HA-Mim1 or HA-Mcp3ΔN, or DHFR-HA as a control. Next, a pull-down with anti-HA beads was performed and bound proteins were analysed. While we could detect only minor binding of native Get3 to HA-tagged proteins, the fraction of bound Get3 was much larger for the ATP hydrolysis-deficient mutant D57N (Fig. 4A,B). Of note, none of the Get3 variants was bound to the control protein, DHFR. Thus, these results indicate that Get3 is able to bind *in vitro* to mitochondrial proteins.

To substantiate these findings by an *in vivo* approach, we employed the cytosolic Split-Ubiquitin System (Asseck et al., 2018; Xing et al., 2016). To this end, we used Get3 as a bait, whereas Mcp3ΔN or GFP-Mcp3ΔN were utilized as preys. Indeed, using these combinations, we observed growth of the yeast cells on stringent Met-containing growth medium, whereas the usage of the negative control NubG as a prey did not result in growth under these conditions (Fig. 4C). Hence, we conclude that Get3 is able to interact *in vivo* with Mcp3.

Conclusions

Our study shows that, when allowed to, the GET pathway is able to recognize newly synthesized mitochondrial proteins. However, this capacity becomes relevant only when the mitochondrial import is compromised. Under normal conditions, the high efficiency and fast kinetics of the mitochondrial import apparatus do not provide factors involved in ER-targeting routes with the option to successfully compete for such interactions. This implies that correct intracellular targeting is dictated by a kinetic competition among various potential pathways.

MATERIALS AND METHODS

Yeast strains and growth conditions

Yeast strains used in the study were isogenic to *Saccharomyces cerevisiae* strain W303α or BY4741. Standard genetic techniques were used for growth and manipulation of yeast strains.

Journal of Cell Science (2018) 131, jcs211110. doi:10.1242/jcs.211110

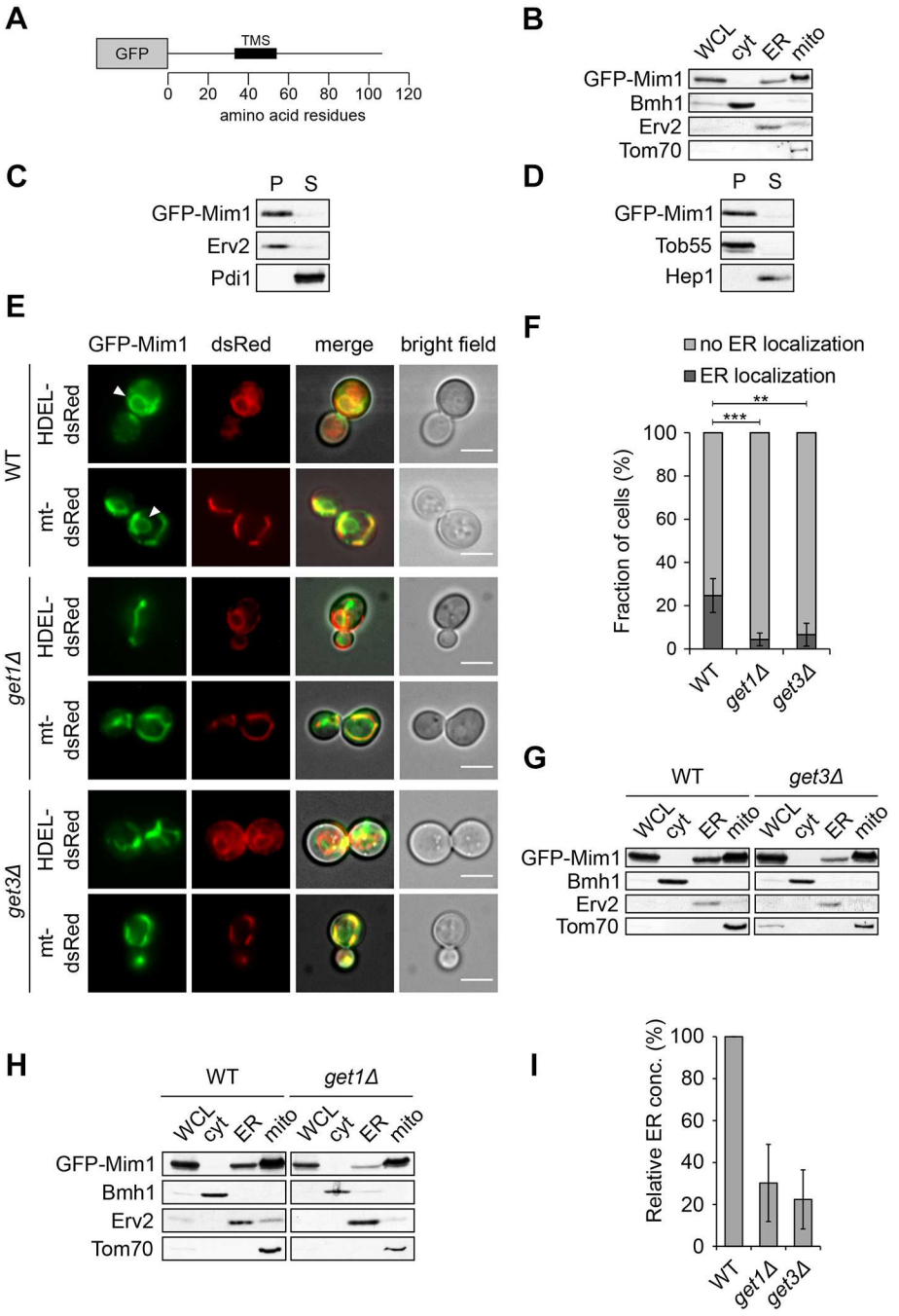

Fig. 3. GET proteins are involved in the mislocalization of GFP-Mim1 to ER. (A) Schematic representation of GFP-Mim1. (B-D) Western blot showing cells expressing GFP-Mim1 subjected to subcellular fractionation (B). (C,D) Western blots of ER (C) and mitochondrial (D) fractions subjected to alkaline extraction. (E) WT, *get1Δ*, and *get3Δ* cells expressing GFP-Mim1 were analysed by fluorescence microscopy as described in the legend to Fig. 2D. Scale bars: 5 µm. (F) Quantification of the intracellular localization of GFP-Mim1 monitored as in E and analysed as described in the legend to Fig. 2E. $^{**}P \leq 0.001$; $^{***}P \leq 0.0001$. (G-H) Western blots of WT, *get3Δ* (G), and *get1Δ* (H) cells expressing GFP-Mim1 subjected to subcellular fractionation. (I) Three independent experiments as shown in G and H were quantified, and the enrichment of GFP-Mim1 in ER fractions are depicted. WCL, whole-cell lysate; cyt, cytosol fraction; ER, microsome fraction; mito, mitochondria fraction; WT, wild type.

Yeast cells were grown in standard rich medium YP (2% [w/v] bacto peptone, 1% [w/v] yeast extract) or synthetic medium S (0.67% [w/v] bacto-yeast nitrogen base without amino acids) with either glucose (2% [w/v], D) or galactose (2% [w/v], Gal) as carbon source. Transformation of yeast cells was performed by the lithium acetate method.

To delete the complete ORFs of *GET1*, *GET2* or *GET3*, they were replaced with KanMX4, CloNAT or Ble cassettes amplified with gene-specific primers. The deletions were confirmed by PCR. The GFP-tag at the N-terminus of the *MCP3* ORF was genomically inserted and encoded under the *SpNOP1* promoter. A GFP-moiety was inserted upstream of the *MIM1* ORF and the fusion protein was expressed under the control of the *ADH* promoter. Table S1 includes a list of strains used in this study.

Recombinant DNA techniques

The cDNAs of rabbit cytochrome b5 ER and its RR variant were amplified by PCR with primers containing EcoRI and HindIII restriction sites from pGEM4-b5ER and pCDNA3-b5RR, respectively (Borgese et al., 2001). The obtained DNA fragments were inserted in-frame with an N-terminal 3HA-tag that was cloned between EcoRI and NcoI sites, into the multi-copy yeast expression plasmid pYX223 (*GAL* promoter). To obtain pGEM4-yk-DHFR-3HA, the DHFR coding sequence was amplified from pGEM4-pSu9-DHFR with primers containing KpnI and BamHI restriction sites as well as the yeast Kozak sequence, and inserted into the pGEM4 plasmid in-frame with a C-terminal 3HA-tag cloned into BamHI and SalI restriction sites.

Plasmid pRS426-TPI-GFP-Mcp3ΔN was obtained by PCR amplification from genomic DNA, of the sequence coding for the 126 most C-terminal amino acids of Mcp3, with primers containing BamHI and HindIII restriction sites. The obtained DNA fragment was inserted in the pRS426-TPI vector in-frame with an N-terminal GFP cloned between two EcoRI sites. The *MCP3*ΔN coding sequence was subcloned, by using BamHI and HindIII restriction enzymes, from this plasmid into a pGEM4 vector

Journal of Cell Science (2018) 131, jcs211110. doi:10.1242/jcs.211110

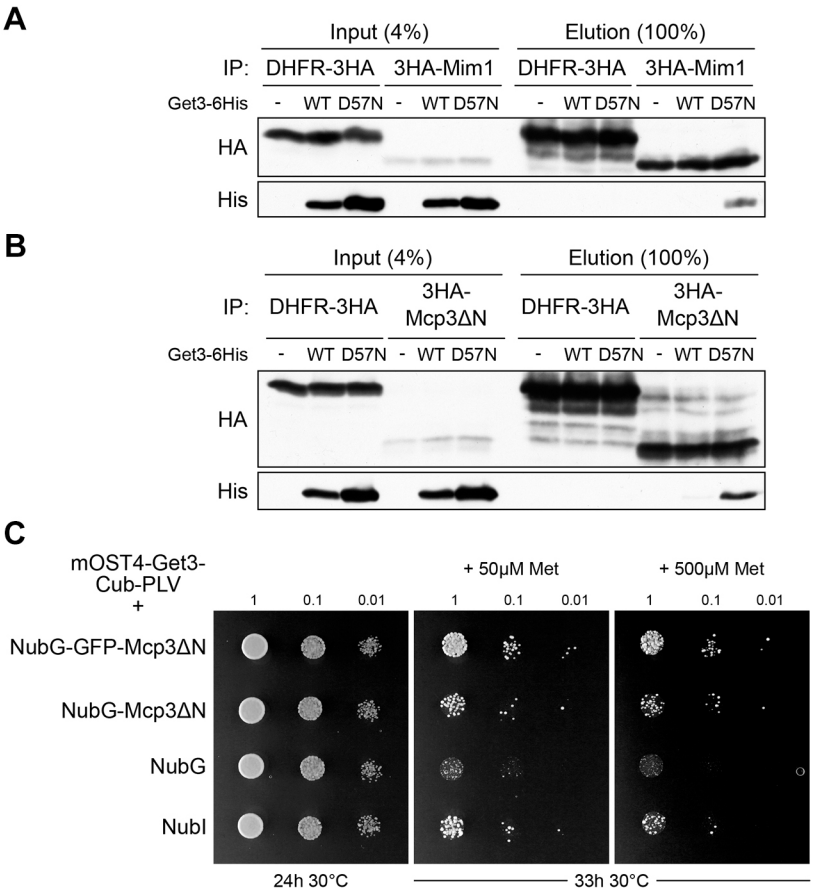

Fig. 4. Get3 physically interacts with Mcp3 and Mim1. (A,B) The indicated radiolabelled HA-tagged proteins were incubated with buffer only (-) or with His-tagged versions of either native Get3 (WT) or the D57N variant. The mixtures were pulled-down with anti-HA beads. Samples from the input and the eluates were analysed by SDS-PAGE and immunoblotting. (C) The cytoSUS was used to monitor interaction of Get3 (used as bait) with Mcp3ΔN (used as prey) with or without GFP-tag together with controls (NubG, negative; NubI, positive). Diploid yeast cells were dropped at OD_{600} of 1.0, 0.1 and 0.01 on complete supplement mixture (CSM) medium to verify mating and on CSM with either 50 or 500 μM methionine to test for the specificity of interaction.

containing the yeast Kozak sequence and an N-terminal 3HA-tag between EcoRI and KpnI sites. The ORF coding for Mim1 was amplified by PCR from pRS426-TPI-*MIM1* with primers containing restriction sites BamHI and HindIII, and four Met residues at the C-terminus. The obtained fragment was inserted in-frame with an N-terminal 3HA-tag, which was cloned between the EcoRI and KpnI restriction sites, into a pGEM4 vector containing the yeast Kozak sequence. To obtain the construct Mim1-GFP, the MIM1 ORF without a stop codon was PCR amplified with primers containing EcoRI and BamHI restriction sites. Then, the PCR product was treated with both restriction enzymes and was inserted into the pRS426-TPI vector in-frame with a C-terminal GFP, which was inserted between KpnI and HindIII restriction sites. Similarly, the *MIM1* ORF was inserted into the pYX223 vector using EcoRI and HindIII.

Biochemical methods

Protein samples for immunoblotting were analysed on 12.5% or 15% SDS-PAGE and subsequently transferred onto nitrocellulose membranes by semi-dry western blotting. Proteins were detected by incubating the membranes, first with primary antibodies and then with horseradish peroxidase-conjugates of goat anti-rabbit or goat anti-rat secondary antibodies. Band intensities were quantified using the AIDA software (Elysia-raytest, Straubenhardt, Germany). Enrichment in the ER fraction was calculated by dividing the signal for the protein of interest in the ER fraction by that in the whole-cell lysate. This value was then divided by the same ratio calculated for the marker ER protein, Erv2 or Sec61 (protein X in ER/protein X in WCL)/(Erv2 or Sec61 in ER/Erv2 or Sec61 in WCL).

Subcellular fractionation was performed as described before (Walther et al., 2009). Isolation of mitochondria from yeast cells was performed by differential centrifugation, as previously described (Daum et al., 1982). To obtain highly pure mitochondria, isolated organelles were layered on top of a Percoll gradient and isolated according to a published procedure (Graham, 2001).

For protease protection assay, 50 μg of microsomes were resuspended in 100 μl of SEM buffer (250 mM sucrose, 1 mM EDTA, 10 mM MOPS pH 7.2). As a control, microsomes were treated with 1% Triton X-100 in SEM buffer and incubated on ice for 30 min. The samples were supplemented with proteinase K (50 μg/ml) and incubated on ice for 30 min. The proteolytic reaction was stopped with 5 mM phenylmethylsulfonyl fluoride (PMSF). The samples were precipitated with trichloroacetic acid (TCA) and resuspended in 40 μl of 2× Laemmli buffer, heated for 10 min at 50°C, and analysed by SDS-PAGE and immunoblotting.

To analyse the membrane topology of proteins, alkaline extraction was performed. Mitochondria or ER fractions (50 μg) were resuspended in 100 μl of buffer containing 10 mM HEPES-KOH pH 11.5 with 100 mM Na_2CO_3, and incubated on ice for 30 min. The membrane fraction was pelleted by centrifugation (76,000 ***g***, at 2°C for 30 min) and the supernatant fraction was precipitated with TCA. Both fractions were resuspended in 40 μl of 2× Laemmli buffer, heated for 10 min at 50°C or 95°C, and analysed by SDS-PAGE and immunoblotting.

The following proteins were used as marker proteins in western blots shown in Figs 1-4: Bmh1, a cytosolic protein; Erv2, an ER membrane protein exposed to the ER lumen; Fis1, a mitochondrial membrane protein; Hep1, a soluble mitochondrial protein; Om14, a mitochondrial membrane protein; Pdi1, a soluble glycosylated ER protein; Tom70, a mitochondrial membrane protein; Sec61, an ER membrane protein; Tob55, a mitochondrial membrane protein; Tom40, a MOM protein. Table S1 includes a list of the antibodies used in this study.

In vitro interactions of recombinant Get3

Plasmids encoding His-tagged versions of Get3 and of its ATP hydrolysis-deficient mutant (D57N) were a kind gift from Irmgard Sinning. Proteins were expressed in *E. coli* cells and purified as described previously (Stefer et al., 2011). 3HA-Mim1, 3HA-Mcp3ΔN or DHFR-3HA were translated *in vitro* in rabbit reticulocyte lysate in the presence of 10 mM DTT and 5 μM of recombinant Get3-6His or Get3D57N-6His. After translation, the lysate was diluted with KHM buffer (110 mM KAc, 20 mM HEPES-KOH pH 7.4, 2 mM $MgCl_2$) supplemented with 50 mM ATP. Then, the lysate was added

to magnetic anti-HA beads (10 µl) that had been equilibrated with KHM buffer for 30 min at 4°C, and incubated with them for 2 h at 4°C. The beads were washed four times with KHM buffer and bound proteins were eluted at either 95°C or 50°C for 10 min with 100 µl of 2× Laemmli buffer lacking β-mercaptoethanol but supplemented with 5% H_2O_2. Samples were analysed by SDS-PAGE and immunoblotting.

Glycosylation assay

To test for glycosylation of proteins, 50 µg of the ER fraction was resuspended in 10 µl glycoprotein denaturing buffer (0.5% SDS, 40 mM DTT) and incubated for 10 min at 95°C. Then, the samples were supplemented with 500 units of either endoglycosidase H (EndoH) or peptide:N-glycosidase F (PNGase) (New England BioLabs) in the respective buffer (according to the manufacturer's instructions) and incubated for 1 h at 37°C. At the end of the incubation period, the samples were precipitated with TCA, resuspended in 40 µl of 2× Laemmli buffer, heated for 10 min at either 50°C or 95°C, and analysed by SDS-PAGE and immunoblotting.

The yeast cytosolic split-ubiquitin system

The yeast cytosolic split-ubiquitin system (cytoSUS) was used to detect physical interaction. The bait protein Get3 was expressed from the Met25 promoter, N-terminally fused to the transmembrane domain of OST4p (mOST4) to ensure membrane anchoring and C-terminally tagged with the C-terminal ubiquitin moiety (Cub) followed by the chimeric ProteinA-LexA-VP16 (PLV) transcription activator (Xing et al., 2016). The bait fusion was transformed in the *S. cerevisiae* strain THY.AP4. N-terminally NubG-2×HA-tagged prey proteins GFP-Mcp3ΔN and Mcp3ΔN, as well as the control peptides NubG (as a positive control) and NubI (wild-type Nub, as a positive control) were transformed in the *S. cerevisiae* strain THY.AP5. After mating, diploids were selected. Interaction analysis was performed by spotting serial dilutions of diploid yeast on interaction-selective complete supplement mixture (CSM) medium lacking adenine and histidine but containing increasing concentrations of methionine (50–500 µM) to decrease bait expression. Protein expression was verified by western blotting utilizing anti-VP16 antibody (rabbit, GeneTex) for bait and anti-HA peroxidase-conjugated (Roche) antibody for prey fusions as described previously (Asseck et al., 2018; Xing et al., 2016).

Fluorescence microscopy

Fluorescence images were acquired using a spinning disk microscope (Zeiss Axio Examiner Z1) equipped with a CSU-X1 real-time confocal system (Visitron), VS-Laser system and SPOT Flex CCD camera (Visitron Systems). Images were analysed with VisiView software (Visitron). Microscopy images of strains expressing GFP-Mim1 were acquired with an Axioskop 20 fluorescence microscope equipped with an Axiocam MRm camera using the 43 Cy3 filter set and the AxioVision software (Carl Zeiss).

Acknowledgements

We thank E. Kracker for excellent technical assistance and Irmgard Sinning, Biochemistry Center (BZH), Heidelberg, Germany, for plasmids.

Competing interests

The authors declare no competing or financial interests.

Author contributions

Conceptualization: D.G.V., C.G., B.S., N.B., D.R.; Methodology: D.G.V., E.P.B., M. Sinzel, A.K., S.Z., D.G.M., A.C., A.F., B.F.C., C.G., D.R.; Formal analysis: D.R.; Investigation: D.G.V., E.P.B., M. Sinzel, A.K., S.Z., A.C., B.F.C., C.G.; Resources: A.C., A.F., M. Schuldiner, B.S., N.B., D.R.; Data curation: E.P.B., M. Sinzel, A.K., S.Z., D.G.M., C.G.; Writing - original draft: D.G.V., M. Schuldiner, B.S., N.B., D.R.; Writing - review & editing: C.G.; Supervision: B.S., N.B., D.R.

Funding

This work was supported by the Deutsche Forschungsgemeinschaft (Sonderforschungsbereich 1190-TP04 to B.S.; RA 1028/7-1 to D.R.; Deutsch-Israelische Projektkooperation to D.R. and M. Schuldiner; and GR 4251/2-1 to C.G.), and the ITN TAMPting network to D.G.V., B.F.C., B.S., N.B. and D.R. [funded by the People Programme (Marie Curie Actions) of the European Union's Seventh Framework Programme FP7/2007-2013/ under REA grant agreement no 607072].

Supplementary information

Supplementary information available online at
http://jcs.biologists.org/lookup/doi/10.1242/jcs.211110.supplemental

References

Asseck, L. Y., Wallmeroth, N. and Grefen, C. (2018). ER membrane protein interactions using the Split-Ubiquitin System (SUS). *Methods Mol. Biol.* **1691**, 191-203.

Aviram, N., Ast, T., Costa, E. A., Arakel, E. C., Chuartzman, S. G., Jan, C. H., Haßdenteufel, S., Dudek, J., Jung, M., Schorr, S. et al. (2016). The SND proteins constitute an alternative targeting route to the endoplasmic reticulum. *Nature* **540**, 134-138.

Borgese, N. and Fasana, E. (2011). Targeting pathways of C-tail-anchored proteins. *Biochim. Biophys. Acta* **1808**, 937-946.

Borgese, N., Gazzoni, I., Barberi, M., Colombo, S. and Pedrazzini, E. (2001). Targeting of a tail-anchored protein to endoplasmic reticulum and mitochondrial outer membrane by independent but competing pathways. *Mol. Biol. Cell* **12**, 2482-2496.

Brambillasca, S., Yabal, M., Soffientini, P., Stefanovic, S., Makarow, M., Hegde, R. S. and Borgese, N. (2005). Transmembrane topogenesis of a tail-anchored protein is modulated by membrane lipid composition. *EMBO J.* **24**, 2533-2542.

Casson, J., McKenna, M., Haßdenteufel, S., Aviram, N., Zimmerman, R. and High, S. (2017). Multiple pathways facilitate the biogenesis of mammalian tail-anchored proteins. *J. Cell Sci.* **130**, 3851-3861.

Colombo, S. F., Longhi, R. and Borgese, N. (2009). The role of cytosolic proteins in the insertion of tail-anchored proteins into phospholipid bilayers. *J. Cell Sci.* **122**, 2383-2392.

D'Arrigo, A., Manera, E., Longhi, R. and Borgese, N. (1993). The specific subcellular localization of two isoforms of cytochrome b5 suggests novel targeting pathways. *J. Biol. Chem.* **268**, 2802-2808.

Daum, G., Böhni, P. C. and Schatz, G. (1982). Import of proteins into mitochondria: cytochrome b2 and cytochrome c peroxidase are located in the intermembrane space of yeast mitochondria. *J. Biol. Chem.* **257**, 13028-13033.

Dukanovic, J. and Rapaport, D. (2011). Multiple pathways in the integration of proteins into the mitochondrial outer membrane. *Biochim. Biophys. Acta* **1808**, 971-980.

Egan, B., Beilharz, T., George, R., Isenmann, S., Gratzer, S., Wattenberg, B. and Lithgow, T. (1999). Targeting of tail-anchored proteins to yeast mitochondria in vivo. *FEBS Lett.* **451**, 243-248.

Fueller, J., Egorov, M. V., Walther, K. A., Sabet, O., Mallah, J., Grabenbauer, M. and Kinkhabwala, A. (2015). Subcellular partitioning of protein tyrosine phosphatase 1B to the endoplasmic reticulum and mitochondria depends sensitively on the composition of its tail anchor. *PLoS ONE* **10**, e0139429.

Graham, J. M. (2001). Isolation of mitochondria from tissues and cells by differential centrifugation. *Curr. Prot. Cell Biol.* Chapter 3: 3.3.1-3.3.15.

Hassdenteufel, S., Sicking, M., Schorr, S., Aviram, N., Fecher-Trost, C., Schuldiner, M., Jung, M., Zimmermann, R. and Lang, S. (2017). hSnd2 protein represents an alternative targeting factor to the endoplasmic reticulum in human cells. *FEBS Lett.* **591**, 3211-3224.

Ishikawa, D., Yamamoto, H., Tamura, Y., Moritoh, K. and Endo, T. (2004). Two novel proteins in the mitochondrial outer membrane mediate β-barrel protein assembly. *J. Cell Biol.* **166**, 621-627.

Kalbfleisch, T., Cambon, A. and Wattenberg, B. W. (2007). A bioinformatics approach to identifying tail-anchored proteins in the human genome. *Traffic* **8**, 1687-1694.

Kemper, C., Habib, S. J., Engl, G., Heckmeyer, P., Dimmer, K. S. and Rapaport, D. (2008). Integration of tail-anchored proteins into the mitochondrial outer membrane does not require any known import components. *J. Cell Sci.* **121**, 1990-1998.

Krumpe, K., Frumkin, I., Herzig, Y., Rimon, N., Özbalci, C., Brügger, B., Rapaport, D. and Schuldiner, M. (2012). Ergosterol content specifies targeting of tail-anchored proteins to mitochondrial outer membranes. *Mol. Biol. Cell* **23**, 3927-3935.

Rao, M., Okreglak, V., Chio, U. S., Cho, H., Walter, P. and Shan, S.-O. (2016). Multiple selection filters ensure accurate tail-anchored membrane protein targeting. *eLife* **5**, e21301.

Schuldiner, M., Metz, J., Schmid, V., Denic, V., Rakwalska, M., Schmitt, H. D., Schwappach, B. and Weissman, J. S. (2008). The GET complex mediates insertion of tail-anchored proteins into the ER membrane. *Cell* **134**, 634-645.

Sinzel, M., Tan, T., Wendling, P., Kalbacher, H., Özbalci, C., Chelius, X., Westermann, B., Brügger, B., Rapaport, D. and Dimmer, K. S. (2016). Mcp3 is a novel mitochondrial outer membrane protein that follows a unique IMP-dependent biogenesis pathway. *EMBO Rep.* **17**, 965-981.

Stefer, S., Reitz, S., Wang, F., Wild, K., Pang, Y.-Y., Schwarz, D., Bomke, J., Hein, C., Lohr, F., Bernhard, F. et al. (2011). Structural basis for tail-anchored

membrane protein biogenesis by the Get3-receptor complex. *Science* **333**, 758-762.

Waizenegger, T., Schmitt, S., Zivkovic, J., Neupert, W. and Rapaport, D. (2005). Mim1, a protein required for the assembly of the TOM complex of mitochondria. *EMBO Rep.* **6**, 57-62.

Walther, D. M., Papic, D., Bos, M. P., Tommassen, J. and Rapaport, D. (2009). Signals in bacterial β-barrel proteins are functional in eukaryotic cells for targeting to and assembly in mitochondria. *Proc. Natl. Acad. Sci. USA* **106**, 2531-2536.

Wang, F., Brown, E. C., Mak, G., Zhuang, J. and Denic, V. (2010). A chaperone cascade sorts proteins for posttranslational membrane insertion into the endoplasmic reticulum. *Mol. Cell* **40**, 159-171.

Wang, F., Whynot, A., Tung, M. and Denic, V. (2011). The mechanism of tail-anchored protein insertion into the ER membrane. *Mol. Cell* **43**, 738-750.

Xing, S., Wallmeroth, N., Berendzen, K. W. and Grefen, C. (2016). Techniques for the Analysis of Protein-Protein Interactions in Vivo. *Plant Phys.* **171**, 727-758.

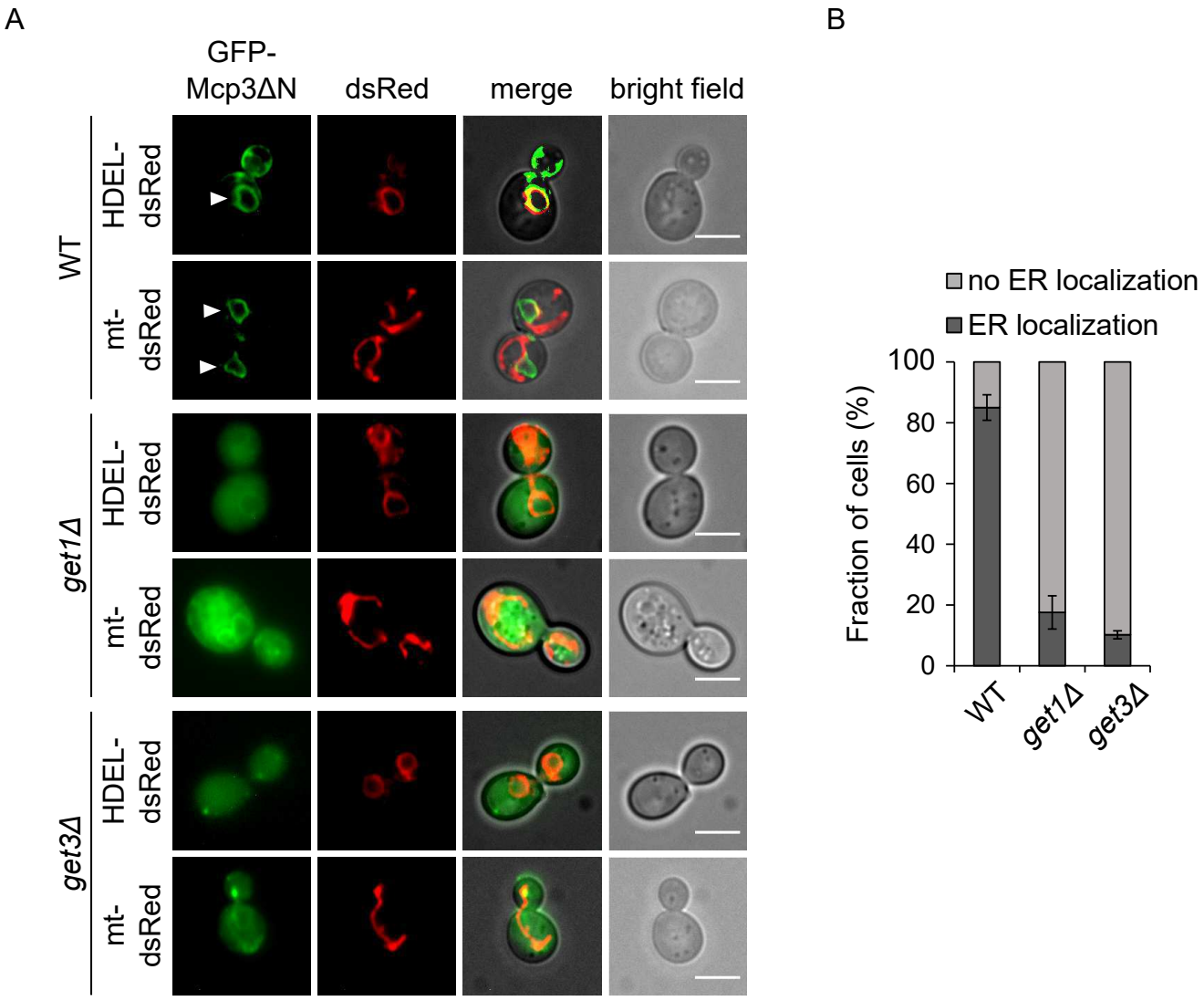

Fig. S1. The partial mistargeting of GFP-Mcp3ΔN to ER requires the GET machinery. (A) WT, *get1Δ* and *get3Δ* cells expressing GFP-Mcp3ΔN and either the ER marker HDEL-dsRed or the mitochondrial marker mt-dsRed were analysed by fluorescence microscopy and representative images are shown. The intensity of the GFP signal in *get1Δ* and *get3Δ* cells was digitaly enhanced compared to WT. Arrowheads indicate the perinuclear ER staining. Scale bars, 5 µm. **(B)** Quantification of the intracellular localization of GFP-Mcp3ΔN monitored as in (A). The figure shows the average and the SD of three independent experiments with at least 100 cells each.

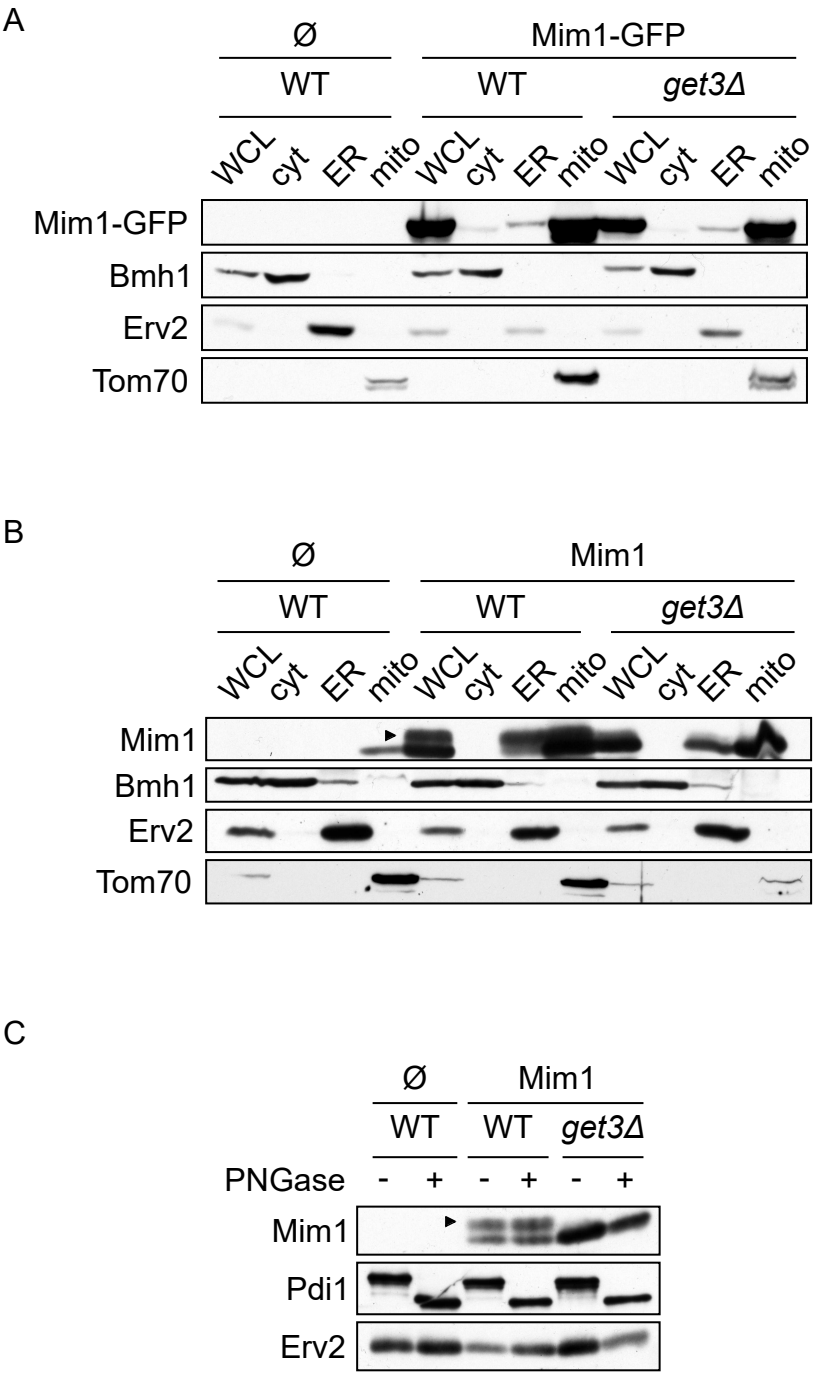

Fig. S2. Mim1 is partially mistargeted to ER independently of the presence and the position of the GFP tag. (A-B) Whole cell lysate (WCL) and fractions corresponding to cytosol (cyt), microsomes (ER) and mitochondria (mito) from WT and *get3Δ* cells transformed with an empty vector (Ø) or with a plasmid expressing either Mim1-GFP (A) or Mim1 (B) were analysed by SDS-PAGE and immunodecoration with the indicated antibodies. **(C)** ER fraction isolated as in (B) was incubated in the presence of Peptide:N-Glycosidase F (PNGase) and analysed by SDS-PAGE and immunodecoration with the indicated antibodies. Pdi1 served as a control for glycosylated protein. Arrowhead, modified form of Mim1.

Table S1: List of yeast strains, plasmids and antibodies used in this study

Strains

Name	Mating type	Genetic background	Source or reference
W303α	*MATα*	*ade2-1 can1-100 his3-11 leu2 3_112 trp1Δ2 ura3-52*	
S288c	*MATa*	BY4741 *his3::kan leu2Δ0 met15Δ0 ura3Δ0*	
YMS412	*MATa*	BY4741 *get1::KanMX*	
YMS414	*MATa*	BY4741 *get3::KanMX*	
	MATa	BY4741 hphΔn::URA3::SpNOP1pr-sfGFP-*MCP3*	Yofe et al., 2016
	MATa	BY4741hphΔn::URA3::SpNOP1pr-sfGFP-*MCP3 get3::CloNAT*	
	MATa	BY4741 hphΔn::URA3::SpNOP1pr-sfGFP-*MCP3 get1::KanMX get2::CloNAT*	
	MATa	BY4741 hphΔn::URA3::SpNOP1pr-sfGFP-*MCP3 get1::KanMX get2::CloNAT get3::Ble*	
YMS1258	*MATa*	BY4741 ADHpr-GFP-*MIM1*::CloNAT	Papic et al., 2013.
YDGV156	*MATa*	BY4741 ADHpr-GFP-*MIM1*::CloNAT *get1::HIS3*	This study
YDGV157	*MATa*	BY4741 ADHpr-GFP-*MIM1*::CloNAT *get3::HIS3*	This study
YDGV257	*MATa*	BY4741 hphΔn::URA3::SpNOP1pr-sfGFP-*MCP3 pdr5::KanMX*	This study
YDGV258	*MATa*	BY4741 hphΔn::URA3:: SpNOP1pr-sfGFP-*MCP3 get3::CloNAT pdr5::KanMX*	This study
THY.AP4	*MATa*	MATa; leu2–3,112 ura3–52 trp1–289 lexA::HIS3 lexA::ADE2 lexA::lacZ	Obrdlik et al., 2004
THY.AP5	*MATα*	MATα; URA3 leu2-3,112 trp1-289 his3-Δ1 ade2Δ::loxP	Obrdlik et al., 2004.

Plasmids

Plasmids	Promoter	Markers	Source or reference
pYX223-3xHA-b5ER	GAL	HIS3, Amp^R	This study
pYX223-3xHA-b5RR	GAL	HIS3, Amp^R	This study
pYX142-pSU9-dsRed	TPI	LEU2, Amp^R	Friedman et al., 2011.
pGEM4-yk-DHFR-3HA	SP6	Amp^R	This study
pGEM4-yk-3HA-Mim1-4M	SP6	Amp^R	This study
pGEM4-yk-3HA-Mcp3ΔN	SP6	Amp^R	This study
pETM13-Get3-6HIS	T7	Kan^R	Stefer et al., 2011 (original name pYLA54)
pETM13-Get3D57N-6HIS	T7	Kan^R	Stefer et al., 2011 (original name pYLA55)
PRS426-TPI-GFP-Mcp3ΔN	TPI	URA3, Amp^R	This study
pRS426-TPI-Mim1-GFP	TPI	URA3, Amp^R	This study
pYX223-Mim1	GAL	HIS3, Amp^R	This study
pRS426-TPI-Mim1-8His	TPI	URA3, Amp^R	Popov-Čeleketić et at., 2008
pNX35-GFP-Mcp3pΔN	ADH1	TRP1, Amp^R	This study
pNX35-Mcp3pΔN	ADH1	TRP1, Amp^R	This study
pMetOYC-Get3	met25	LEU2, , Amp^R	This study
pNubWtXgate	ADH1	TRP1, Amp^R, CM^R	Obrdlik et al., *PNAS*, 2004.
pNX35-Dest	ADH1	TRP1, Amp^R, CM^R	Grefen and Blatt, 2012.

Antibodies

Antibodies	dilution	Source
polyclonal rat anti-HA	1 : 1500	11867423001 (Roche)
polyclonal rabbit anti-Bmh1	1 : 1500	Lab stocks
polyclonal rabbit anti-Erv2	1 : 1000	Lab stocks
polyclonal rabbit anti-Tom40	1 : 4000	Lab stocks
polyclonal rabbit anti-Sec61	1 : 10000	Lab stocks
polyclonal rabbit anti-Pdi1	1 : 3000	Lab stocks
polyclonal rabbit anti-Tob55	1 : 2000	Lab stocks
polyclonal rabbit anti-Hep1	1 : 3000	Lab stocks
polyclonal rabbit anti-Om14	1 : 4000	Lab stocks
polyclonal rabbit anti-GFP	1 : 1000	TP401 (Torrey Pines)
polyclonal rabbit anti-Fis1	1 : 1000	Lab stocks
polyclonal rabbit anti-Tom70	1 : 2000	Lab stocks
polyclonal rabbit anti-6HIS	1 : 4000	A190-114A (Biomol)

References

Friedman, J.R., Lackner, L.L., West, M., DiBenedetto, J.R., Nunnari, J., Voeltz, G.K. (2011) ER Tubules Mark Sites of Mitochondrial Division. *Science* **334**, 358-362

Grefen, C., and Blatt, M.R. (2012) Do calcineurin B-like proteins interact independently of the serine threonine kinase CIPK23 with the K^+ channel AKT1? Lessons learned from a ménage à trois. *Plant Physiol.* **159**, 915-919

Obrdlik, P., El-Bakkoury, M., Hamacher, T., Cappellaro, C., Vilarino, C., Fleischer, C., Ellerbrok, H., Kamuzinzi, R., Ledent, V., Blaudez, D., Sanders, D., Revuelta, J.L., Boles, E., Andre´, B., and Frommer, W.B. (2004) K^+ channel interactions detected by a genetic system optimized for systematic studies of membrane protein interactions. *Proc. Natl. Acad. Sci. USA* **101**, 12242–12247

Papic, D., Elbaz-Alon, Y., Koerdt, S.N., Leopold, K., Worm, D., Jung, M., Schuldiner, M., and Rapaport D. (2013) The Role of Djp1 in Import of the Mitochondrial Protein Mim1 Demonstrates Specificity between a Cochaperone and Its Substrate Protein. *Mol. Cell. Biol.* **33**, 4083–4094

Popov-Celeketić, J., Waizenegger, T., Rapaport D. (2008) Mim1 functions in an oligomeric form to facilitate the integration of Tom20 into the mitochondrial outer membrane. *J. Mol. Biol.* **376**, 671-680

Stefer, S., Reitz, S., Wang, F., Wild, K., Pang, Y.Y., Schwarz, D., Bomke, J., Hein, C., Lohr, F., Bernhard, F., Denic, V., Dotsch, V., and Sinning, I. (2011) Structural basis for tail-anchored membrane protein biogenesis by the Get3-receptor complex. *Science* **333**, 758-762

Yofe, I., Weill, U., Meurer, M., Chuartzman, S., Zalckvar, E., Goldman, O., Ben-Dor, S., Schütze, C., Wiedemann, N., Knop, M., Khmelinskii, A., and Schuldiner M. (2016) One library to make them all: streamlining the creation of yeast libraries via a SWAp-Tag strategy. *Nature Meth.* **13**, 371-378

eLIFE elifesciences.org

RESEARCH ARTICLE

Independent evolution of functionally exchangeable mitochondrial outer membrane import complexes

Daniela G Vitali[1†], Sandro Käser[2†], Antonia Kolb[1†], Kai S Dimmer[1], Andre Schneider[2*], Doron Rapaport[1*]

[1]Interfaculty Institute of Biochemistry, University of Tübingen, Tübingen, Germany; [2]Department of Chemistry and Biochemistry, University of Bern, Bern, Switzerland

Abstract Assembly and/or insertion of a subset of mitochondrial outer membrane (MOM) proteins, including subunits of the main MOM translocase, require the fungi-specific Mim1/Mim2 complex. So far it was unclear which proteins accomplish this task in other eukaryotes. Here, we show by reciprocal complementation that the MOM protein pATOM36 of trypanosomes is a functional analogue of yeast Mim1/Mim2 complex, even though these proteins show neither sequence nor topological similarity. Expression of pATOM36 rescues almost all growth, mitochondrial biogenesis, and morphology defects in yeast cells lacking Mim1 and/or Mim2. Conversely, co-expression of Mim1 and Mim2 restores the assembly and/or insertion defects of MOM proteins in trypanosomes ablated for pATOM36. Mim1/Mim2 and pATOM36 form native-like complexes when heterologously expressed, indicating that additional proteins are not part of these structures. Our findings indicate that Mim1/Mim2 and pATOM36 are the products of convergent evolution and arose only after the ancestors of fungi and trypanosomatids diverged.
DOI: https://doi.org/10.7554/eLife.34488.001

***For correspondence:** andre.schneider@dcb.unibe.ch (AS); doron.rapaport@uni-tuebingen.de (DR)

[†]These authors contributed equally to this work

Competing interests: The authors declare that no competing interests exist.

Funding: See page 19

Received: 19 December 2017
Accepted: 06 May 2018
Published: 20 June 2018

Reviewing editor: Nikolaus Pfanner, University of Freiburg, Germany

Introduction

Mitochondrial outer membrane (MOM) proteins include a diverse set of enzymes, components of protein import machineries, pore forming proteins, as well as proteins mediating mitochondrial fusion, fission, and motility. In addition, the MOM harbours proteins that regulate apoptosis and mitophagy and hence are of central importance for the fate of the organelle and the whole cell. All these MOM proteins are nuclear-encoded and synthesised on cytosolic ribosomes. Therefore, they have to bear appropriate signals that ensure both their correct targeting to the organelle and their ability to acquire different topologies in the lipid bilayer. Despite their well-recognised importance, the diverse molecular mechanisms by which MOM proteins are specifically targeted to the organelle and inserted into their target membrane remain incompletely defined (***Dukanovic and Rapaport, 2011***).

MOM proteins can be divided into several topological groups (***Dukanovic and Rapaport, 2011***). Some of them span the lipid bilayer with one transmembrane segment (TMS), while others transverse the membrane with multiple β-strands or α-helical structures. Depending on their orientation, single-span proteins can be classified into three groups: the first two are signal- or tail-anchored proteins, which face the intermembrane space (IMS) with either the N- or C-terminus, respectively. These proteins typically expose the bulk of the protein to the cytosol and only a very short segment faces the IMS. A third subclass of single-span proteins exposes soluble domains towards both the IMS and the cytosol. Other integral MOM proteins span the bilayer either with several α-helical TMSs or as β-barrel structures. Whereas the import pathway taken by β-barrel precursor proteins has been studied in some detail (***Becker et al., 2008b***; ***Endo and Yamano, 2009***; ***Walther et al.,***

2009), much less is known about the factors and the mechanisms that assure the membrane integration of MOM proteins with helical TMSs.

MOM helical multispan proteins follow a unique import pathway in yeast cells (*Becker et al., 2011*; *Papic et al., 2011*). Precursors of these proteins are integrated into the membrane in a process where the MOM protein *m*itochondrial *im*port 1 (Mim1) cooperates with the import receptor Tom70 in binding precursor proteins and facilitating their insertion into the lipid bilayer. Interestingly, it appears that neither other subunits of the translocase of the outer membrane (TOM) nor components residing in the mitochondrial IMS are involved in this process. Currently, it is unresolved whether the MIM complex has only a receptor-like function or it acts also as an insertase (*Vögtle et al., 2015*). In addition to mediating the membrane integration of multi-span proteins, Mim1 is also involved in the biogenesis of the import receptors Tom20 and Tom70 and therefore the protein is also required for the proper assembly of the TOM complex (*Becker et al., 2008a*; *Dimmer et al., 2012*; *Hulett et al., 2008*; *Lueder and Lithgow, 2009*; *Thornton et al., 2010*; *Waizenegger et al., 2005*). Mim1 is known to interact with Mim2, another protein of the MOM that has a crucial role in the biogenesis of α-helical multispan proteins (*Dimmer et al., 2012*; *Krüger et al., 2017*). Both proteins form a high-molecular-weight complex (MIM complex). They transverse the MOM once and expose their N-terminal domains to the cytosol whereas their C-terminal regions are facing the IMS (*Dimmer et al., 2012*; *Ishikawa et al., 2004*; *Lueder and Lithgow, 2009*; *Waizenegger et al., 2005*).

Considering their multifaceted functions, it is not surprising that the absence of Mim1 and/or Mim2 results in severe growth retardation and multiple cellular defects like hampered assembly of the TOM complex, alteration in mitochondrial morphology, and accumulation of unprocessed mitochondrial precursor proteins (*Dimmer et al., 2012*; *Ishikawa et al., 2004*; *Mnaimneh et al., 2004*; *Popov-Celeketić et al., 2008*; *Waizenegger et al., 2005*). Mim1 and Mim2 are conserved among various fungi but homologues in any other eukaryotes were not identified so far (*Dimmer et al., 2012*; *Ishikawa et al., 2004*; *Otera et al., 2007*; *Waizenegger et al., 2005*). This situation raises the question which factor(s) facilitate the membrane integration of helical MOM proteins in non-fungal organisms.

Recently, a first candidate for such a factor was reported in the parasitic protozoan *Trypanosoma brucei*. It was shown that the integral MOM protein, *p*eripheral *a*rchaic *t*ranslocase of the *o*uter *m*embrane 36 (pATOM36), in analogy to the MIM complex, is involved in the assembly and/or membrane insertion of a small subset of MOM proteins including subunits of the main trypanosomal outer membrane protein translocase (ATOM complex) (*Bruggisser et al., 2017*; *Käser et al., 2016*). However, in contrast to the MIM complex, pATOM36 is also directly required for the inheritance of the single unit mitochondrial genome of trypanosomes, termed kinetoplast DNA (kDNA). A fraction of the protein localises to the tripartite attachment complex (TAC) (*Käser et al., 2016*), which connects the kDNA across the two mitochondrial membranes with the basal body of the flagellum (*Schnarwiler et al., 2014*).

Although pATOM36 and Mim1/2 do not share any sequence or topological similarities (*Figure 1—figure supplement 1*), we wondered whether convergent evolution allowed these unrelated proteins to fulfil similar tasks in the biogenesis of MOM proteins. To address this question, we expressed pATOM36 in yeast cells. Remarkably, introduction of pATOM36 could complement the deletion of *MIM1, MIM2,* or even of both genes. Accordingly, the presence of pATOM36 in the deletion strains could reverse the known alterations resulting from the absence of the MIM complex. Importantly, the reciprocal complementation was also successful and co-expression of Mim1 and Mim2 in *T. brucei* cells ablated for pATOM36 could rescue all phenotypes associated with the MOM protein biogenesis function of pATOM36. Taken together, we present the first reciprocal functional rescue of two evolutionary unrelated mitochondrial biogenesis complexes between eukaryotic supergroups.

Results

pATOM36 forms a native-like complex in yeast cells

To better understand the functional relation between yeast Mim1/2 and *T. brucei* pATOM36, we wanted to investigate whether the trypanosomal protein can complement the phenotypes observed in yeast cells lacking the MIM complex. To that aim, plasmids encoding for pATOM36 or its

C-terminally 3xHA-tagged version (pATOM36-HA), as well as an empty plasmid (Ø) as a control, were transformed into wild type (WT), *mim1Δ*, *mim2Δ* or *mim1Δ/mim2Δ* cells. In *T. brucei*, pATOM36 is an integral MOM protein with the C-terminus exposed to the cytosol (***Pusnik et al., 2012***). Blue native (BN)-PAGE analysis has shown that the endogenous protein occurs in two groups of protein complexes of unknown composition with molecular weights of approximately 140–250 kDa and larger than 480 kDa (***Käser et al., 2016***; ***Pusnik et al., 2012***).

Initially, we verified that pATOM36-HA can be expressed in the aforementioned yeast strains (***Figure 1—figure supplement 2***). Next, we isolated mitochondria from either control or *mim1Δ/mim2Δ* cells harbouring pATOM36-HA. We observed that the C-terminally HA-tagged pATOM36, similar to the yeast import receptor Tom70, is accessible to added proteinase K in isolated mitochondria, whereas the matrix protein Hep1 was protected as would be expected for intact organelles

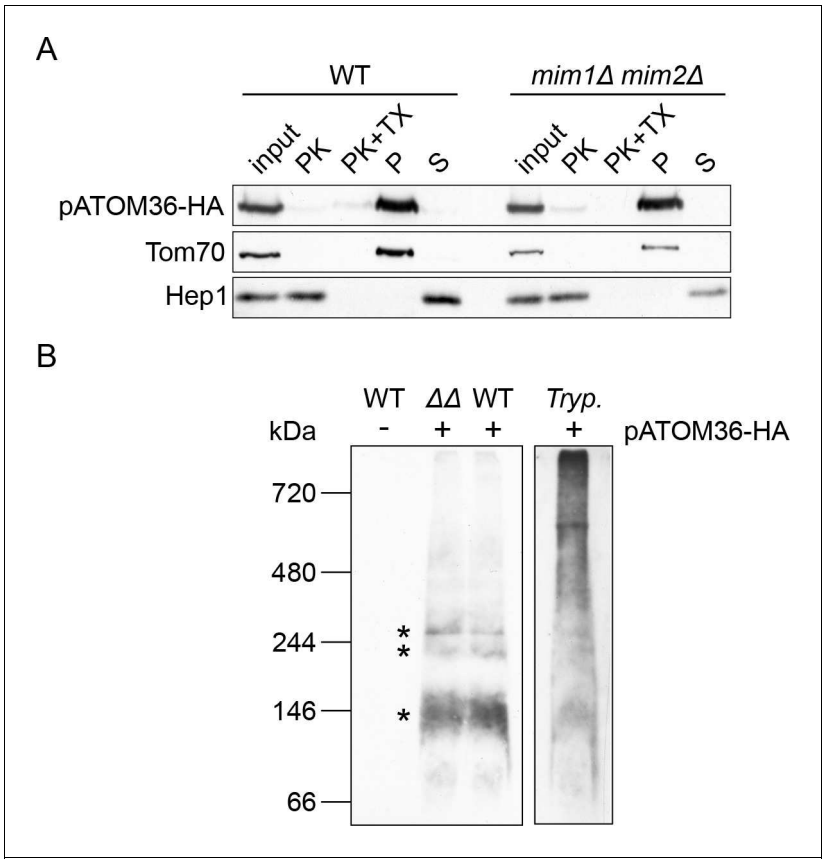

Figure 1. pATOM36 forms native-like complexes in the yeast mitochondrial OM. (**A**) Mitochondria isolated from WT or *mim1Δ/mim2Δ* cells expressing pATOM36-HA were left intact or lysed with Triton X-100 (TX) before they were subjected to treatment with proteinase K (PK). Alternatively, other samples were subjected to alkaline extraction followed by separation by centrifugation to pellet (P) and supernatant (S) fractions. All samples were analysed by SDS-PAGE followed by immunodecoration with antibodies against the HA-epitope, the OM receptor protein Tom70, or the matrix soluble protein Hep1. (**B**) Mitochondria were isolated from yeast WT cells transformed with an empty plasmid (-) or from WT and *mim1Δ/mim2Δ* (ΔΔ) cells expressing pATOM36-HA (+). Isolated yeast organelles and mitochondria-enriched fraction from *T. brucei* (Tryp.) cells expressing pATOM36-HA were lysed with 1% digitonin. All samples were then subjected to BN-PAGE followed by immunodecoration with an antibody against the HA-tag. pATOM36-containing complexes are indicated with an asterisk.

DOI: https://doi.org/10.7554/eLife.34488.002

The following figure supplements are available for figure 1:

Figure supplement 1. Topologies and protein sequence alignments of Mim1, Mim2 and pATOM36.

DOI: https://doi.org/10.7554/eLife.34488.003

Figure supplement 2. pATOM36-HA is expressed in the transformed cells.

DOI: https://doi.org/10.7554/eLife.34488.004

(*Figure 1A*). Alkaline extraction of the isolated organelles showed that pATOM36, as Tom70 but unlike the soluble matrix protein Hep1, was detected in the pellet fraction indicating that it is an integral membrane protein (*Figure 1A*). Finally, a BN-PAGE analysis demonstrated that pATOM36 expressed in yeast forms complexes of similar size to the 140 and 250 kDa complexes observed in *T. brucei* mitochondria (*Figure 1B*). However, the higher molecular weight complex, which likely corresponds to a TAC subcomplex required for kDNA maintenance (*Käser et al., 2016*), was not detected. In summary, these results suggest that pATOM36 expressed in yeast cells behaves essentially identical to the endogenous protein: it is embedded into the MOM with its C-terminus facing the cytosol and it forms oligomeric complexes of ca. 140–250 kDa.

pATOM36 can replace the MIM complex in yeast

We next asked whether pATOM36 can rescue the growth defect on respiratory carbon sources of *mim1*Δ or *mim2*Δ cells. To that aim, plasmids encoding for pATOM36 or its HA-tagged version, as well as *MIM1* or *MIM2* and an empty plasmid (Ø) as a control, were transformed into wild type, *mim1*Δ and *mim2*Δ strains. The growth of the transformed cells was analysed by drop dilution assays on synthetic fermentative glucose-containing (SD-Leu) and respiratory glycerol-containing media (SG-Leu) at three different temperatures (15°C, 30°C and 37°C). Of note, the expression of pATOM36 and its HA-tagged version did not alter the growth of WT cells. Under all the tested conditions, pATOM36 and pATOM36-HA were able to rescue the growth defect caused by the absence of either Mim1 or Mim2 (*Figure 2A*). Of note, the rescue capacity of pATOM36 was similar to that of Mim1 or Mim2 in the corresponding deletion strains.

These results suggest that pATOM36 is active in yeast cells but it remained unclear whether pATOM36 can function alone or if it requires one of the remaining Mim proteins. To address this question, we monitored the capacity of pATOM36 to rescue the growth retardation of the double deletion *mim1*Δ/*mim2*Δ cells. We observed that pATOM36 could functionally compensate for the absence of both Mim1 and Mim2, since it was able to rescue the growth defect on non-fermentable carbon sources, a condition which requires fully functional mitochondria (*Figure 2B* and *Figure 2—figure supplement 1*).

The absence of Mim1 and/or Mim2 in yeast cells results in a variety of mitochondrial defects including reduction in the steady-state levels of Mim1/2 substrates like the outer membrane proteins Ugo1, Tom20 and Tom70 (*Dimmer et al., 2012*; *Ishikawa et al., 2004*; *Popov-Celeketić et al., 2008*; *Waizenegger et al., 2005*). We therefore monitored whether expression of pATOM36 restores the reduced levels of these MIM substrates. To that aim we isolated mitochondria from WT and *mim1*Δ/*mim2*Δ cells transformed with either an empty plasmid or a plasmid encoding pATOM36-HA and monitored the levels of the proteins by immunodecoration. The results indicate that, whereas expression of pATOM36-HA in WT cells did not alter the abundance of the tested proteins or did it only to a minor extent, it did restore the levels of Mim1/2 substrates Tom20 and Tom70 in mitochondria from the double deletion cells (*Figure 3A and B*). Interestingly, the effect of pATOM36 on the levels of Ugo1 was only marginal, suggesting that pATOM36 has preferences to certain MIM substrates.

A further phenotype of cells lacking Mim1/2 is the accumulation of mitochondrial precursor proteins due to hampered assembly of the TOM complex (*Ishikawa et al., 2004*; *Mnaimneh et al., 2004*; *Waizenegger et al., 2005*). To test whether pATOM36 is able to reverse this situation, we obtained whole cell lysates from the cells described above. As can be seen in *Figure 3C*, the presence of pATOM36-HA in the deletion strains completely eliminated the appearance of the precursor form of mitochondrial Hsp60. The presence of pATOM36-HA in the deletion cell lines resulted also in enhanced levels of Tom40 whereas the amounts of aconitase (Aco1) were not affected (*Figure 3C*).

These results suggest that the function of the MIM complex in TOM complex assembly can be replaced by pATOM36. To substantiate this assumption, we used digitonin-solubilised mitochondria, which were isolated from control and deletion strains, and analysed them by BN-PAGE. To detect the TOM complex, the corresponding immunoblots were probed with antibodies against either Tom40 or Tom22. Of note, pATOM36-HA did not affect the assembly of the TOM complex in WT cells (*Figure 3D*). As expected, in the absence of Mim1/2, a dramatic reduction in the amount of assembled TOM complex and an appearance of an unassembled Tom40-containing species can be

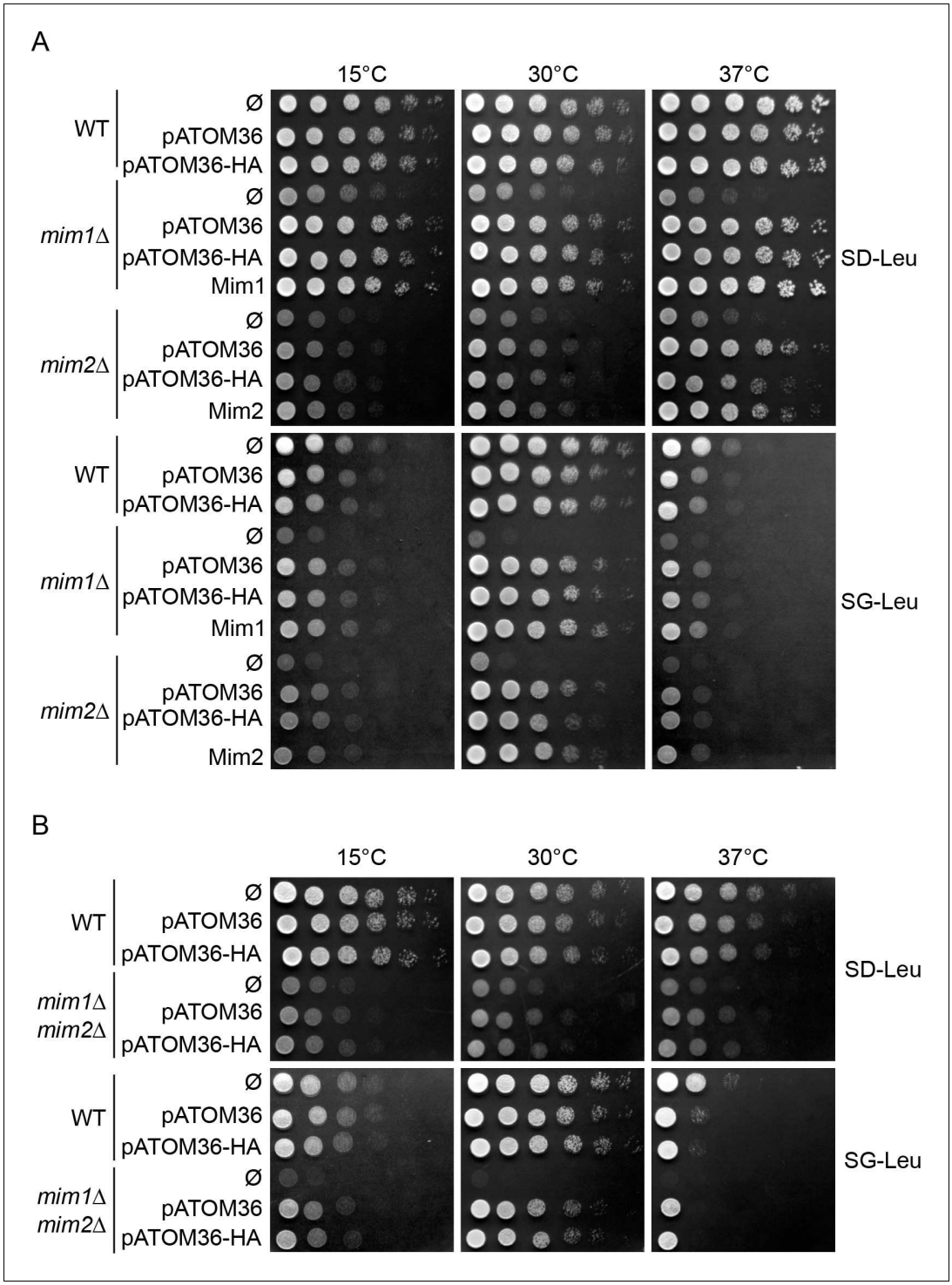

Figure 2. pATOM36 rescues the growth defects of cells lacking Mim1, Mim2 or both. (**A**) The indicated strains transformed with an empty plasmid (Ø) or with a plasmid expressing pATOM36 or its HA-tagged variant were tested at three different temperatures by drop-dilution assay for growth on synthetic medium containing either glucose (SD-Leu) or glycerol (SG-Leu). For comparison, plasmid-encoded Mim1 or Mim2 were transformed into *mim1Δ* or *mim2Δ* cells, respectively. All dilutions are in fivefold increment. (**B**) Cells deleted for both *MIM1* and *MIM2* (*mim1Δ/mim2Δ*) were transformed with the empty plasmid (Ø) or a plasmid encoding either native pATOM36 or pATOM36-HA. Transformed cells were analysed by drop-dilution assay at the indicated temperatures on synthetic medium containing either glucose (SD-Leu) or glycerol (SG-Leu). All dilutions are in fivefold increment.

Figure 2 continued on next page

Figure 2 continued

DOI: https://doi.org/10.7554/eLife.34488.005

The following figure supplement is available for figure 2:

Figure supplement 1. pATOM36 rescues the growth defect of mim1Δmim2Δ cells.

DOI: https://doi.org/10.7554/eLife.34488.006

observed. Strikingly, these alterations completely disappeared upon the introduction of pATOM36-HA into these cells (***Figure 3D***).

To investigate the specificity of the complementation by pATOM36, we asked whether it can functionally replace another import factor that mediates the biogenesis of other MOM proteins. To that goal, pATOM36 was introduced into cells lacking Mas37/Sam37, a subunit of the TOB/SAM complex that facilitates membrane integration of β-barrel proteins and the TOM subunit Tom22 (***Chan and Lithgow, 2008***; ***Dukanovic et al., 2009***; ***Wiedemann et al., 2003***). ***Figure 3—figure supplement 1*** shows that pATOM36 could revert neither the drop in the steady-state levels of the TOB complex and its altered assembly behaviour nor the reduced levels of either the β-barrel proteins Tom40 and Porin or the single-span protein Tom22. Thus, the effect of pATOM36 is specific for MIM substrates. These findings further support the notion that the single-span protein Tom22 follows an import pathway that is distinct from that taken by the signal-anchored subunits Tom20 and Tom70.

Previous reports suggested that Tom70 works together with Mim1 in the biogenesis of multi-span helical MOM proteins (***Becker et al., 2011***; ***Papic et al., 2011***). To test whether pATOM36 can also interact with Tom70, we utilised a recombinant protein composed of the cytosolic domain of Tom70 fused to GST moiety (GST-Tom70). When this protein was incubated with newly synthesised radiolabelled pATOM36, or with Mim1 as a control, we observed a specific binding to both proteins (***Figure 3E***). Although we cannot exclude the possibility that Tom70, as an import receptor for MOM proteins, recognises Mim1 and pATOM36 as substrates, it can be envisaged that, similarly to Mim1, pATOM36 can also cooperate with Tom70 in the biogenesis of MOM proteins.

The aforementioned results indicate that pATOM36 can compensate for the loss of the MIM machinery. To demonstrate directly a role of pATOM36 in protein import into the outer membrane of yeast mitochondria, we performed in vitro import assays. To that aim, we tested whether the presence of pATOM36 in mitochondria lacking the MIM complex can rescue the reduced import capacity of the MIM substrates Tom20 and Ugo1 observed for these organelles. To monitor the import efficiency of radiolabelled Tom20 into isolated organelles, we employed an established assay based on the formation of a proteolytic fragment of an N-terminally extended variant of Tom20 (***Ahting et al., 2005***). This assay clearly demonstrated that the presence of pATOM36 is sufficient to improve dramatically the capacity of organelles lacking Mim1/2 to import radiolabelled Tom20 molecules (***Figure 4A***). Along the same line, the assembly of newly synthesised Tom20 molecules into pre-existing TOM complexes was markedly improved when pATOM36 was present in mitochondria lacking the MIM complex (***Figure 4B***). Similarly to its minor effect on the steady state levels of Ugo1, the presence of pATOM36 did not improve the capacity of isolated mitochondria to import radiolabelled Ugo1 (***Figure 4C***). As a control, we checked the effect of pATOM36 on the import of proteins that are not known as MIM substrates like the matrix-targeted model protein pSu9-DHFR or the MOM tail-anchored protein Fis1. In both cases, we did not observe altered import upon expression of pATOM36 (***Figure 4D and E***). Collectively, pATOM36 can support the biogenesis of MIM substrates but appears to have preferences to certain ones.

Finally, we tested whether the trypanosomal protein is able to rescue the mitochondrial fragmentation that is observed in cells lacking Mim proteins. To that goal, we transformed a plasmid encoding pATOM36 into WT, *mim1Δ*, *mim2Δ*, or *mim1Δ*/*mim2Δ* cells expressing mitochondrial targeted GFP (mito-GFP). Analysis of mitochondria from the resulting cell lines by fluorescence microscopy revealed that pATOM36 is able to revert the mitochondrial fragmentation observed in cells lacking Mim1 and/or Mim2 to the tubular-like morphology of organelles in control cells (***Figure 5A and B***).

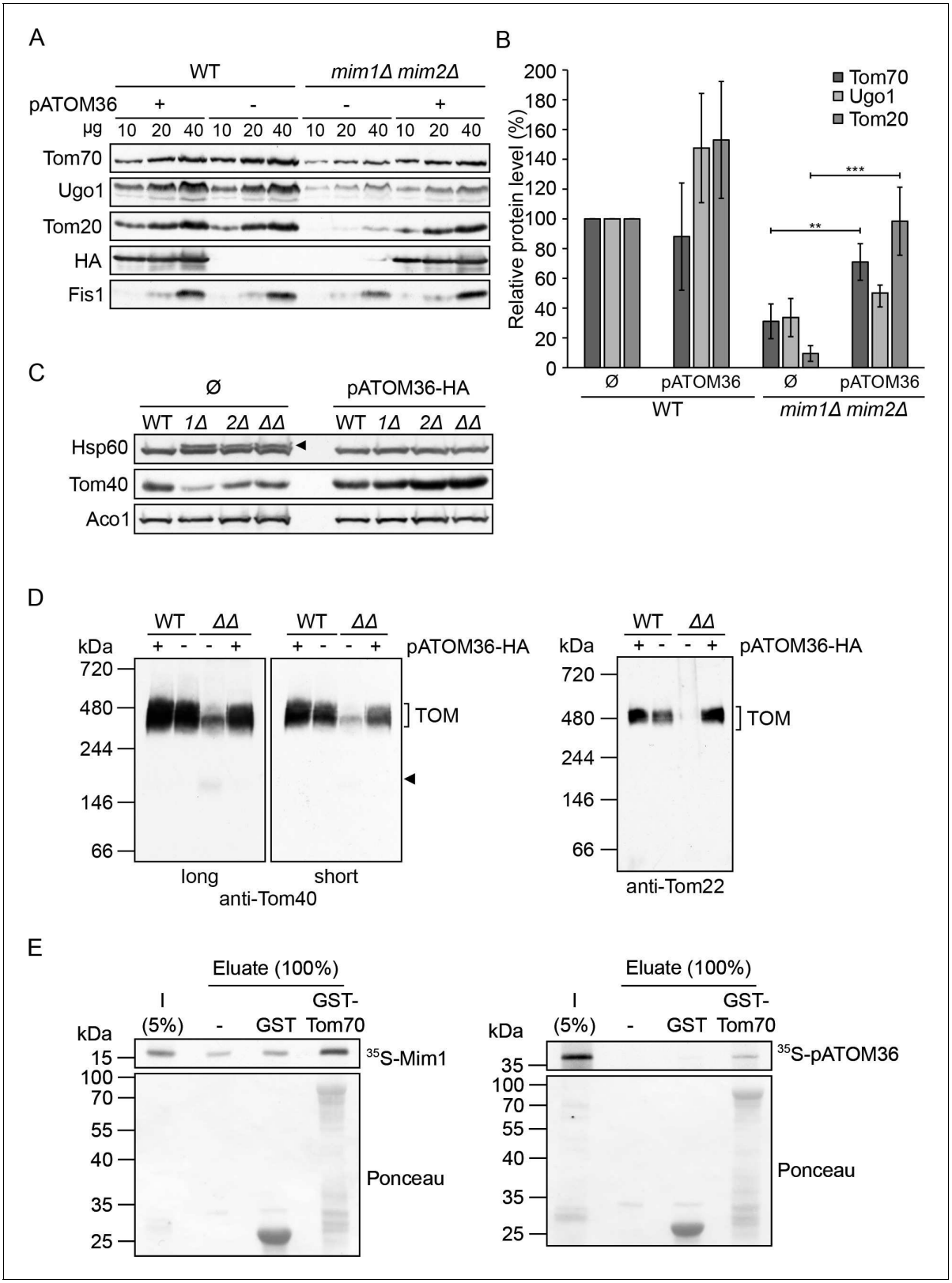

Figure 3. pATOM36 can compensate for the reduced steady state levels and assembly defects in cells lacking both Mim1 and Mim2. (**A**) Mitochondria were isolated from WT or *mim1Δ/mim2Δ* cells transformed with either an empty plasmid (-) or with a plasmid encoding pATOM36-HA (+). The specified amounts were analysed by SDS-PAGE and immunodecoration with antibodies against either the indicated mitochondrial proteins or the HA-tag. (**B**) The intensity of the bands from three independent experiments such as those presented in (**A**) was monitored. The amounts of Tom70, Ugo1 and

Figure 3 continued on next page

Figure 3 continued

Tom20 in the various mitochondria samples are presented as mean percentage of their levels in control organelles (WT+ Ø). The levels of Fis1 were taken as loading control. Error bars represent ± SD. **p≤0.005, ***p≤0.0005. (**C**) Whole cell lysates were obtained from WT, *mim1Δ (1Δ), mim2Δ (2Δ),* or the double deletion *mim1Δ/mim2Δ (ΔΔ)* cells transformed with either an empty plasmid (Ø) or with a plasmid encoding pATOM36-HA. Samples were analysed by SDS-PAGE and immunodecoration with antibodies against the indicated mitochondrial proteins. The precursor form of mitochondrial Hsp60 is indicated with an arrowhead. (**D**) The mitochondria described in (**A**) were solubilised in a buffer containing 1% digitonin and then analysed by BN-PAGE followed by western blotting. The membranes were immunodecorated with antibodies against the TOM subunits, Tom40 (long and short exposures) and Tom22. The TOM complex is signposted. A Tom40-containing low molecular weight complex is indicated with an arrowhead. (**E**) Mim1 and pATOM36 interact directly with Tom70. Radiolabelled Mim1 or pATOM36 (input, **I**) were incubated with glutathione beads (-) or with beads that were pre-bound to recombinant GST alone or to GST fused to the cytosolic domain of Tom70 (GST-Tom70). After washing, bound material was eluated and proteins were analysed by SDS–PAGE followed by blotting onto a membrane, and detection with either autoradiography (upper panel) or Ponceau staining (lower panel).

DOI: https://doi.org/10.7554/eLife.34488.007

The following source data and figure supplement are available for figure 3:

Source data 1. pATOM36 can compensate for the reduced steady state levels in cells lacking both Mim1 and Mim2.

DOI: https://doi.org/10.7554/eLife.34488.009

Figure supplement 1. pATOM36-HA does not rescue biogenesis defects in mas37Δ cells.

DOI: https://doi.org/10.7554/eLife.34488.008

Mim1/2 form a native-like MIM complex in trypanosomes

Observing the rescue capacity of pATOM36 in yeast cells, we asked whether the functional similarity between Mim1/2 and pATOM36 allows the yeast proteins to replace the function pATOM36 has in the biogenesis of trypanosomal MOM proteins. To that end, we constructed a plasmid for the co-expression of myc-tagged Mim1 and HA-tagged Mim2 in *T. brucei* (***Figure 6A***). Next, this plasmid was introduced into a cell line allowing controlled ablation of pATOM36. In these cells, addition of tetracycline simultaneously initiates the RNAi-mediated degradation of the pATOM36 mRNA as well as the expression of the tagged Mim1 and Mim2.

Subcellular fractionation of induced cells showed that both proteins are expressed and, like the mitochondrial marker protein ATOM40, they are exclusively localised in the mitochondrial fraction (***Figure 6B***, top panels). Alkaline extraction of the latter revealed that, as the endogenous proteins in yeast, both Mim1 and Mim2 are recovered in the pellet, together with the integral membrane protein ATOM40, whereas the soluble protein CytC was present in the supernatant (***Figure 6B***, lower panels). To monitor whether Mim1 and Mim2 are inserted into the membrane in their native orientation, mitochondria-enriched fractions were treated with proteinase K. This treatment resulted for both proteins in the formation of protease-resistant C-terminal fragments (***Figure 6C***). Thus, Mim1 and Mim2 acquired their native topology in *T. brucei* mitochondria with their N-terminus exposed to the cytosol and the C-terminus located in the IMS. Mim1 and Mim2 of yeast cells form a complex of approx. 200 kDa (***Dimmer et al., 2012***; ***Ishikawa et al., 2004***; ***Waizenegger et al., 2005***). BN-PAGE shows that similar complexes of ca. 230 kDa, which contain both Mim1-myc and Mim2-HA, could be detected in *T. brucei* (***Figure 6D***). Importantly, these complexes migrated similarly to complexes harbouring Mim1-HA and Mim2-HA of yeast mitochondria (***Figure 6E***). The slightly higher molecular weight than that observed for native complexes in yeast can be explained by the fact that both proteins are tagged. Thus, expression of Mim1 and Mim2 results in a native-like MIM complex in mitochondria from *T. brucei*.

The MIM complex can replace the protein biogenesis function of pATOM36 in *T. brucei*

The next question we addressed was whether the MIM complex can take over the function of pATOM36. Ablation of pATOM36 has been shown to cause a growth arrest. Due to its dual function the lack of pATOM36 does not only interfere with the assembly and/or insertion of MOM proteins but it also prevents assembly of the TAC, which causes loss of the kDNA (***Figure 7A***) (***Käser et al., 2016***). Interestingly, introducing Mim1/2 into the pATOM36-depleted cells could not prevent the loss of kDNA but it did cause a milder growth phenotype (***Figure 7A***). When mitochondrial proteins from pATOM36-depleted cells expressing Mim1/2 were analysed, we observed that the steady-state levels of the ATOM complex subunits ATOM46, ATOM19, and ATOM14, all of which are greatly

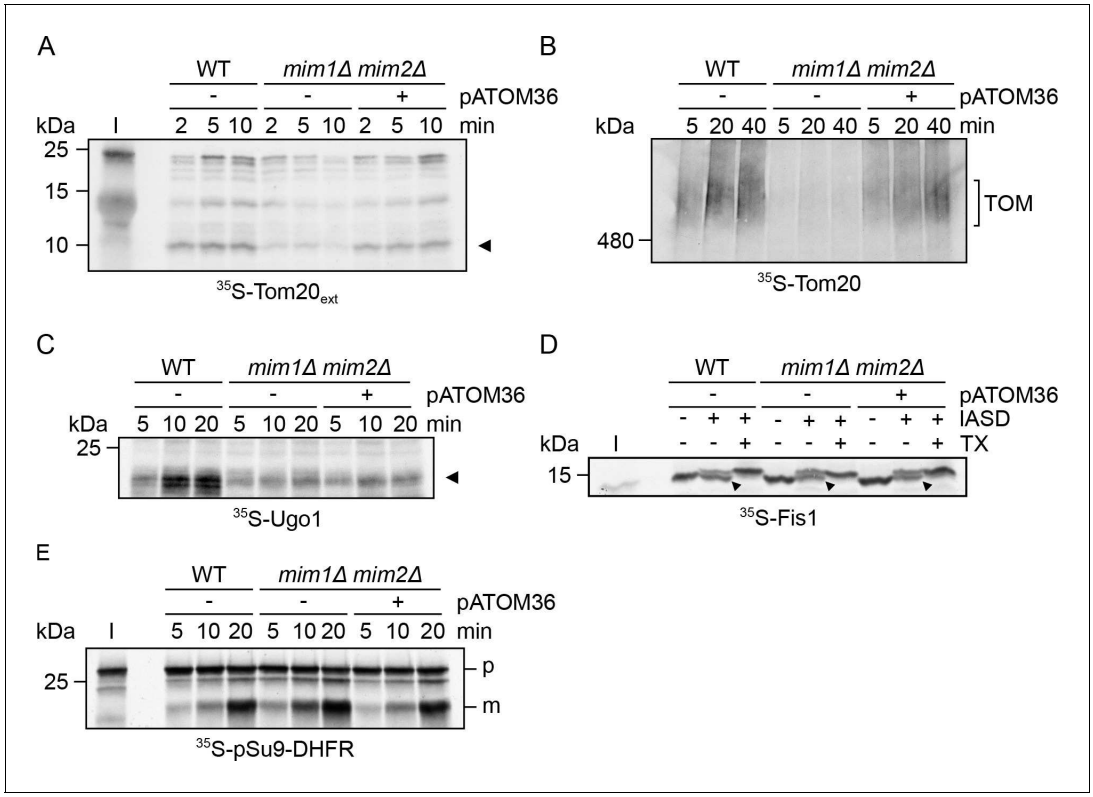

Figure 4. pATOM36 can rescue some of the import defects of cells lacking the MIM complex. (**A**) Mitochondria were isolated from WT cells transformed with an empty plasmid (WT-) or from *mim1Δ/mim2Δ* cells transformed with either an empty plasmid (-) or with a plasmid encoding pATOM36-HA (+). Radiolabelled $Tom20_{ext}$ molecules (5% input, I) were incubated with the indicated isolated organelles for the specified time periods. Then, mitochondria were treated with PK and analysed by SDS-PAGE and autoradiography. A proteolytic fragment of $Tom20_{ext}$, which reflects correct membrane integration, is indicated by an arrowhead. (**B**) Radiolabelled Tom20 was incubated with isolated mitochondria as in (**A**). At the end of the import reactions, mitochondria were solubilised with 0.2% digitonin and samples were analysed by BN-PAGE followed by autoradiography. The migration of Tom20 molecules assembled into the TOM complex is indicated. (**C**) Radiolabelled Ugo1 was incubated with isolated mitochondria as in (**A**). Then, mitochondria were treated with trypsin and analysed by SDS-PAGE and autoradiography. A proteolytic fragment of Ugo1, which reflects correct membrane integration, is indicated by an arrowhead. (**D**) Radiolabelled Fis1-TMC (5% input, I) was incubated with isolated mitochondria as in (**A**). Then, mitochondria were subjected to an IASD assay, re-isolated and analysed by SDS-PAGE and autoradiography. Bands representing correctly integrated Fis1-TMC are marked by an arrowhead. (**E**) Radiolabelled pSu9-DHFR (5% input, I) was incubated with isolated mitochondria as in (**A**). Then, mitochondria were re-isolated and analysed by SDS-PAGE and autoradiography. The precursor and mature forms are indicated by p and m, respectively.

DOI: https://doi.org/10.7554/eLife.34488.010

reduced in the absence of pATOM36, were restored (***Figure 7B***) (***Käser et al., 2016***). Furthermore, not only the abundance of the ATOM subunits was back to normal levels, but also the subunits were incorporated into the high-molecular-weight ATOM complexes. Of note, in the cell lines complemented by the MIM complex the ATOM subunit complexes were shifted to a slightly higher molecular weight (***Figure 8A***). Moreover, complementation of the ATOM40-containing complexes was somewhat incomplete, since the 200 kDa ATOM40 complexes that accumulate after ablation of pATOM36 were still visible (***Figure 8A***).

It has previously been described that ablation of pATOM36 in trypanosomes, reminiscent to deletion of the MIM complex in yeast, causes a condensation of the network-like structure of the trypanosomal mitochondrion (***Bruggisser et al., 2017***) (***Figure 8B***, left panel). The immunofluorescence analysis in the right panel of ***Figure 8B*** indicates that in the presence of the MIM complex also this phenotype is reversed and the wild type morphology of the mitochondrion is fully restored. Hence, similarly to the rescue capacity of pATOM36 in yeast cells, Mim1/2 can replace the function of endogenous pATOM36 in MOM protein biogenesis in trypanosomes.

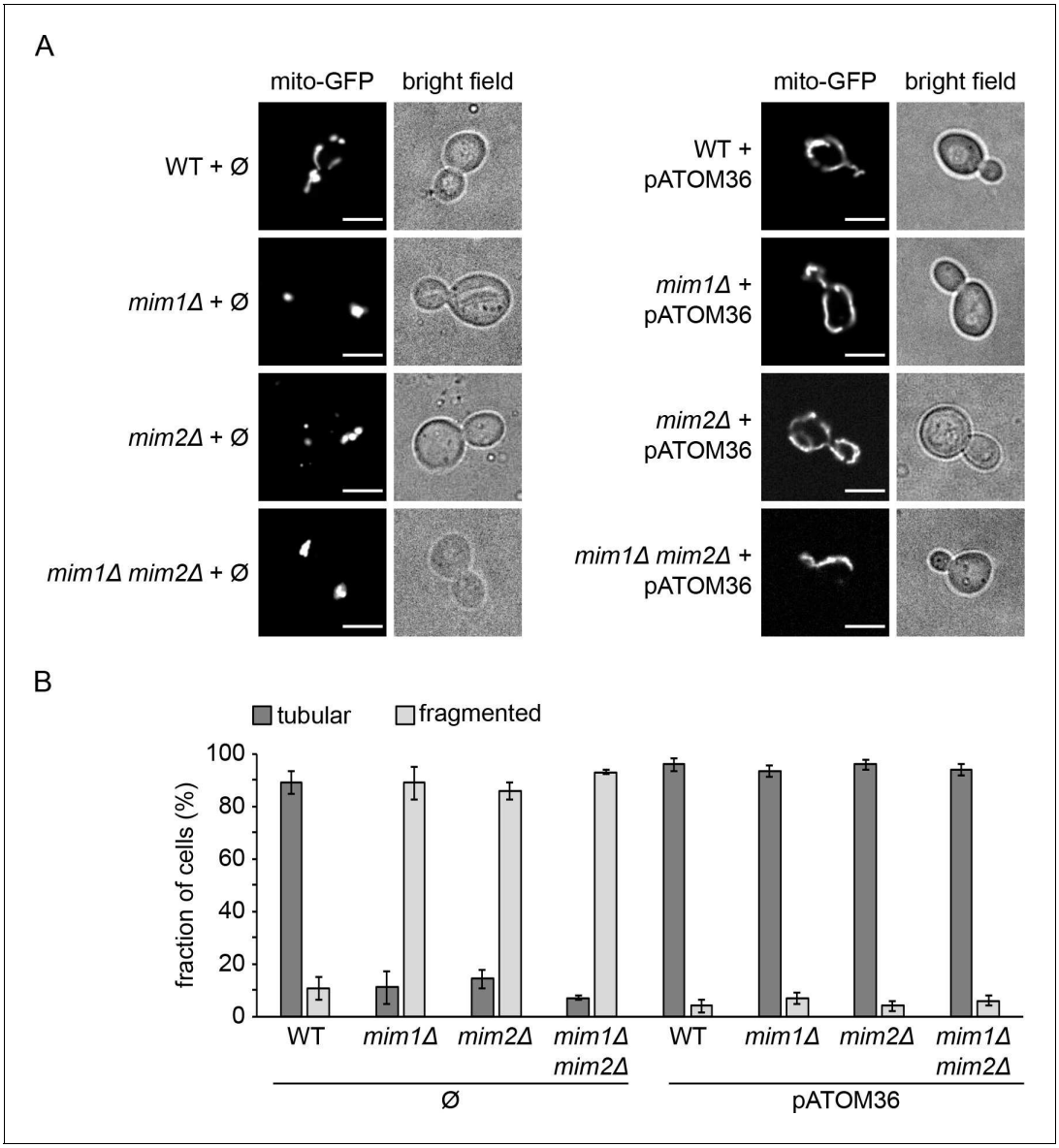

Figure 5. *mim1*Δ and *mim2*Δ cells expressing pATOM36 do not show altered mitochondrial morphology. (**A**) WT, *mim1*Δ, *mim2*Δ, and *mim1*Δ/*mim2*Δ cells harbouring mitochondria-targeted GFP (mito-GFP) were transformed with either an empty plasmid (Ø) as a control (left panels) or a plasmid encoding pATOM36 (right panels). Cells were analysed by fluorescence microscopy and representative images of the predominant morphology for each strain are shown. Scale bar, 5 µm. (**B**) Statistical analysis of the cells described in (**A**). Average values with standard deviation bars of three independent experiments with at least n = 100 cells in each experiment are shown.

DOI: https://doi.org/10.7554/eLife.34488.011

The following source data is available for figure 5:

Source data 1. *mim1*Δ and *mim2*Δ cells expressing pATOM36 have normal mitochondrial morphology

DOI: https://doi.org/10.7554/eLife.34488.012

Complementing the biogenesis function of pATOM36 requires both Mim1 and Mim2

When we transfected the *T. brucei* pATOM36-RNAi cell line with distinct plasmids encoding myc-tagged Mim1 and HA-tagged Mim2 we obtained also clones that mainly expressed either Mim1-myc or Mim2-HA while the other Mim subunit was expressed only in residual amounts (***Figure 8—figure supplement 1***). In the cell line that mainly expresses Mim1-myc, the protein is found in a complex of approximately 440 kDa (***Figure 8—figure supplement 1A***, middle panel), whereas in the cell

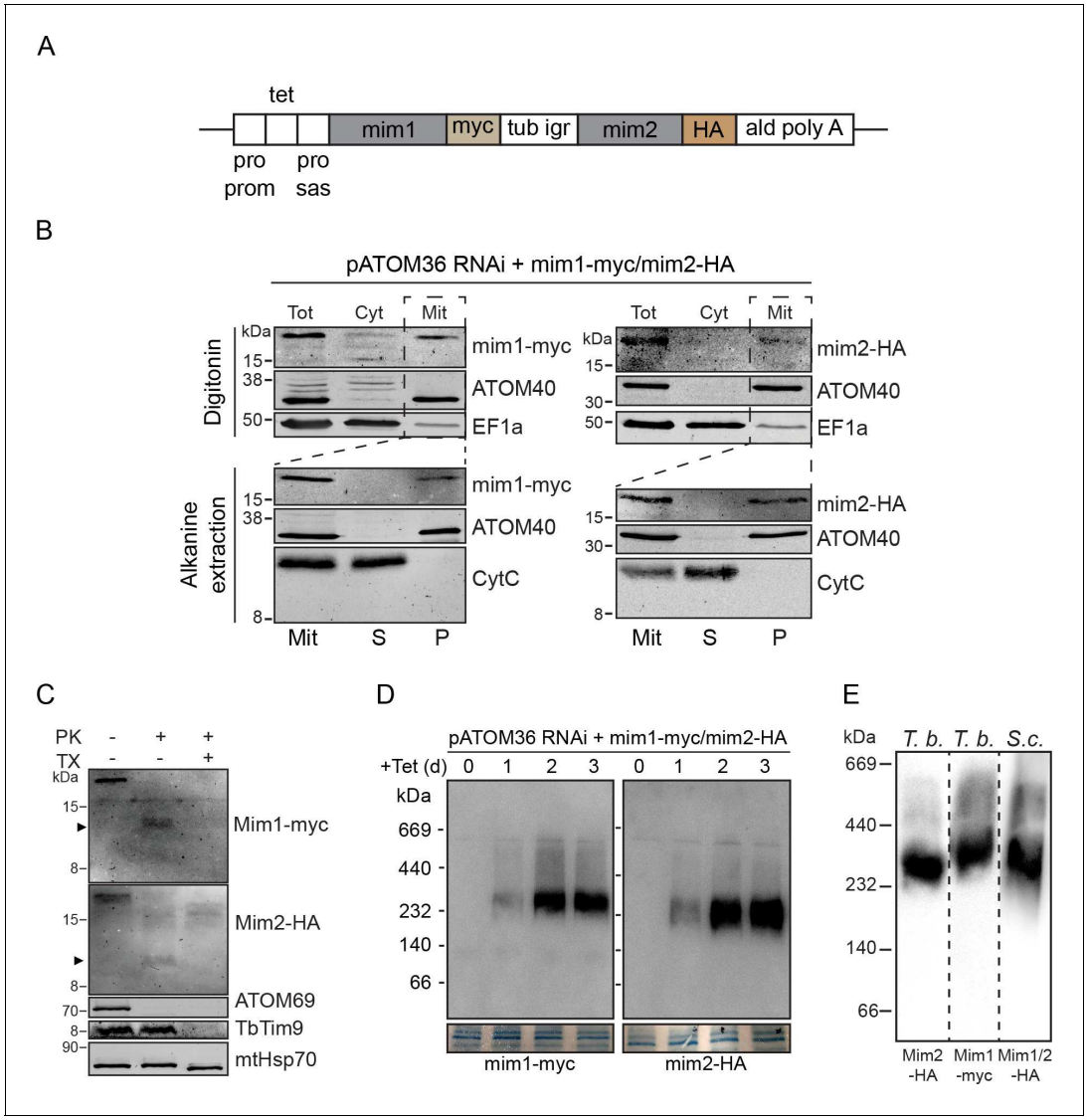

Figure 6. Yeast Mim1 and Mim2 form a high-molecular-weight complex in mitochondria of *T. brucei*. (**A**) Schematic representation of the insert of the pLew100-based vector that allows tetracycline-inducible expression of C-terminally myc-tagged Mim1 and HA-tagged Mim2 in *T. brucei*. Pro prom, procyclin promotor; tet, tetracycline operator; pro sas, procycline splice acceptor site; tub igr, α- and β-tubulin intergenic region; ald polyA, 3'-UTR of the aldolase gene. (**B**) Top panels: immunoblot analysis of whole cells (Tot), soluble (Cyt) and digitonin-extracted mitochondria-enriched pellet (Mit) fractions of a tetracycline-inducible pATOM36-RNAi cell line expressing Mim1-myc and Mim2-HA. Duplicate blots were analysed for the expression of Mim1-myc (left panels) and Mim2-HA (right panels). ATOM40 and EF1a serve as mitochondrial and cytosolic markers, respectively. Bottom panels: Alkaline extraction of the mitochondria-enriched fraction (Mit) shown in the top panels. The pellet (**P**) and the supernatant (**S**) fractions corresponding to integral membrane and soluble proteins, respectively, were analysed by SDS-PAGE and immunodecoration. ATOM40 and CytC serve as markers for integral and peripheral membrane proteins, respectively. (**C**) Mitochondria-enriched fractions of the same cell line describe in (**B**) were left intact or lysed with Triton X-100 (TX) before they were subjected to treatment with proteinase K (PK). All samples were analysed by SDS-PAGE followed by immunodecoration with antibodies against myc and HA tags, the OM protein ATOM69, the IMS protein TbTim9, or the matrix protein mtHsp70. Note that mtHsp70 contains a folded core, which is protease resistant. A proteolytic fragment of Mim1 and Mim2 is indicated with an arrowhead. (**D**) Duplicate immunoblots from BN-PAGE analysis of mitochondria-enriched fractions of the same cell line describe in (**B**) were probed for Mim1-myc (left panels) and Mim2-HA (right panels). Sections of the coomassie-stained gels serve as loading control. (**E**) Immunoblots of a BN-PAGE analysis of mitochondria-enriched fractions of the *T. brucei* (*T.b.*) cell line simultaneously expressing myc-tagged Mim1 (Mim1-myc) and HA-tagged Mim2 (Mim2-HA) and isolated yeast (*S.c.*) mitochondria simultaneously expressing HA-tagged versions of Mim1 and Mim2. The immunoblots are probed with antibodies against HA- or myc-tag.

DOI: https://doi.org/10.7554/eLife.34488.013

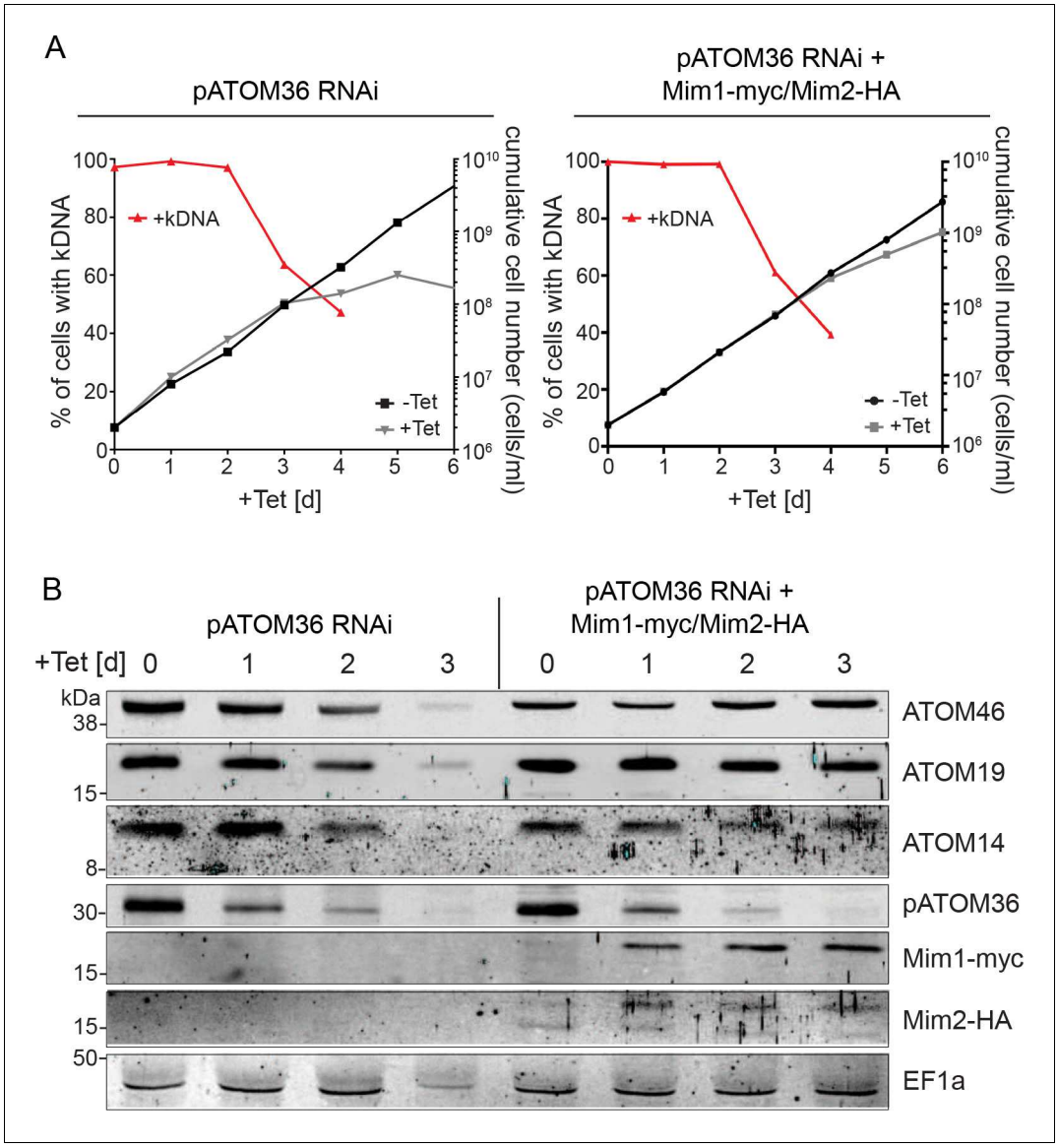

Figure 7. Yeast Mim1 and Mim2 complement the mitochondrial OM biogenesis phenotype of *T. brucei* cells ablated for pATOM36. (**A**) Left panel: growth in the presence and absence of tetracycline (black and grey lines, respectively) and loss of kDNA (red line) in the presence of tetracycline of the pATOM36-RNAi parent cell line. Right panel: as in the left but the analysis was done for the pATOM36-RNAi cell line that co-expresses Mim1-myc and Mim2-HA. (**B**) Whole cell lysates from the cell lines as in (**A**) were obtained after the indicated time of induction. Proteins of these samples were analysed by SDS-PAGE and immunodecoration with the indicated antibodies. ATOM46, ATOM19 and ATOM14 are subunits of the ATOM complex. Cytosolic EF1a serves as a loading control.

DOI: https://doi.org/10.7554/eLife.34488.014

line preferentially expressing Mim2-HA this protein is present in a complex of approximately 230 kDa (***Figure 8—figure supplement 1B***, bottom panel). These complexes are of either higher (Mim1-myc) or similar molecular weights (Mim2-HA) to the one that is formed when both proteins are expressed in similar amounts (***Figure 6D and E***). Most importantly, both cell lines show a strong deficiency of ATOM complex assembly (***Figure 8—figure supplement 1***, top panels) and a growth arrest (***Figure 8—figure supplement 1***, bottom graphs) that are indistinguishable from the parent pATOM36-RNAi cell line (***Figure 8A***, left panels and ***Figure 7***, left graph, respectively). This indicates that expression of Mim1 or Mim2 alone cannot complement for the protein biogenesis

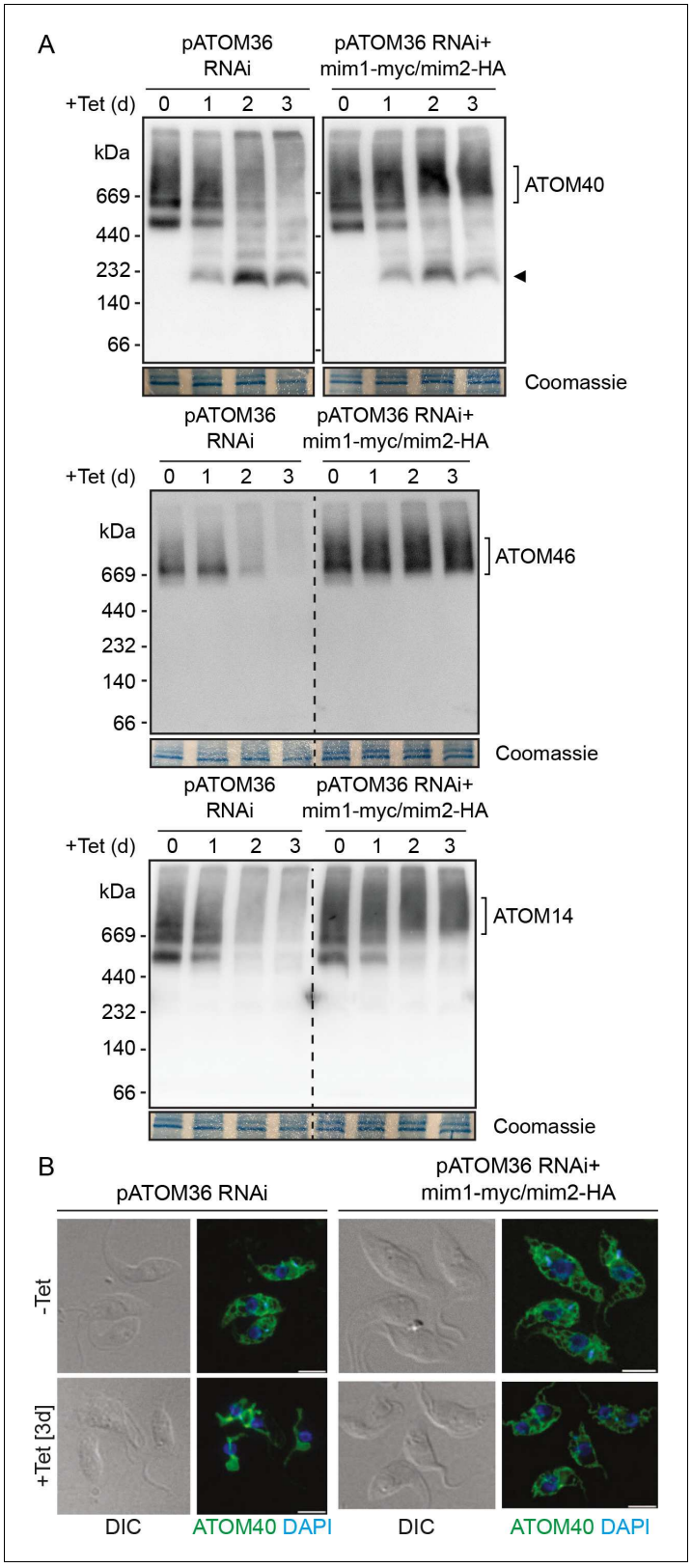

Figure 8. Mim1 and Mim2 rescue the assembly defect of the ATOM complex and the altered mitochondrial morphology in cells lacking pATOM36. (**A**) Mitochondria-enriched fractions from the cell lines as in ***Figure 7A*** were obtained after the indicated time of induction. Samples were analysed by BN-PAGE followed by immunodecoration with antibodies against the indicated subunits of the ATOM complex. The migration of the

Figure 8 continued on next page

Figure 8 continued

ATOM complex is signposted. Sections of the coomassie-stained gels serve as loading controls. Arrowhead indicates an ATOM40-containing lower molecular weight complex. (**B**) Left images: Immunofluorescence analyses of mitochondrial morphology in the pATOM36 RNAi cell line after 0 or 3 days of induction. Right images: as in the left panels but the analysis was performed with the RNAi cell line co-expressing Mim1-myc and Mim2-HA. ATOM40 is shown in green and DAPI-stained DNA is shown in blue. DIC, differential interference contrast. Scale bar, 5 μm.

DOI: https://doi.org/10.7554/eLife.34488.015

The following figure supplement is available for figure 8:

Figure supplement 1. Complementing the biogenesis function of pATOM36 requires both Mim1 and Mim2.

DOI: https://doi.org/10.7554/eLife.34488.016

phenotype caused by the lack of pATOM36. Furthermore, these results suggest that successful complementation requires similar amounts of Mim1 and Mim2.

Discussion

Our study shows that the MIM complex of yeast, consisting of Mim1 and Mim2, and trypanosomal pATOM36 have identical functions, even though they do not share sequence similarity, the same membrane topology, or a similar size (***Figure 1—figure supplement 1***). This conclusion is based on the stringent criteria that the two proteins can replace each other in reciprocal complementation experiments. The only major limitation is that the role of pATOM36 in mitochondrial DNA inheritance in trypanosomes cannot be carried out by the MIM complex, which is expected since unlike the MIM complex pATOM36 has a dual function (***Käser et al., 2016***).

The reciprocal complementation is surprising because yeast belongs to the eukaryotic supergroup of the Opisthokonts whereas trypanosomes are Excavates (***Burki, 2014***). Thus, except for being eukaryotes the two systems are essentially unrelated. The most parsimonious explanation for the observed phylogenetic distribution of the two functional analogues is that the MIM complex and pATOM36 evolved after the eukaryotic supergroups were already established. Moreover, the observation that within the Opisthokonts the MIM complex is restricted to fungi suggests that it evolved only after the divergence of the ancestors of fungi and metazoans. Thus, the last eukaryotic common ancestor (LECA) likely did not contain the MIM complex, pATOM36 or any other functional analogue of these proteins. This assumption is in line with the notion that LECA had a much simpler MOM protein import system consisting possibly only of a Tom40-like β-barrel protein (***Dolezal et al., 2006***; ***Mani et al., 2016***), whose integration into the MOM is mediated by the TOB/SAM complex, the core subunit of which, Tob55/Sam50, is conserved in all eukaryotes (***Dolezal et al., 2006***; ***Gentle et al., 2004***; ***Kozjak et al., 2003***; ***Paschen et al., 2003***). During evolution, additional subunits that are anchored in the membrane by α-helices joined the TOM complex to increase its specificity and efficiency. This scenario is supported by the fact that the TOM complexes of yeast, plants and trypanosomes, representatives of three different eukaryotic supergroups, contain three distinct evolutionary unrelated pairs of protein import receptors (***Mani et al., 2015***; ***Mani et al., 2016***). The appearance of the new TOM subunits required the evolution of a system, such as the MIM complex or pATOM36, that facilitates their assembly with Tom40.

Interestingly, the capacity of pATOM36 expressed in yeast cells to support the biogenesis of MIM substrates is variable with the import receptor Tom20 as the most favourable substrate and the fusion-modulator Ugo1 as the least favourable one. Ugo1 is a carrier-like protein with several TMSs that lack clear homologues in higher eukaryotes. Hence, one can speculate that pATOM36 cannot deal with it well since there are no similar substrates in the MOM of *T. brucei*.

Both Mim1 and Mim2 as well as pATOM36 occur in protein complexes of unknown composition. The successful complementation experiments together with the fact that they form complexes of similar sizes when expressed in the heterologous systems strongly suggest that these complexes do not contain any additional proteins. Their ability for reciprocal rescue also suggests that their essential function does not require any further proteins since it is very unlikely that such factors would be present in the other species.

It is established that pATOM36 and Mim1/Mim2 are integral MOM proteins. However, whereas Mim1 and Mim2 have each a single TMS with the N-terminus facing the cytosol, the topology of pATOM36 is largely unknown (***Figure 1—figure supplement 1***). It has been demonstrated by antibody shift experiments that the C-terminus of pATOM36 is exposed to the cytosol (***Pusnik et al., 2012***), but depending on the prediction programs the protein is postulated to have either one, two or even three TMSs (***Käser et al., 2016***). While Mim1/Mim2 and pATOM36 do not share sequence similarity and also have different molecular weights (Mim1, 13 kDa; Mim2, 11 kDa; pATOM36, 36 kDa), they all have GxxxG(A) motifs within their putative TMSs (***Figure 1—figure supplement 1***), which is in line with their oligomeric quaternary structures. It has recently been shown by electrophysiological experiments that Mim1, on its own or in complex with Mim2, can form a cation-selective channel (***Krüger et al., 2017***). Should this channel activity of Mim1 be functionally relevant, we would expect pATOM36 to form also a pore.

Presently, it is unclear whether the convergent evolution of the MIM complex and pATOM36 demonstrated in the present study, resulted in a similar 3D-structure of the two oligomers. Should this be the case, the two complexes may independently have evolved the same mechanisms to perform the equivalent functions. Alternatively, it cannot be excluded that they use structurally different solutions resulting in different mechanisms that nevertheless allow them to carry out the same functions.

There is evidence that both the yeast MIM complex as well as trypanosomal pATOM36 mediate assembly of already integrated MOM proteins and at least for some substrates also the insertion process itself (***Becker et al., 2008a***; ***Becker et al., 2011***; ***Bruggisser et al., 2017***; ***Dimmer et al., 2012***; ***Hulett et al., 2008***; ***Käser et al., 2016***; ***Lueder and Lithgow, 2009***; ***Papic et al., 2011***; ***Thornton et al., 2010***; ***Waizenegger et al., 2005***). Whether the two oligomers directly catalyse protein insertion or whether they form microdomains in the MOM that facilitate membrane integration of helical segments is unclear. In any case, we hypothesise that the MIM complex and pATOM36 should behave similarly in this respect.

The successful complementation of the functions of the yeast MIM complex by trypanosomal pATOM36 and vice versa opens the way for future comparative studies to define the fundamental features the two biogenesis complexes share. The constraints imposed by their identical functions will help to reveal their mechanism of action. Taken together, our work offers new insights into the evolution of mitochondrial import factors and sheds new light on basic aspects of the biogenesis of mitochondrial outer membrane proteins.

Materials and methods

Key resources table

Reagent type (species) or resource	Designation	Source or reference	Identifiers	Additional information
Strain, strain background (*Saccharomyces cerevisiae*)	WT; W303α; MATα leu2-3,112 trp1-1 can1-100 ura3-1 ade2-1 his3-11,15	NA		
Strain, strain background (*S. cerevisiae*)	*mim1*Δ; W303α; MATα leu2-3,112 trp1-1 can1-100 ura3-1 ade2-1 his3-11,15 MIM1::KanMX	DOI: 10.1242/jcs.103804		
Strain, strain background (*S. cerevisiae*)	*mim2*Δ; W303α; MATα leu2-3, 112 trp1-1 can1-100 ura3-1 ade2-1 his3-11,15 MIM2::HIS3	DOI: 10.1242/jcs.103804		
Strain, strain background (*S. cerevisiae*)	*mim1*Δ *mim2*Δ; W303α; MATα leu2-3,112 trp1-1 can1-100 ura3-1 ade2-1 his3-11,15 MIM1::KanMX MIM2::HIS3	DOI: 10.1242/jcs.103804		
Strain, strain background (*S. cerevisiae*)	WT; YPH499; MATa ura3-52 lys2-801_amber ade2-101 _ochre trp1-Δ63 his3-Δ200 leu2-Δ1			

Continued on next page

Continued

Reagent type (species) or resource	Designation	Source or reference	Identifiers	Additional information
Strain, strain background (*S. cerevisiae*)	*mas37Δ*; YPH499; MATa ura3-52 lys2-801_amber ade2-101_ochre trp1-Δ63 his3-Δ200 leu2-Δ1 MAS37::HIS3	DOI: 10.1074/jbc.M411510200		
Cell line (*Trypanosoma brucei*)	29–13, procyclic, pATOM36 RNAi	PMID: 22787278		
Transfected construct (*S. cerevisiae*)	pATOM36 RNAi + mim1-myc/ mim2-HA (***Figures 6***, ***7*** and ***8***)	this paper		see Materials and methods
Transfected constructs (*S. cerevisiae*)	pATOM36 RNAi + mim1-myc/ mim2-HA (***Figure 8—figure supplement 1***)	this paper		see Materials and methods
Antibody	anti-HA (polyclonal rat)	Roche	11867423001; AB_390918	WB 1:15000
Antibody	anti-Tom70 (polyclonal rabbit)	N/A		WB 1:2000
Antibody	anti-Hep1 (polyclonal rabbit)	N/A		WB 1:3000
Antibody	anti-Ugo1 (polyclonal rabbit)	N/A		WB 1:500
Antibody	anti-Tom20 (polyclonal rabbit)	N/A		WB 1:1600
Antibody	anti-Fis1 (polyclonal rabbit)	N/A		WB 1:1000
Antibody	anti-Hsp60 (polyclonal rabbit)	N/A		WB 1:100000
Antibody	anti-Tom40 (polyclonal rabbit)	N/A		WB 1:4000
Antibody	anti-Aco1 (polyclonal rabbit)	N/A		WB 1:7000
Antibody	anti-Tom22 (polyclonal rabbit)	N/A		WB 1:2000
Antibody	anti-Tob55 (polyclonal rabbit)	N/A		WB 1:2000
Antibody	anti-Por1 (polyclonal rabbit)	N/A		WB 1:4000
Antibody	anti-rat (HRP coupled goat)	Abcam	ab6845; AB_955449	WB 1:3000
Antibody	anti-rabbit (HRP coupled goat)	Bio-Rad	1721019; AB_11125143	WB 1:10000
Antibody	anti-myc (monoclonal mouse)	Invitrogen	132500	WB 1:2000
Antibody	anti-HA (monoclonal mouse)	Enzo Life Sciences AG	CO-MMS-101 R-1000	WB 1:5000
Antibody	anti-EF1a (monoclonal mouse)	Merck Millipore	05–235	WB 1:10000
Antibody	anti-ATOM40 (polyclonal rabbit)	N/A		WB 1:10000, IF 1:1000
Antibody	anti-CytC (polyclonal rabbit)	N/A		WB 1:1000
Antibody	anti-ATOM69 (polyclonal rabbit, affinity purified)	N/A		WB 1:50
Antibody	anti-TbTim9 (polyclonal rabbit)	N/A		WB 1:20

Continued on next page

Continued

Reagent type (species) or resource	Designation	Source or reference	Identifiers	Additional information
Antibody	anti-mtHsp70 (mouse)	N/A		WB 1:1000
Antibody	anti-ATOM46 (polyclonal rabbit; affinity purified)	N/A		WB 1:50
Antibody	anti-ATOM19 (mouse)	N/A		WB 1:500
Antibody	anti-ATOM14 (polyclonal rabbit)	N/A		WB 1:500
Antibody	anti-pATOM36 (polyclonal rabbit; affintiy purified)	N/A		WB 1:250
Antibody	anti-rabbit Alexa488	ThermoFisher Scientific		IF 1:1000
Antibody	anti-rabbit IRDye 800CW	LI-COR Biosciences	P/N 925–32211	WB 1:20000
Antibody	anti-mouse IRDye LT680	LI-COR Biosciences	P/N 925–68020; AB_2687826	WB 1:20000
Antibody	anti-mouse (HRP-coupled goat)	Sigma Aldrich	AP308P	WB 1:5000
Antibody	anti-rabbit (HRP coupled goat)	Sigma Aldrich	AP307P	WB 1:5000
Recombinant DNA reagent	Ø; pYX142 (plasmid)			
Recombinant DNA reagent	pATOM36; pYX142-pATOM36 (plasmid)	this paper		pATOM36 ORF was amplified from pFT33 and cloned in pYX142 between EcoRI and BamHI
Recombinant DNA reagent	pATOM36-HA; pYX142-pATOM36-3HA (plasmid)	this paper		pATOM36 ORF was amplified from pFT33 and cloned in pYX142 between EcoRI and BamHI
Recombinant DNA reagent	^{35}S-Mim1; pGEM4-Mim1-4M (plasmid)	DOI: 10.1038/sj.embor.7400318		
Recombinant DNA reagent	^{35}S-pATOM36; pGEM4-pATOM36 (plasmid)	this paper		pATOM36 ORF was subcloned from pYX142-pATOM36 in pGEM4 with EcoRI and BamHI
Recombinant DNA reagent	^{35}S-Tom20$_{ext}$; pGEM4-Tom20$_{ext}$ (plasmid)	DOI: 10.1074/jbc.M410905200		
Recombinant DNA reagent	^{35}S-Tom20; pGEM3-Tom20 (plasmid)	DOI: 10.1074/jbc.M410905200		
Recombinant DNA reagent	^{35}S-Ugo1; pGEM4-Ugo1 (plasmid)	DOI: 10.1083/jcb.201102041		
Recombinant DNA reagent	^{35}S-Fis1; pGEM4-Fis1-TMC (plasmid)	DOI: 10.1242/jcs.024034		
Recombinant DNA reagent	^{35}S-pSu9-DHFR; pGEM4-pSu9-DHFR (plasmid)	PMID: 2892669		
Recombinant DNA reagent	mito-GFP; pRS426-TPI -pSu9-eGFP (plasmid)	this paper		pSu9-eGFP was subcloned from pYX142-pSu9-GFP (Westermann B. and Neupert W. *Yeast*, 2000) to pRS426 with EcoRI and HindIII
Peptide, recombinant protein GST	GST	DOI: 10.1128/MCB.00227–13		
Peptide, recombinant protein GST-Tom70	GST-Tom70	DOI: 10.1128/MCB.00227–13		

Yeast strains and growth conditions

Yeast strains used in the study were isogenic to *Saccharomyces cerevisiae* strain W303α beside *mas37Δ*, which is isogenic to YPH499. Standard genetic techniques were used for growth and manipulation of yeast strains. Yeast cells were grown in synthetic medium S (0.67% [w/v] bacto-yeast nitrogen base without amino acids) with glucose (2% [w/v]), glycerol (3% [w/v]), or lactate (2% [w/v]) as carbon source. Transformation of yeast cells was performed by the lithium acetate method. Strains deleted for *MIM1*, *MIM2* or both were previously described (**Dimmer et al., 2012**). For drop-dilution assay, cells were grown in a synthetic medium to an OD_{600} of 1.0 and diluted in fivefold increments followed by spotting 5 µl of the diluted cells on solid media.

Transgenic cell lines and growth of *T. brucei*

Transgenic procyclic cell lines are based on *T. brucei* 29–13 cells (**Wirtz et al., 1999**) and were grown at 27˚C in SDM-79 medium supplemented with 10% FCS (v/v). The RNAi cell line targeting the open reading frame of pATOM36 (Tb927.7.5700, Q582I5) was previously described (**Pusnik et al., 2012**). For growth curves, tetracycline induced and uninduced cell lines were diluted to 2×10^6 cells/ml every 2 days and the cumulative cell number was calculated.

Recombinant DNA techniques

pATOM36 and its 3xHA-tagged variant were cloned into the yeast expression plasmid pYX142-TPI-$_{pro}$ using the EcoRI and BamHI cutting sites. For simultaneous and inducible expression of *S.c.* Mim1-myc and Mim2-HA in *T. brucei*, the appropriate cell line was transfected with a pLew100-based plasmid (**Bochud-Allemann and Schneider, 2002**; **Wirtz et al., 1999**). For optimal expression of the proteins, the ORFs were adapted to the codon usage of *T. brucei* according to **Horn (2008)**. The intergenic region of the α- and β-tubulin genes was cloned in between the ORFs. The insert was synthesised by GenScript with flanking HindIII and BamHI sites for cloning into the pLew100 vector.

For expression from distinct plasmids, the ORFs of *MIM1* and *MIM2* were amplified from yeast genomic DNA and cloned into pLew100-based expression vectors using HindIII and BamHI for *MIM1* and HindIII and XbaI for *MIM2*.

Biochemical methods

Protein samples for immunodecoration were analysed on 8, 12, 12.5, or 15% SDS-PAGE and subsequently transferred onto nitrocellulose membranes by semi-dry western blotting. Proteins were detected by incubating the membranes first with primary antibodies and then with either horseradish peroxidase-conjugates of goat anti-rabbit, goat anti-mouse or goat anti-rat secondary antibodies or with secondary antibodies coupled to fluorescent dye and usage of the LI-COR system.

Isolation of mitochondria from yeast cells was performed by differential centrifugation, as previously described (**Daum et al., 1982**). For protease protection assay, 50 µg of mitochondria were resuspended in 100 µl of SEM buffer (250 mM sucrose, 1 mM EDTA, 10 mM MOPS, pH 7.2). As a control, mitochondria were treated with 1% Triton X-100 in SEM buffer and incubated on ice for 30 min. The samples were supplemented with Proteinase K (50 µg/ml) and incubated on ice for 30 min. The proteolytic reaction was stopped with 5 mM Phenylmethylsulfonyl fluoride (PMSF). The samples were precipitated with trichloroacetic acid (TCA) and resuspended in 40 µl of 2x Laemmli buffer, heated for 10 min at 95˚C, and analysed by SDS-PAGE and immunoblotting.

To analyse the membrane topology of proteins, alkaline extraction was performed. Mitochondria (50 µg) were resuspended in 100 µl of buffer containing 10 mM HEPES-KOH, 100 mM Na_2CO_3, pH 11.5 and incubated 30 min on ice. The membrane fraction was pelleted by centrifugation (76000xg, 30 min, 2˚C) and the supernatant fraction was precipitated with TCA. Both fractions were resuspended in 40 µl of 2x Laemmli buffer, heated for 10 min at 95˚C, and analysed by SDS-PAGE and immunoblotting.

GST-pulldown with radiolabelled proteins was performed as previously described (**Papić et al., 2013**).

For mitochondria enriched fractions by digitonin extraction of *T. brucei*, the cells were incubated for 10 min on ice in 20 mM Tris-HCl pH 7.5, 0.6 M sorbitol, 2 mM EDTA containing 0.025% (w/v) digitonin. After centrifugation (6,800 g, 4˚C), the resulting mitochondria enriched fraction was separated

from the supernatant and subjected to SDS-PAGE. The mitochondria enriched pellets were also used for further experiments.

In vitro synthesis and mitochondrial import of radiolabelled proteins

In vitro transcription was performed with SP6 polymerase from either pGEM4 or pGEM3 plasmid encoding the gene of interest. Proteins were then in vitro translated from the acquired mRNA in the presence of ^{35}S-methionine in rabbit reticulocyte lysate (Promega, Madison, WI, USA). Protein import was performed by adding 50 µg of isolated organelles to 100 µl of import buffer harboring 1 mM NADH and 2 mM ATP. Then, the translation reaction was added to the mitochondria solution and import of precursor proteins was performed at either 25˚C for pSu9-DHFR, Tom20 and Ugo1 or at 2˚C for Fis1 and Tom20$_{ext}$. Import of Tom20, Fis1-TMC, and Ugo1 was monitored according to established assays (***Ahting et al., 2005***; ***Kemper et al., 2008***; ***Papic et al., 2011***).

Blue native gel electrophoresis (BN-PAGE)

Assembly of native complexes was analysed by BN-PAGE. Mitochondria or mitochondria-enriched fractions were solubilised with buffer (1% digitonin or 0.2% TritonX-100, 20 mM Tris, 0.1 mM EDTA, 50 mM NaCl, 10% glycerol, pH 7.4) for 30 min at 4˚C on an overhead shaker. After a clarifying spin (30,000xg, 15 min, 2˚C), 10x sample buffer (5% [wt/vol] Coomassie brilliant blue G-250, 100 mM Bis-Tris, 500 mM 6-aminocaproic acid, pH 7.0) was added and the mixture was analysed by electrophoresis in a blue native gel containing either 6–14% or 8–13% gradient of acrylamide (***Schägger et al., 1994***). To analyse the assembly of radiolabelled Tom20 molecules, the organelles were solubilised with 0.2% digitonin. BN-PAGE was followed by either western blotting or autoradiography. The mixture NativeMark Unstained Protein Standard was used to monitor the migration of molecular weight marker proteins.

Fluorescence microscopy

Fluorescence images of yeast cells were acquired with spinning disk microscope Zeiss Axio Examiner Z1 equipped with a CSU-X1 real-time confocal system (Visitron, Puchheim, Germany), VS-Laser system, and SPOT Flex CCD camera (Visitron Systems). Images were analysed with VisiView software (Visitron). Immunofluorescence images of *T. brucei* were acquired with a DFC360 FX monochrome camera (Leica Microsystrems, Nussloch, Germany) and a DMI6000B microscope (Leica Microsystems). Image analysis was done using LAS X software (Leica Microsystems), ImageJ, and Adobe Photoshop CS5.1 (Adobe).

Acknowledgements

We thank E Kracker for technical assistance. This work was supported by the Deutsche Forschungsgemeinschaft (RA 1028/7–1,2 and DIP to DR), the ITN TAMPting to DV and DR (funded by the Marie Curie Actions of the EU [grant number 607072]). KSD was supported by the PROFILplus program of the Faculty of Medicine of the University of Tübingen. Research in the Schneider group was supported by grant 175563 and in part by the NCCR 'RNA and Disease' both funded by the Swiss National Science Foundation.

Additional information

Funding

Funder	Grant reference number	Author
H2020 Marie Skłodowska-Curie Actions	ITN TAMPting, 607072	Daniela G Vitali Doron Rapaport
Schweizerischer Nationalfonds zur Förderung der Wissenschaftlichen Forschung	138355	Andre Schneider
Deutsche Forschungsgemeinschaft	RA 1028/7-1,RA 1028/10-1	Doron Rapaport

The funders had no role in study design, data collection and interpretation, or the decision to submit the work for publication.

Author contributions

Daniela G Vitali, Conceptualization, Investigation, Methodology; Sandro Käser, Conceptualization, Investigation, Methodology, Writing—original draft; Antonia Kolb, Investigation, Methodology; Kai S Dimmer, Resources, Funding acquisition; Andre Schneider, Doron Rapaport, Conceptualization, Supervision, Funding acquisition, Writing—original draft

Author ORCIDs

Doron Rapaport http://orcid.org/0000-0003-3136-1207

Decision letter and Author response

Decision letter https://doi.org/10.7554/eLife.34488.018
Author response https://doi.org/10.7554/eLife.34488.019

Additional files

Data availability

All data generated or analysed during this study are included in the manuscript and supporting files.

References

Ahting U, Waizenegger T, Neupert W, Rapaport D. 2005. Signal-anchored proteins follow a unique insertion pathway into the outer membrane of mitochondria. *Journal of Biological Chemistry* **280**:48–53. DOI: https://doi.org/10.1074/jbc.M410905200, PMID: 15501820

Becker T, Pfannschmidt S, Guiard B, Stojanovski D, Milenkovic D, Kutik S, Pfanner N, Meisinger C, Wiedemann N. 2008a. Biogenesis of the mitochondrial TOM complex: mim1 promotes insertion and assembly of signal-anchored receptors. *The Journal of Biological Chemistry* **283**:120–127. DOI: https://doi.org/10.1074/jbc.M706997200, PMID: 17974559

Becker T, Vögtle FN, Stojanovski D, Meisinger C. 2008b. Sorting and assembly of mitochondrial outer membrane proteins. *Biochimica et Biophysica Acta (BBA) - Bioenergetics* **1777**:557–563. DOI: https://doi.org/10.1016/j.bbabio.2008.03.017, PMID: 18423394

Becker T, Wenz LS, Krüger V, Lehmann W, Müller JM, Goroncy L, Zufall N, Lithgow T, Guiard B, Chacinska A, Wagner R, Meisinger C, Pfanner N. 2011. The mitochondrial import protein Mim1 promotes biogenesis of multispanning outer membrane proteins. *The Journal of Cell Biology* **194**:387–395. DOI: https://doi.org/10.1083/jcb.201102044, PMID: 21825073

Bochud-Allemann N, Schneider A. 2002. Mitochondrial substrate level phosphorylation is essential for growth of procyclic Trypanosoma brucei. *Journal of Biological Chemistry* **277**:32849–32854. DOI: https://doi.org/10.1074/jbc.M205776200, PMID: 12095995

Bruggisser J, Käser S, Mani J, Schneider A. 2017. Biogenesis of a mitochondrial outer membrane protein in *Trypanosoma brucei*: Targeting signal and dependence on a unique biogenesis factor. *The Journal of Biological Chemistry* **292**:3400–3410. DOI: https://doi.org/10.1074/jbc.M116.755983, PMID: 28100781

Burki F. 2014. The eukaryotic tree of life from a global phylogenomic perspective. *Cold Spring Harbor Perspectives in Biology* **6**:a016147. DOI: https://doi.org/10.1101/cshperspect.a016147, PMID: 24789819

Chan NC, Lithgow T. 2008. The peripheral membrane subunits of the SAM complex function codependently in mitochondrial outer membrane biogenesis. *Molecular Biology of the Cell* **19**:126–136. DOI: https://doi.org/10.1091/mbc.e07-08-0796, PMID: 17978093

Daum G, Böhni PC, Schatz G. 1982. Import of proteins into mitochondria. cytochrome b2 and cytochrome c peroxidase are located in the intermembrane space of yeast mitochondria. *The Journal of Biological Chemistry* **257**:13028–13033. PMID: 6290489

Dimmer KS, Papić D, Schumann B, Sperl D, Krumpe K, Walther DM, Rapaport D. 2012. A crucial role for Mim2 in the biogenesis of mitochondrial outer membrane proteins. *Journal of Cell Science* **125**:3464–3473. DOI: https://doi.org/10.1242/jcs.103804, PMID: 22467864

Dolezal P, Likic V, Tachezy J, Lithgow T. 2006. Evolution of the molecular machines for protein import into mitochondria. *Science* **313**:314–318. DOI: https://doi.org/10.1126/science.1127895, PMID: 16857931

Dukanovic J, Dimmer KS, Bonnefoy N, Krumpe K, Rapaport D. 2009. Genetic and functional interactions between the mitochondrial outer membrane proteins Tom6 and Sam37. *Molecular and Cellular Biology* **29**:5975–5988. DOI: https://doi.org/10.1128/MCB.00069-09, PMID: 19797086

Dukanovic J, Rapaport D. 2011. Multiple pathways in the integration of proteins into the mitochondrial outer membrane. *Biochimica et Biophysica Acta (BBA) - Biomembranes* **1808**:971–980. DOI: https://doi.org/10.1016/j.bbamem.2010.06.021, PMID: 20599689

Endo T, Yamano K. 2009. Multiple pathways for mitochondrial protein traffic. *Biological Chemistry* **390**:723–730. DOI: https://doi.org/10.1515/BC.2009.087, PMID: 19453276

Gentle I, Gabriel K, Beech P, Waller R, Lithgow T. 2004. The Omp85 family of proteins is essential for outer membrane biogenesis in mitochondria and bacteria. *The Journal of Cell Biology* **164**:19–24. DOI: https://doi.org/10.1083/jcb.200310092, PMID: 14699090

Horn D. 2008. Codon usage suggests that translational selection has a major impact on protein expression in trypanosomatids. *BMC Genomics* **9**:2. DOI: https://doi.org/10.1186/1471-2164-9-2, PMID: 18173843

Hulett JM, Lueder F, Chan NC, Perry AJ, Wolynec P, Likić VA, Gooley PR, Lithgow T. 2008. The transmembrane segment of Tom20 is recognized by Mim1 for docking to the mitochondrial TOM complex. *Journal of Molecular Biology* **376**:694–704. DOI: https://doi.org/10.1016/j.jmb.2007.12.021, PMID: 18187149

Ishikawa D, Yamamoto H, Tamura Y, Moritoh K, Endo T. 2004. Two novel proteins in the mitochondrial outer membrane mediate beta-barrel protein assembly. *The Journal of Cell Biology* **166**:621–627. DOI: https://doi.org/10.1083/jcb.200405138, PMID: 15326197

Käser S, Oeljeklaus S, Tyc J, Vaughan S, Warscheid B, Schneider A. 2016. Outer membrane protein functions as integrator of protein import and DNA inheritance in mitochondria. *PNAS* **113**:E4467–E4475. DOI: https://doi.org/10.1073/pnas.1605497113, PMID: 27436903

Kemper C, Habib SJ, Engl G, Heckmeyer P, Dimmer KS, Rapaport D. 2008. Integration of tail-anchored proteins into the mitochondrial outer membrane does not require any known import components. *Journal of Cell Science* **121**:1990–1998. DOI: https://doi.org/10.1242/jcs.024034, PMID: 18495843

Kozjak V, Wiedemann N, Milenkovic D, Lohaus C, Meyer HE, Guiard B, Meisinger C, Pfanner N. 2003. An essential role of Sam50 in the protein sorting and assembly machinery of the mitochondrial outer membrane. *Journal of Biological Chemistry* **278**:48520–48523. DOI: https://doi.org/10.1074/jbc.C300442200, PMID: 14570913

Krüger V, Becker T, Becker L, Montilla-Martinez M, Ellenrieder L, Vögtle FN, Meyer HE, Ryan MT, Wiedemann N, Warscheid B, Pfanner N, Wagner R, Meisinger C. 2017. Identification of new channels by systematic analysis of the mitochondrial outer membrane. *The Journal of Cell Biology* **216**:3485–3495. DOI: https://doi.org/10.1083/jcb.201706043, PMID: 28916712

Lueder F, Lithgow T. 2009. The three domains of the mitochondrial outer membrane protein Mim1 have discrete functions in assembly of the TOM complex. *FEBS Letters* **583**:1475–1480. DOI: https://doi.org/10.1016/j.febslet.2009.03.064, PMID: 19345216

Mani J, Desy S, Niemann M, Chanfon A, Oeljeklaus S, Pusnik M, Schmidt O, Gerbeth C, Meisinger C, Warscheid B, Schneider A. 2015. Mitochondrial protein import receptors in Kinetoplastids reveal convergent evolution over large phylogenetic distances. *Nature Communications* **6**:6646. DOI: https://doi.org/10.1038/ncomms7646, PMID: 25808593

Mani J, Meisinger C, Schneider A. 2016. Peeping at TOMs-Diverse entry gates to mitochondria provide insights into the evolution of eukaryotes. *Molecular Biology and Evolution* **33**:337–351. DOI: https://doi.org/10.1093/molbev/msv219, PMID: 26474847

Mnaimneh S, Davierwala AP, Haynes J, Moffat J, Peng WT, Zhang W, Yang X, Pootoolal J, Chua G, Lopez A, Trochesset M, Morse D, Krogan NJ, Hiley SL, Li Z, Morris Q, Grigull J, Mitsakakis N, Roberts CJ, Greenblatt JF, et al. 2004. Exploration of essential gene functions via titratable promoter alleles. *Cell* **118**:31–44. DOI: https://doi.org/10.1016/j.cell.2004.06.013, PMID: 15242642

Otera H, Taira Y, Horie C, Suzuki Y, Suzuki H, Setoguchi K, Kato H, Oka T, Mihara K. 2007. A novel insertion pathway of mitochondrial outer membrane proteins with multiple transmembrane segments. *The Journal of Cell Biology* **179**:1355–1363. DOI: https://doi.org/10.1083/jcb.200702143, PMID: 18158327

Papic D, Krumpe K, Dukanovic J, Dimmer KS, Rapaport D. 2011. Multispan mitochondrial outer membrane protein Ugo1 follows a unique Mim1-dependent import pathway. *The Journal of Cell Biology* **194**:397–405. DOI: https://doi.org/10.1083/jcb.201102041, PMID: 21825074

Papić D, Elbaz-Alon Y, Koerdt SN, Leopold K, Worm D, Jung M, Schuldiner M, Rapaport D. 2013. The role of Djp1 in import of the mitochondrial protein Mim1 demonstrates specificity between a cochaperone and its substrate protein. *Molecular and Cellular Biology* **33**:4083–4094. DOI: https://doi.org/10.1128/MCB.00227-13, PMID: 23959800

Paschen SA, Waizenegger T, Stan T, Preuss M, Cyrklaff M, Hell K, Rapaport D, Neupert W. 2003. Evolutionary conservation of biogenesis of beta-barrel membrane proteins. *Nature* **426**:862–866. DOI: https://doi.org/10.1038/nature02208, PMID: 14685243

Popov-Celeketić J, Waizenegger T, Rapaport D. 2008. Mim1 functions in an oligomeric form to facilitate the integration of Tom20 into the mitochondrial outer membrane. *Journal of Molecular Biology* **376**:671–680. DOI: https://doi.org/10.1016/j.jmb.2007.12.006, PMID: 18177669

Pusnik M, Mani J, Schmidt O, Niemann M, Oeljeklaus S, Schnarwiler F, Warscheid B, Lithgow T, Meisinger C, Schneider A. 2012. An essential novel component of the noncanonical mitochondrial outer membrane protein import system of trypanosomatids. *Molecular Biology of the Cell* **23**:3420–3428. DOI: https://doi.org/10.1091/mbc.e12-02-0107, PMID: 22787278

Schägger H, Cramer WA, von Jagow G. 1994. Analysis of molecular masses and oligomeric states of protein complexes by blue native electrophoresis and isolation of membrane protein complexes by two-dimensional

native electrophoresis. *Analytical Biochemistry* **217**:220–230. DOI: https://doi.org/10.1006/abio.1994.1112, PMID: 8203750

Schnarwiler F, Niemann M, Doiron N, Harsman A, Käser S, Mani J, Chanfon A, Dewar CE, Oeljeklaus S, Jackson CB, Pusnik M, Schmidt O, Meisinger C, Hiller S, Warscheid B, Schnaufer AC, Ochsenreiter T, Schneider A. 2014. Trypanosomal TAC40 constitutes a novel subclass of mitochondrial β-barrel proteins specialized in mitochondrial genome inheritance. *PNAS* **111**:7624–7629. DOI: https://doi.org/10.1073/pnas.1404854111, PMID: 24821793

Thornton N, Stroud DA, Milenkovic D, Guiard B, Pfanner N, Becker T. 2010. Two modular forms of the mitochondrial sorting and assembly machinery are involved in biogenesis of alpha-helical outer membrane proteins. *Journal of Molecular Biology* **396**:540–549. DOI: https://doi.org/10.1016/j.jmb.2009.12.026, PMID: 20026336

Vögtle FN, Keller M, Taskin AA, Horvath SE, Guan XL, Prinz C, Opalińska M, Zorzin C, van der Laan M, Wenk MR, Schubert R, Wiedemann N, Holzer M, Meisinger C. 2015. The fusogenic lipid phosphatidic acid promotes the biogenesis of mitochondrial outer membrane protein Ugo1. *The Journal of Cell Biology* **210**:951–960. DOI: https://doi.org/10.1083/jcb.201506085, PMID: 26347140

Waizenegger T, Schmitt S, Zivkovic J, Neupert W, Rapaport D. 2005. Mim1, a protein required for the assembly of the TOM complex of mitochondria. *EMBO reports* **6**:57–62. DOI: https://doi.org/10.1038/sj.embor.7400318, PMID: 15608614

Walther DM, Rapaport D, Tommassen J. 2009. Biogenesis of beta-barrel membrane proteins in bacteria and eukaryotes: evolutionary conservation and divergence. *Cellular and Molecular Life Sciences* **66**:2789–2804. DOI: https://doi.org/10.1007/s00018-009-0029-z, PMID: 19399587

Wiedemann N, Kozjak V, Chacinska A, Schönfisch B, Rospert S, Ryan MT, Pfanner N, Meisinger C. 2003. Machinery for protein sorting and assembly in the mitochondrial outer membrane. *Nature* **424**:565–571. DOI: https://doi.org/10.1038/nature01753, PMID: 12891361

Wirtz E, Leal S, Ochatt C, Cross GA. 1999. A tightly regulated inducible expression system for conditional gene knock-outs and dominant-negative genetics in *Trypanosoma brucei*. *Molecular and Biochemical Parasitology* **99**:89–101. DOI: https://doi.org/10.1016/S0166-6851(99)00002-X, PMID: 10215027

eLIFE elifesciences.org

RESEARCH ARTICLE

Figures and figure supplements

Independent evolution of functionally exchangeable mitochondrial outer membrane import complexes

Daniela G Vitali *et al*

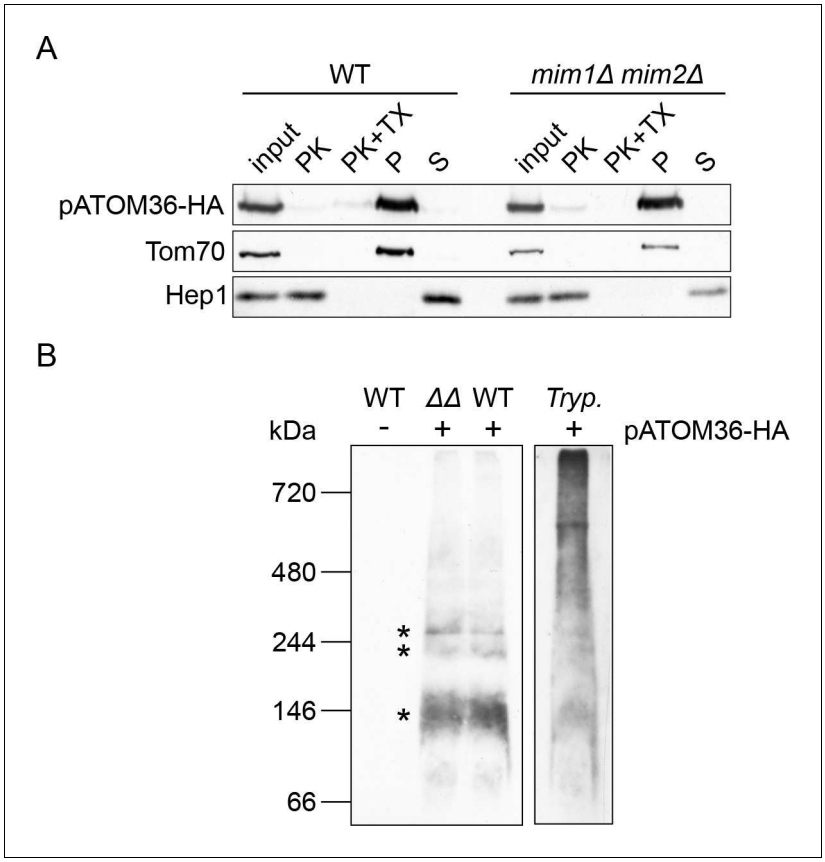

Figure 1. pATOM36 forms native-like complexes in the yeast mitochondrial OM. (**A**) Mitochondria isolated from WT or *mim1Δ/mim2Δ* cells expressing pATOM36-HA were left intact or lysed with Triton X-100 (TX) before they were subjected to treatment with proteinase K (PK). Alternatively, other samples were subjected to alkaline extraction followed by separation by centrifugation to pellet (P) and supernatant (S) fractions. All samples were analysed by SDS-PAGE followed by immunodecoration with antibodies against the HA-epitope, the OM receptor protein Tom70, or the matrix soluble protein Hep1. (**B**) Mitochondria were isolated from yeast WT cells transformed with an empty plasmid (-) or from WT and *mim1Δ/mim2Δ* (*ΔΔ*) cells expressing pATOM36-HA (+). Isolated yeast organelles and mitochondria-enriched fraction from *T. brucei* (Tryp.) cells expressing pATOM36-HA were lysed with 1% digitonin. All samples were then subjected to BN-PAGE followed by immunodecoration with an antibody against the HA-tag. pATOM36-containing complexes are indicated with an asterisk.

DOI: https://doi.org/10.7554/eLife.34488.002

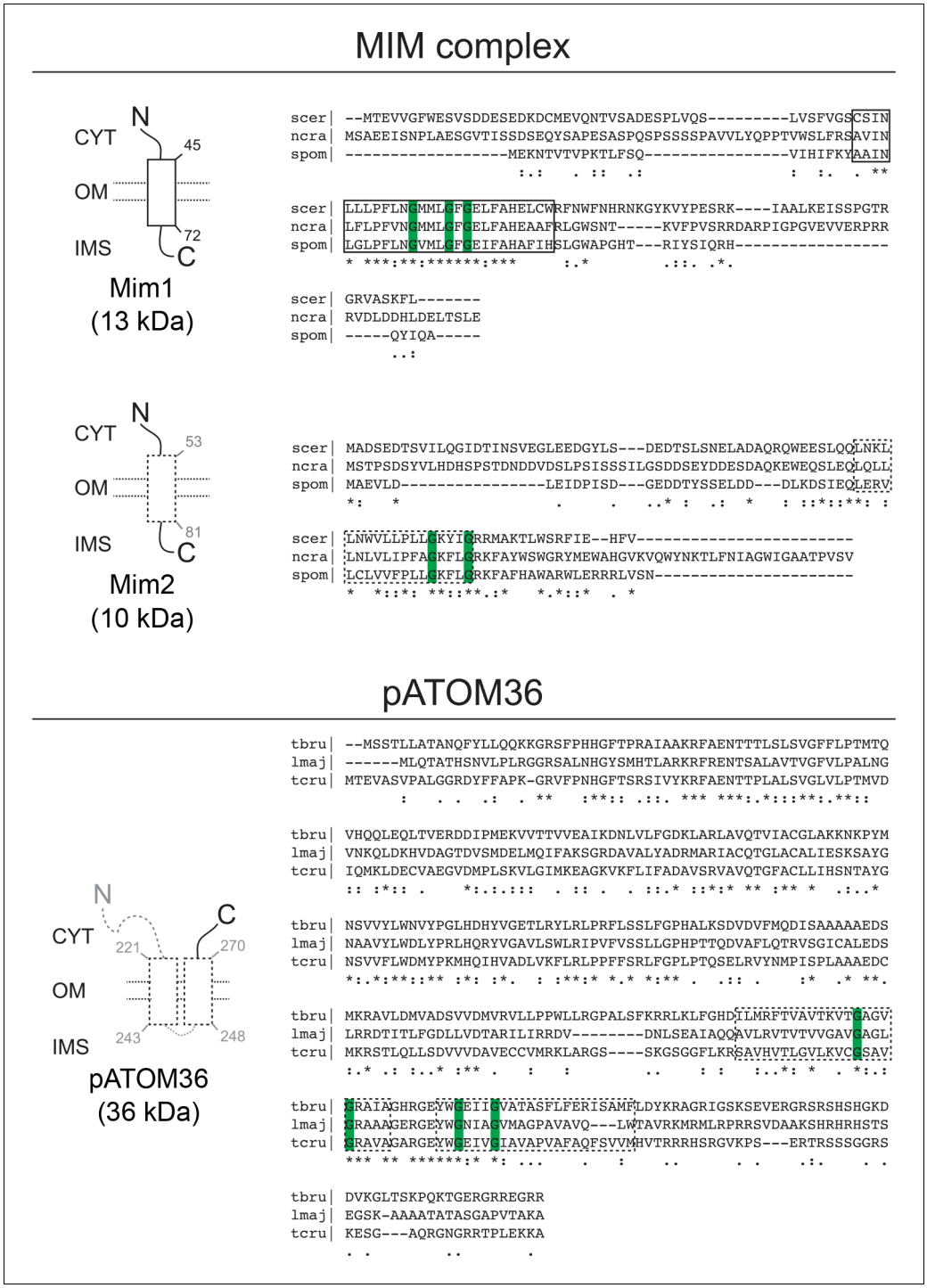

Figure 1—figure supplement 1. Topologies and protein sequence alignments of Mim1, Mim2 and pATOM36. Left panels: Schematic representation of the experimentally determined and predicted topologies of Mim1, Mim2 and pATOM36. The transmembrane segment (TMS) of Mim1 has been experimentally characterised (solid line), whereas those of Mim2 and pATOM36 are predicted by PolyPhobius with TOPCONS (dashed lines). The amino acid positions of the TMSs are illustrated and the protein sizes are in brackets. CYT, cytosol; OM, outer mitochondrial membrane; IMS, intermembrane space. Right panels: Multiple protein sequence alignments of Mim1, Mim2 and pATOM36. Verified and predicted TMSs are highlighted by solid and dashed lines, respectively. Conserved glycine residues are marked in green. scer, *Saccharomyces cerevisiae*; ncra, *Neurospora crassa*; spom, *Schizosaccharomyces pombe*; tbru, *Trypanosoma brucei*; lmaj, Leishmania major; tcru, *Trypanosoma cruzi*.
DOI: https://doi.org/10.7554/eLife.34488.003

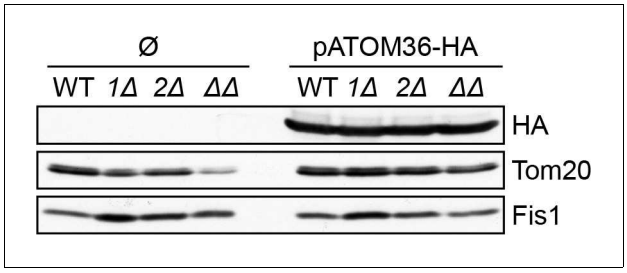

Figure 1—figure supplement 2. pATOM36-HA is expressed in the transformed cells. Whole cell lysate of wild type (WT), mim1Δ (1Δ), mim2Δ (2Δ) and mim1Δmim2Δ (ΔΔ) cells transformed with either an empty plasmid (Ø) or a plasmid encoding for pATOM36-HA were obtained. The samples were analysed by SDS-PAGE and immunodecoration with the indicated antibodies.

DOI: https://doi.org/10.7554/eLife.34488.004

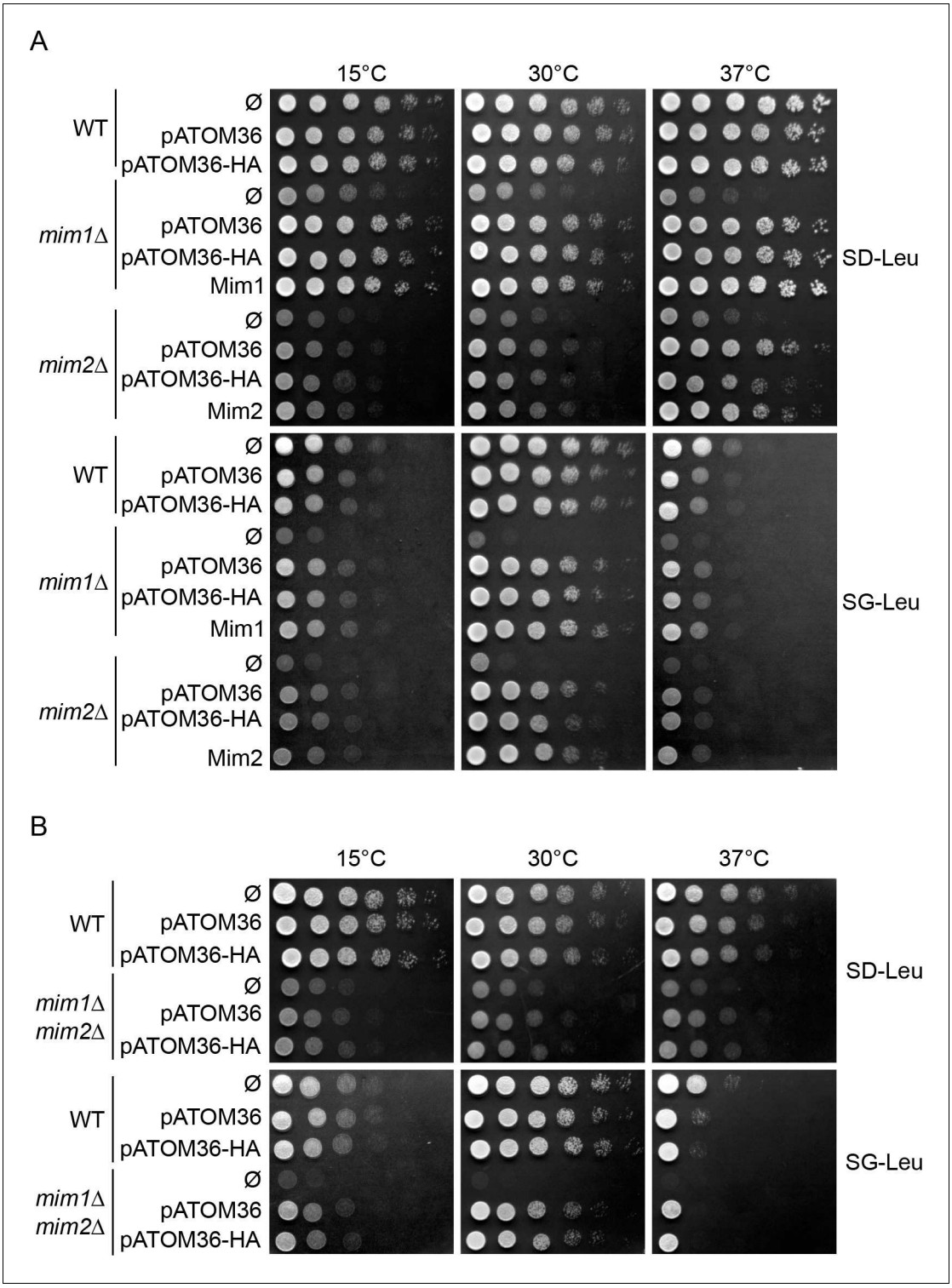

Figure 2. pATOM36 rescues the growth defects of cells lacking Mim1, Mim2 or both. (**A**) The indicated strains transformed with an empty plasmid (Ø) or with a plasmid expressing pATOM36 or its HA-tagged variant were tested at three different temperatures by drop-dilution assay for growth on synthetic medium containing either glucose (SD-Leu) or glycerol (SG-Leu). For comparison, plasmid-encoded Mim1 or Mim2 were transformed into *mim1Δ* or *mim2Δ* cells, respectively. All dilutions are in fivefold increment. (**B**) Cells deleted for both *MIM1* and *MIM2* (*mim1Δ/mim2Δ*) were transformed with the empty plasmid (Ø) or a plasmid encoding either native pATOM36 or pATOM36-HA. Transformed cells were analysed by drop-dilution assay at the indicated temperatures on synthetic medium containing either glucose (SD-Leu) or glycerol (SG-Leu). All dilutions are in fivefold increment.

DOI: https://doi.org/10.7554/eLife.34488.005

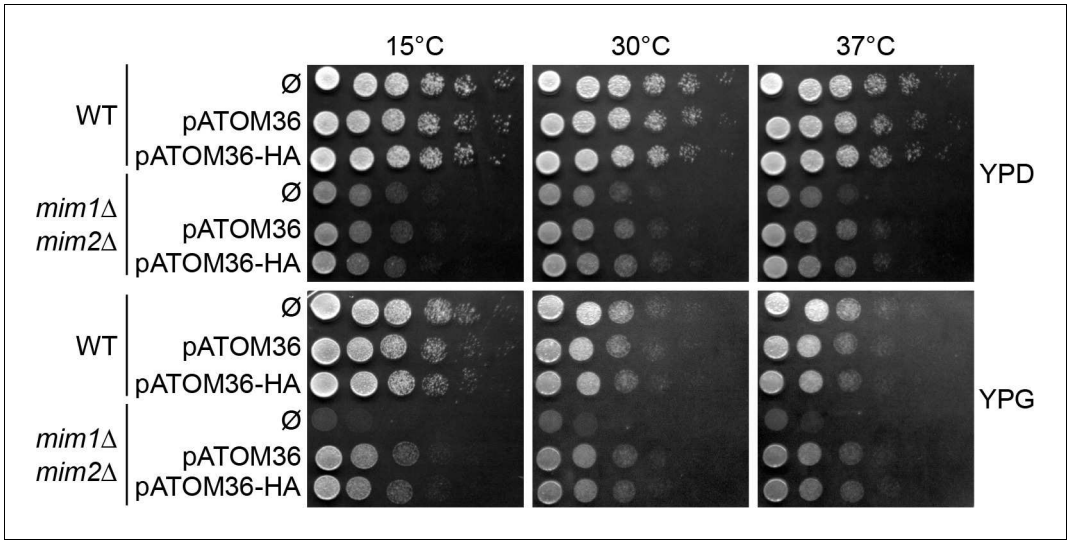

Figure 2—figure supplement 1. pATOM36 rescues the growth defect of mim1Δmim2Δ cells. The indicated strains transformed with an empty plasmid (Ø), a plasmid expressing pATOM36, or its HA-tagged variant were tested at three different temperatures by drop-dilution assay for growth on rich media containing either glucose (YPD) or glycerol (YPG). All dilutions are in fivefold increment.

DOI: https://doi.org/10.7554/eLife.34488.006

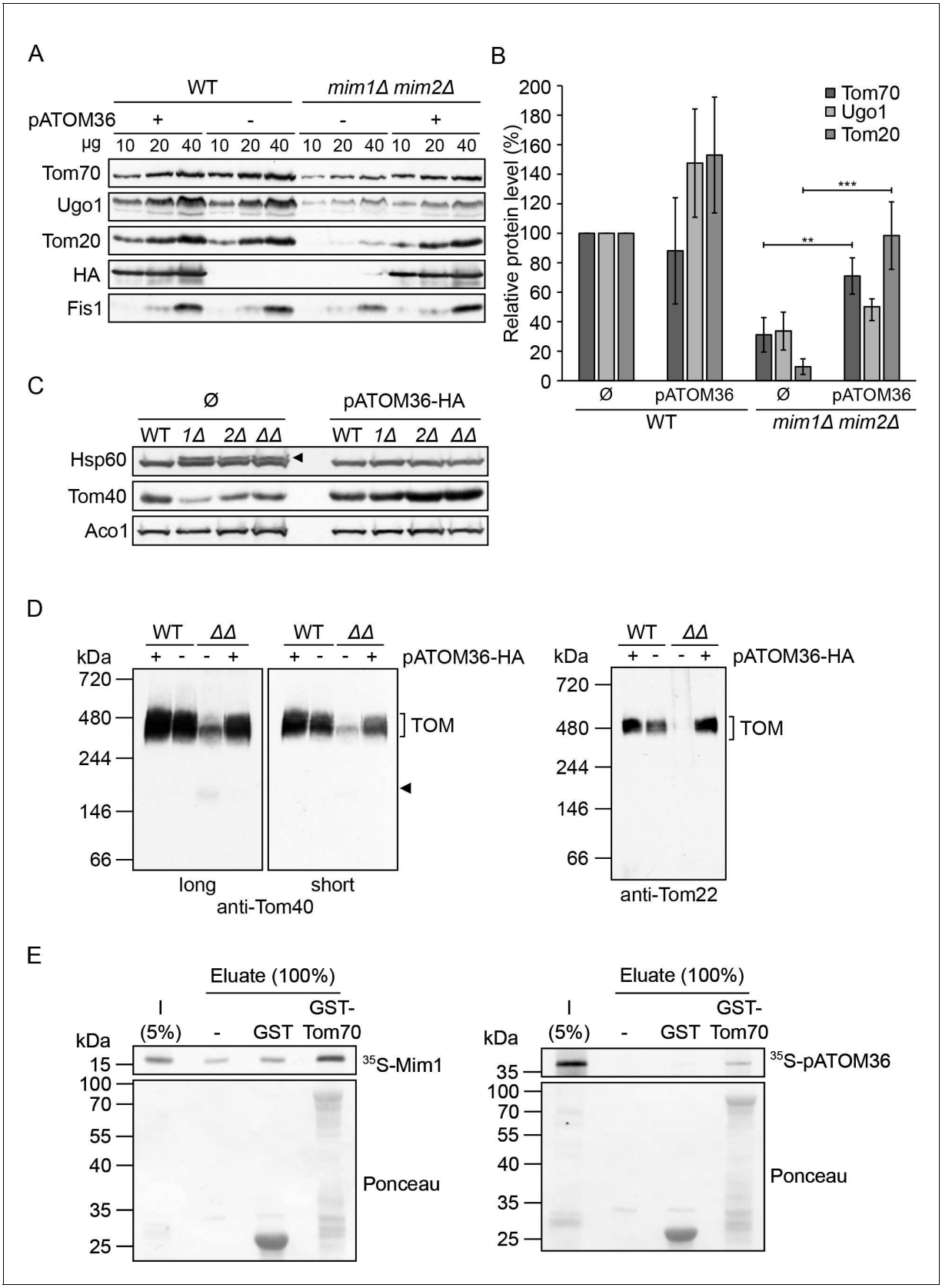

Figure 3. pATOM36 can compensate for the reduced steady state levels and assembly defects in cells lacking both Mim1 and Mim2. (**A**) Mitochondria were isolated from WT or *mim1Δ/mim2Δ* cells transformed with either an empty plasmid (-) or with a plasmid encoding pATOM36-HA (+). The

Figure 3 continued on next page

Figure 3 continued

specified amounts were analysed by SDS-PAGE and immunodecoration with antibodies against either the indicated mitochondrial proteins or the HA-tag. (**B**) The intensity of the bands from three independent experiments such as those presented in (**A**) was monitored. The amounts of Tom70, Ugo1 and Tom20 in the various mitochondria samples are presented as mean percentage of their levels in control organelles (WT+ Ø). The levels of Fis1 were taken as loading control. Error bars represent ± SD. **p≤0.005, ***p≤0.0005. (**C**) Whole cell lysates were obtained from WT, *mim1Δ (1Δ), mim2Δ (2Δ),* or the double deletion *mim1Δ/mim2Δ (ΔΔ)* cells transformed with either an empty plasmid (Ø) or with a plasmid encoding pATOM36-HA. Samples were analysed by SDS-PAGE and immunodecoration with antibodies against the indicated mitochondrial proteins. The precursor form of mitochondrial Hsp60 is indicated with an arrowhead. (**D**) The mitochondria described in (**A**) were solubilised in a buffer containing 1% digitonin and then analysed by BN-PAGE followed by western blotting. The membranes were immunodecorated with antibodies against the TOM subunits, Tom40 (long and short exposures) and Tom22. The TOM complex is signposted. A Tom40-containing low molecular weight complex is indicated with an arrowhead. (**E**) Mim1 and pATOM36 interact directly with Tom70. Radiolabelled Mim1 or pATOM36 (input, **I**) were incubated with glutathione beads (-) or with beads that were pre-bound to recombinant GST alone or to GST fused to the cytosolic domain of Tom70 (GST-Tom70). After washing, bound material was eluated and proteins were analysed by SDS–PAGE followed by blotting onto a membrane, and detection with either autoradiography (upper panel) or Ponceau staining (lower panel).

DOI: https://doi.org/10.7554/eLife.34488.007

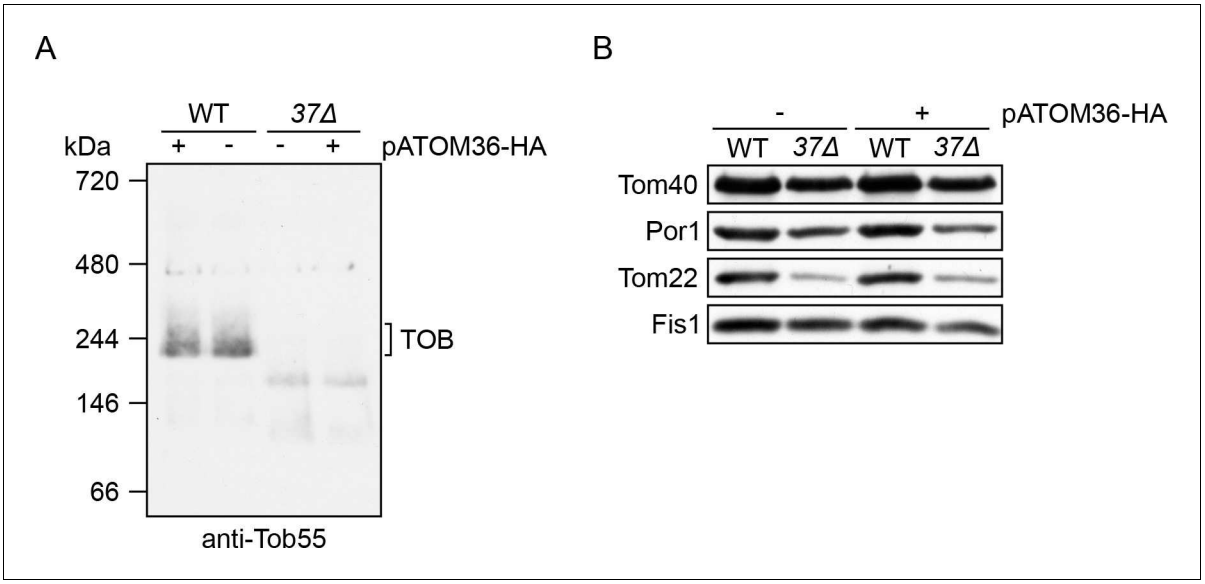

Figure 3—figure supplement 1. pATOM36-HA does not rescue biogenesis defects in mas37Δ cells. (**A**) Mitochondria isolated from wild type (WT) and mas37Δ (37Δ) cells transformed with either an empty plasmid (-) or a plasmid encoding for pATOM36-HA (+) were solubilised in 0.2% Triton X-100. Samples were analysed by BN-PAGE and immunodecoration with an antibody against Tob55. (**B**) Isolated mitochondria as in (**A**) were subjected to SDS-PAGE and immunodecoration with the indicated antibodies.

DOI: https://doi.org/10.7554/eLife.34488.008

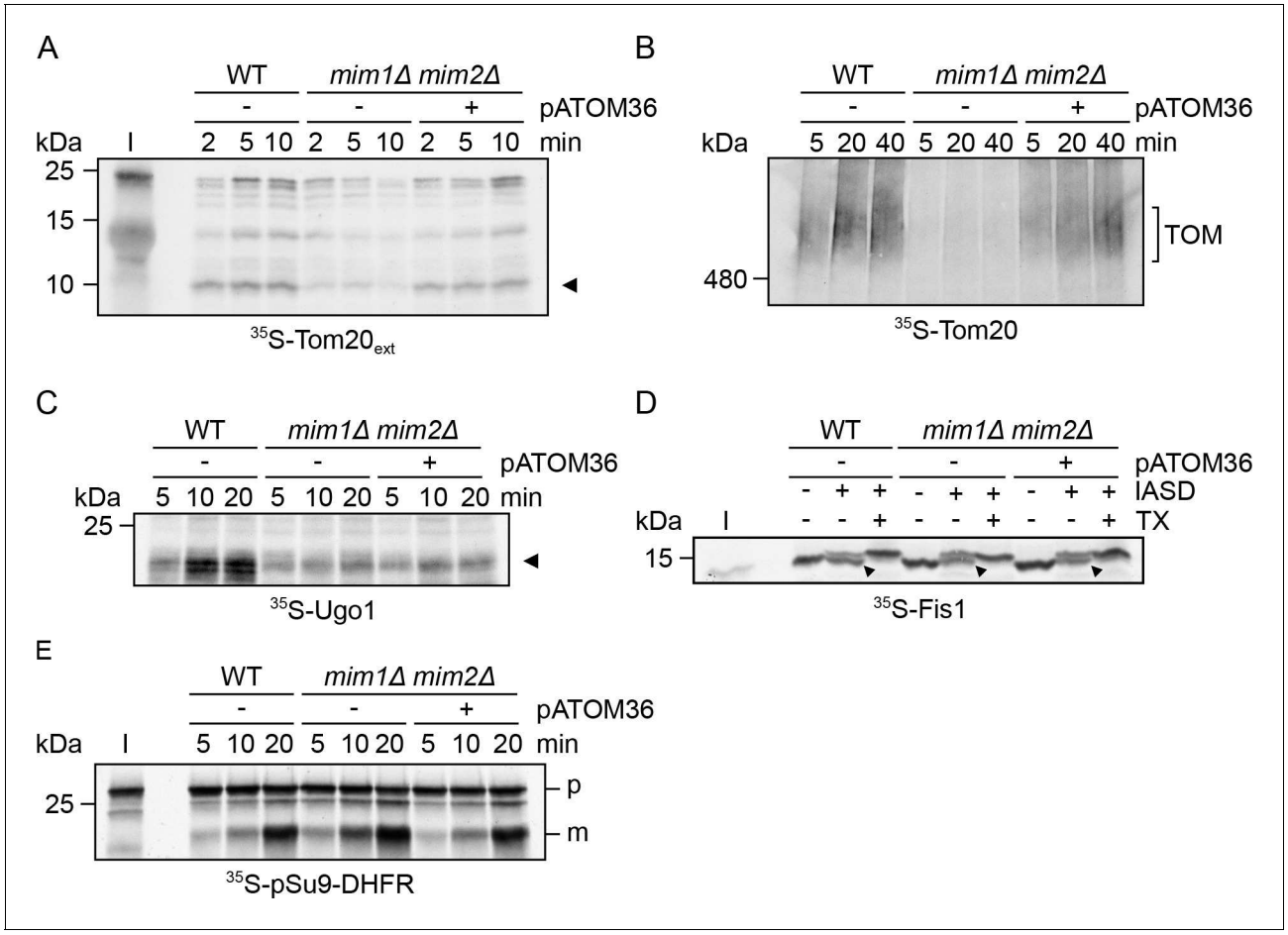

Figure 4. pATOM36 can rescue some of the import defects of cells lacking the MIM complex. (**A**) Mitochondria were isolated from WT cells transformed with an empty plasmid (WT-) or from *mim1Δ/mim2Δ* cells transformed with either an empty plasmid (-) or with a plasmid encoding pATOM36-HA (+). Radiolabelled $Tom20_{ext}$ molecules (5% input, **I**) were incubated with the indicated isolated organelles for the specified time periods. Then, mitochondria were treated with PK and analysed by SDS-PAGE and autoradiography. A proteolytic fragment of $Tom20_{ext}$, which reflects correct membrane integration, is indicated by an arrowhead. (**B**) Radiolabelled Tom20 was incubated with isolated mitochondria as in (**A**). At the end of the import reactions, mitochondria were solubilised with 0.2% digitonin and samples were analysed by BN-PAGE followed by autoradiography. The migration of Tom20 molecules assembled into the TOM complex is indicated. (**C**) Radiolabelled Ugo1 was incubated with isolated mitochondria as in (**A**). Then, mitochondria were treated with trypsin and analysed by SDS-PAGE and autoradiography. A proteolytic fragment of Ugo1, which reflects correct membrane integration, is indicated by an arrowhead. (**D**) Radiolabelled Fis1-TMC (5% input, I) was incubated with isolated mitochondria as in (**A**). Then, mitochondria were subjected to an IASD assay, re-isolated and analysed by SDS-PAGE and autoradiography. Bands representing correctly integrated Fis1-TMC are marked by an arrowhead. (**E**) Radiolabelled pSu9-DHFR (5% input, I) was incubated with isolated mitochondria as in (**A**). Then, mitochondria were re-isolated and analysed by SDS-PAGE and autoradiography. The precursor and mature forms are indicated by p and m, respectively.

DOI: https://doi.org/10.7554/eLife.34488.010

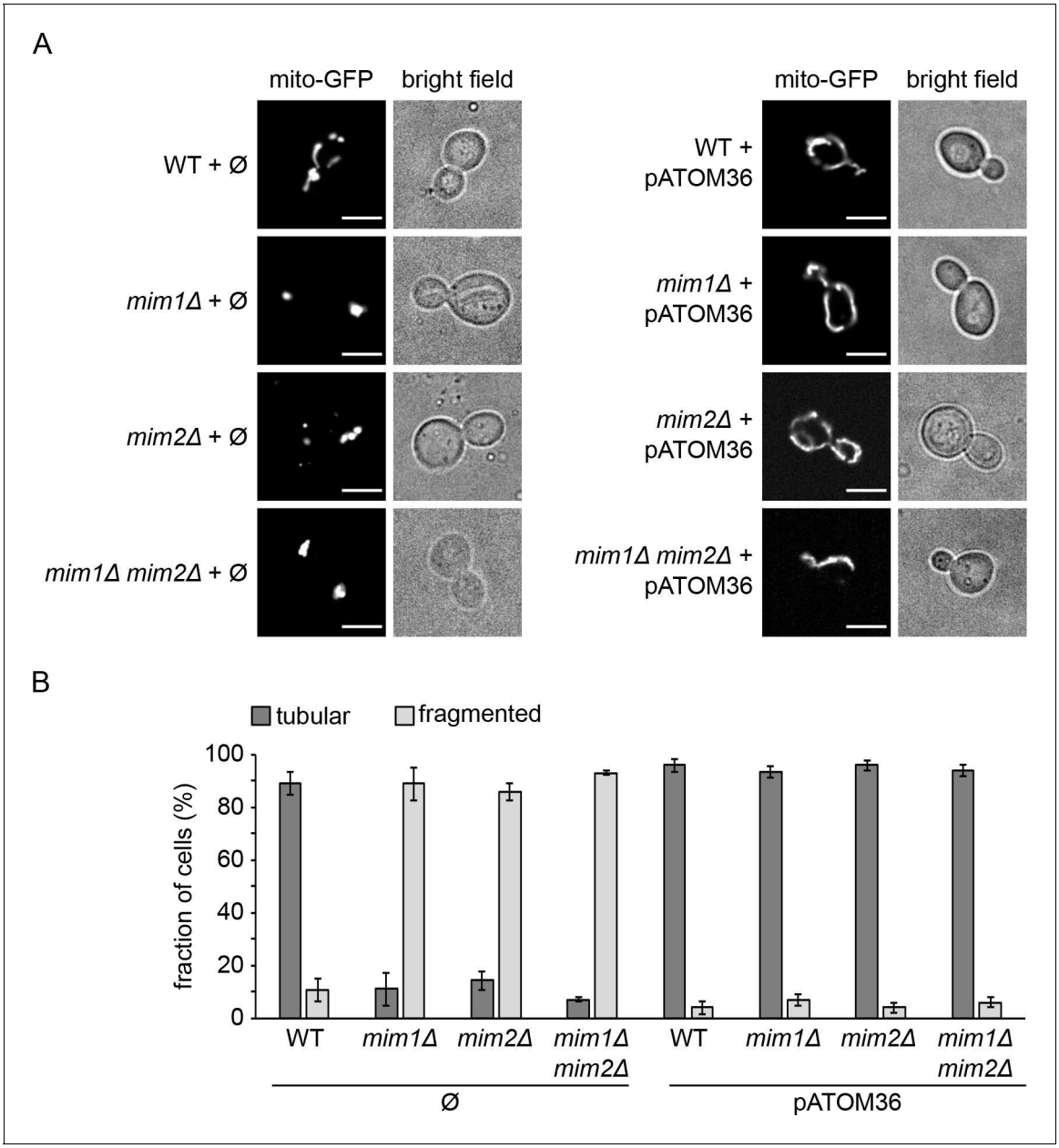

Figure 5. *mim1Δ* and *mim2Δ* cells expressing pATOM36 do not show altered mitochondrial morphology. (**A**) WT, *mim1Δ*, *mim2Δ*, and *mim1Δ/mim2Δ* cells harbouring mitochondria-targeted GFP (mito-GFP) were transformed with either an empty plasmid (Ø) as a control (left panels) or a plasmid encoding pATOM36 (right panels). Cells were analysed by fluorescence microscopy and representative images of the predominant morphology for each strain are shown. Scale bar, 5 µm. (**B**) Statistical analysis of the cells described in (**A**). Average values with standard deviation bars of three independent experiments with at least n = 100 cells in each experiment are shown.

DOI: https://doi.org/10.7554/eLife.34488.011

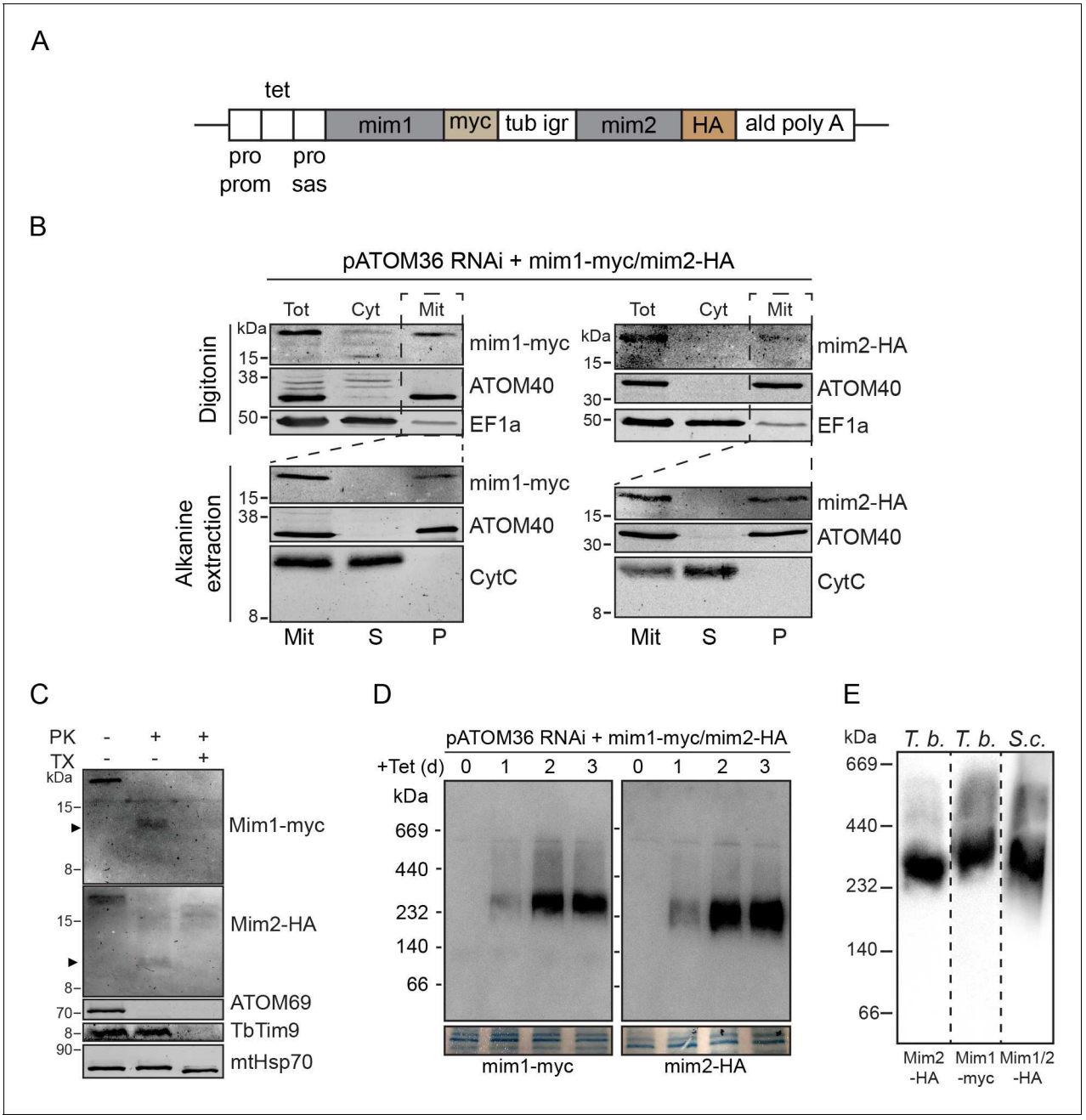

Figure 6. Yeast Mim1 and Mim2 form a high-molecular-weight complex in mitochondria of *T. brucei*. (**A**) Schematic representation of the insert of the pLew100-based vector that allows tetracycline-inducible expression of C-terminally myc-tagged Mim1 and HA-tagged Mim2 in *T. brucei*. Pro prom, procyclin promotor; tet, tetracycline operator; pro sas, procycline splice acceptor site; tub igr, α- and β-tubulin intergenic region; ald polyA, 3'-UTR of the aldolase gene. (**B**) Top panels: immunoblot analysis of whole cells (Tot), soluble (Cyt) and digitonin-extracted mitochondria-enriched pellet (Mit) fractions of a tetracycline-inducible pATOM36-RNAi cell line expressing Mim1-myc and Mim2-HA. Duplicate blots were analysed for the expression of Mim1-myc (left panels) and Mim2-HA (right panels). ATOM40 and EF1a serve as mitochondrial and cytosolic markers, respectively. Bottom panels: Alkaline extraction of the mitochondria-enriched fraction (Mit) shown in the top panels. The pellet (**P**) and the supernatant (**S**) fractions corresponding to integral membrane and soluble proteins, respectively, were analysed by SDS-PAGE and immunodecoration. ATOM40 and CytC serve as markers for integral and peripheral membrane proteins, respectively. (**C**) Mitochondria-enriched fractions of the same cell line describe in (**B**) were left intact or lysed with Triton X-100 (TX) before they were subjected to treatment with proteinase K (PK). All samples were analysed by SDS-PAGE followed by immunodecoration with antibodies against myc and HA tags, the OM protein ATOM69, the IMS protein TbTim9, or the matrix protein mtHsp70. Note that mtHsp70 contains a folded core, which is protease resistant. A proteolytic fragment of Mim1 and Mim2 is indicated with an arrowhead. (**D**) Duplicate immunoblots from BN-PAGE analysis of mitochondria-enriched fractions of the same cell line describe in (**B**) were probed for Mim1-myc (left panels) and Mim2-HA (right panels). Sections of the coomassie-stained gels serve as loading control. (**E**) Immunoblots of a BN-PAGE analysis of

Figure 6 continued on next page

Figure 6 continued

mitochondria-enriched fractions of the *T. brucei* (*T.b.*) cell line simultaneously expressing myc-tagged Mim1 (Mim1-myc) and HA-tagged Mim2 (Mim2-HA) and isolated yeast (*S.c.*) mitochondria simultaneously expressing HA-tagged versions of Mim1 and Mim2. The immunoblots are probed with antibodies against HA- or myc-tag.

DOI: https://doi.org/10.7554/eLife.34488.013

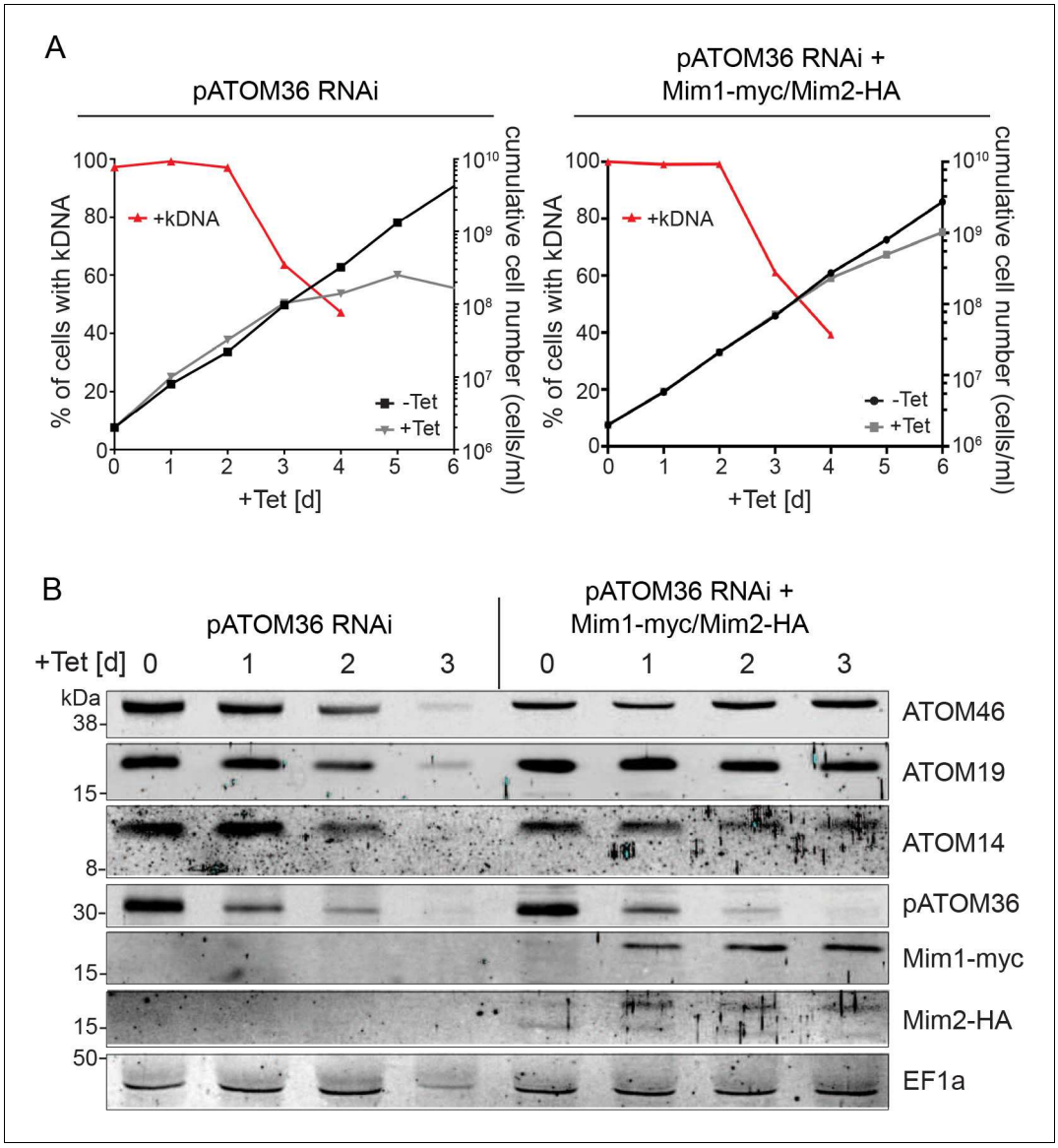

Figure 7. Yeast Mim1 and Mim2 complement the mitochondrial OM biogenesis phenotype of *T. brucei* cells ablated for pATOM36. (**A**) Left panel: growth in the presence and absence of tetracycline (black and grey lines, respectively) and loss of kDNA (red line) in the presence of tetracycline of the pATOM36-RNAi parent cell line. Right panel: as in the left but the analysis was done for the pATOM36-RNAi cell line that co-expresses Mim1-myc and Mim2-HA. (**B**) Whole cell lysates from the cell lines as in (**A**) were obtained after the indicated time of induction. Proteins of these samples were analysed by SDS-PAGE and immunodecoration with the indicated antibodies. ATOM46, ATOM19 and ATOM14 are subunits of the ATOM complex. Cytosolic EF1a serves as a loading control.

DOI: https://doi.org/10.7554/eLife.34488.014

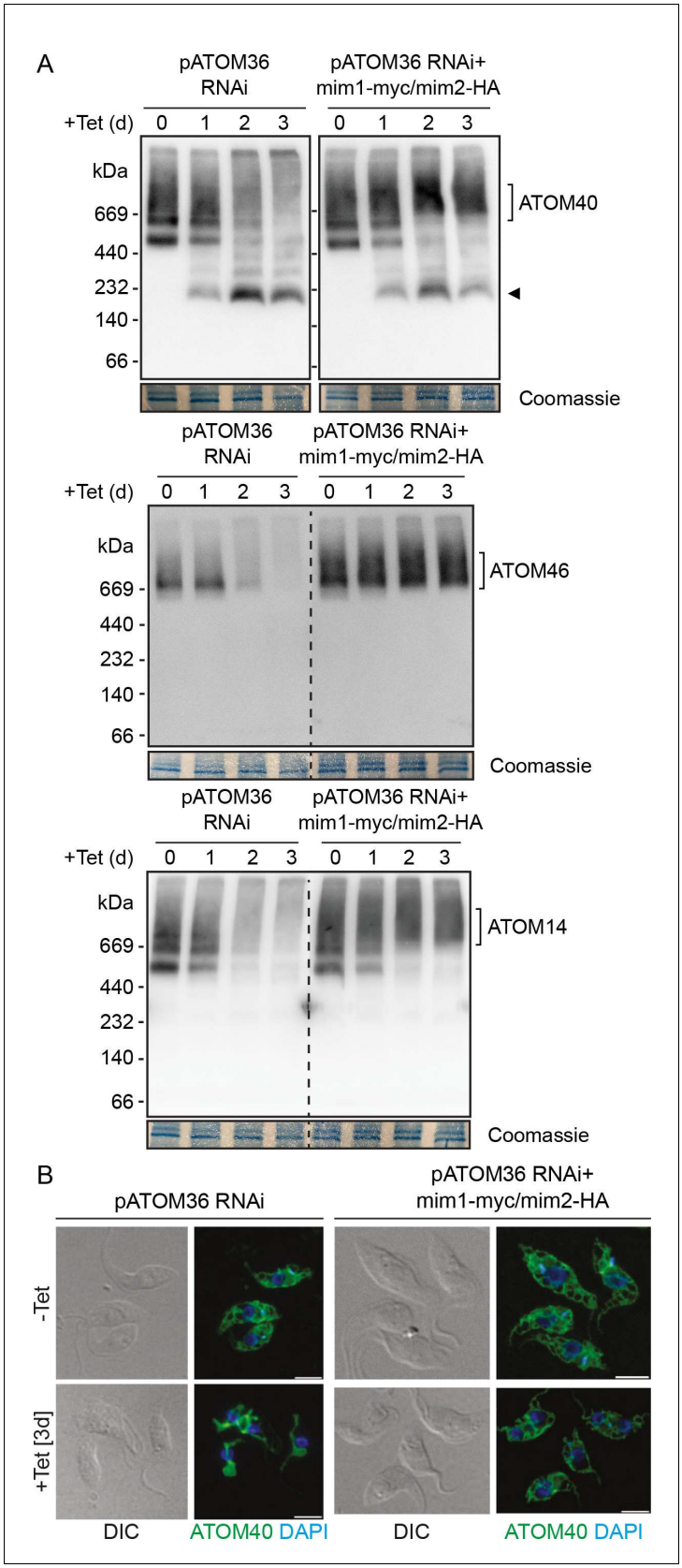

Figure 8. Mim1 and Mim2 rescue the assembly defect of the ATOM complex and the altered mitochondrial morphology in cells lacking pATOM36. (**A**) Mitochondria-enriched fractions from the cell lines as in ***Figure 7A***

Figure 8 continued on next page

Figure 8 continued

were obtained after the indicated time of induction. Samples were analysed by BN-PAGE followed by immunodecoration with antibodies against the indicated subunits of the ATOM complex. The migration of the ATOM complex is signposted. Sections of the coomassie-stained gels serve as loading controls. Arrowhead indicates an ATOM40-containing lower molecular weight complex. (**B**) Left images: Immunofluorescence analyses of mitochondrial morphology in the pATOM36 RNAi cell line after 0 or 3 days of induction. Right images: as in the left panels but the analysis was performed with the RNAi cell line co-expressing Mim1-myc and Mim2-HA. ATOM40 is shown in green and DAPI-stained DNA is shown in blue. DIC, differential interference contrast. Scale bar, 5 µm.

DOI: https://doi.org/10.7554/eLife.34488.015

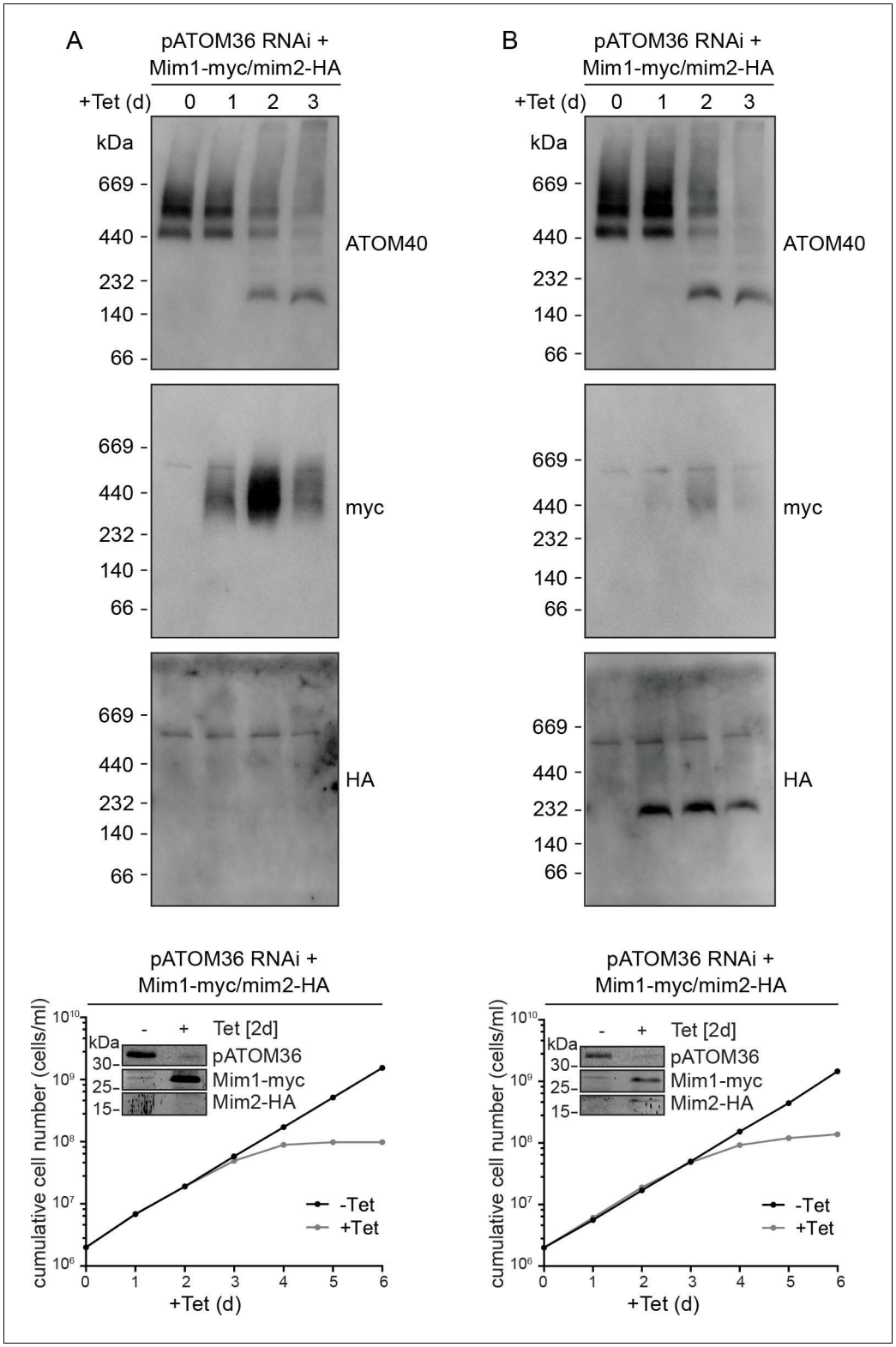

Figure 8—figure supplement 1. Complementing the biogenesis function of pATOM36 requires both Mim1 and Mim2. Individual clones of a pATOM36-RNAi cell line transfected with plasmids encoding myc-tagged Mim1 and HA-tagged Mim2 were analysed by BN-PAGE and subsequent immunodecoration. Clones that primarily express either myc-tagged Mim1 (**A**) or HA-tagged Mim2 (**B**) were analysed. The BN-PAGE blots were probed with anti-ATOM40 (upper panel), anti-myc (middle panel), and anti-HA (bottom panel) antibodies. Days of tetracycline

Figure 8—figure supplement 1 continued on next page

Figure 8—figure supplement 1 continued

induction (+Tet (**d**)) are indicated. Bottom graphs: growth curve for the same clone as above analysed in the presence and absence of tetracycline. Days of induction with tetracycline (+Tet [d]) are indicated. Inset: whole cell lysates of the clones were analysed by SDS-PAGE and immunodecoration with the indicated antibodies.
DOI: https://doi.org/10.7554/eLife.34488.016